MAP3K Regulation of MAPK Activation *in vitro* and Tumor Growth and Metastasis *in vivo*

Mark Robert Cronan

A dissertation submitted to the faculty of the University of North Carolina at Chapel Hill in partial fulfillment of the requirements for the degree of Doctor of Philosophy in the Department Biochemistry and Biophysics

Chapel Hill
2010

Approved by:

Gary L. Johnson, Ph.D.

Henrik G. Dohlman, Ph.D.

Beverly Errede, Ph.D.

Lee M. Graves, Ph.D.

Brian Kuhlman, Ph.D.

Abstract

Mark Robert Cronan. MAP3K Regulation of MAPK Activation *in vitro* and Tumor Growth and Metastasis *in vivo*
(Under the Direction of Gary L. Johnson, Ph.D.)

Mitogen activated protein kinase (MAPK) signaling is frequently dysregulated in cancer and contributes to both tumor growth and metastasis. These signaling networks consist of a three-tiered phospho-relay system in which the upstream MAPK kinase kinase (MAP3Ks) control magnitude and duration of downstream MAPK activation. MAPK activation drives the subsequent physiological outcomes in the cell based on the location, strength and pattern of MAPK activation. While work to date has focused on activation and dysregulation of MAPK signaling in tumors, it has largely ignored the role of upstream MAP3Ks, despite the critical role of MAP3Ks in pathogenic MAPK signaling.

Herein, I use multiple screening methods to assess the role of MAP3Ks in MAPK network activation *in vitro* and physiological outcome in cancer *in vivo*. Specifically, I have devised an immunofluorescent based MAPK activation screen that I use to identify MAP3Ks that regulate MAPK network activation in response to seven stimuli. Screening identified novel positive and negative regulators of growth factor, cytokine and stress stimulated ERK1/2, JNK and p38 activation. *In vivo*, I use an orthotopic xenograft system with a library of shRNAs to nine MAP3Ks to screen for novel roles of MAP3Ks

in tumor growth and metastasis. I identified new roles for six MAP3Ks in tumor growth and/or metastasis *in vivo*. Of these six MAP3Ks, I focus particularly on MEKK2 and MLK3 that control both tumor growth and metastasis *in vivo*. I demonstrate that MLK3 regulates cell growth and activation of JNK and p38 *in vitro* and controls macrophage recruitment to tumors *in vivo*. By contrast, I find MEKK2 regulates ERK5 activation by ERBB family members and I demonstrate that loss of ERK5 activation inhibits metastasis *in vivo*. Taken together, these results demonstrate the varied modes of MAP3K regulation of MAPK network activation and how altered MAPK signaling through MAP3Ks contributes to pathogenic signaling in cancer.

To my parents

Acknowledgements

First, I would like to thank Gary Johnson for his mentorship on this project, without which this project wouldn't have been possible. His knowledge and enthusiasm for science was a constant boon and was instrumental to my growth as a scientist and the success of this project. Equally, I would like to thank Henrik Dohlman, who has been my co-advisor on this project with Gary, for his constant patience and support. He went above and beyond and I can't thank him enough. I would also like to thank my committee members Beverly Errede, Lee Graves, Brian Kuhlman and JoAnn Trejo for their time and help in making this a better project.

To the Johnson lab members, both past and present, thank you for your warmth, good humor and technical know how. I would particularly like to thank Nancy Johnson for her tireless help with all of the tumor biology experiments, she was truly instrumental to this project.

Last, I would like to thank my friends and family who have been a constant source of support throughout this process and have always helped me keep my perspective. I would particularly like to thank my parents, John and Betsey. I am truly lucky to have had you as my parents. I would like to thank my brother, Glen for his support and for always challenging the way I think. I also would like to thank Emily for her love and support and for always tolerating my lab induced tardiness.

Table of Contents

List of Figures

List of Abbreviations and Symbols

ASK: Apoptosis signal-regulating kinase

DLK: Dual leucine zipper kinase

ECM: Extracellular Matrix

EGF: Epidermal growth factor

EGFR: Epidermal growth factor receptor

EMT: Epithelial to Mesenchymal transition

ERK: Extracellular regulated kinase

FGF: Fibroblast growth factor

GPCR: G-protein coupled receptor

HCC: Hepatocellular carcinoma

HGF: Hepatocyte growth factor

IL-1: Interleukin 1

JNK: c-Jun N-terminal kinase

LZK: Leucine zipper kinase

MAPK: Mitogen activated protein kinase

MAP2K: Mitogen activated protein kinase kinase

MAP3K: Mitogen activated protein kinase kinase kinase

MEF: Mouse embryo fibroblast

MEK: MAPK and ERK kinase

MEKK: MAPK and ERK kinase kinase

miR: MicroRNA

miRNA: MicroRNA

MLK: Mixed lineage kinase

MMP: Matrix metalloproteinase

MMTV: Murine mammary tumor virus

PAR: Proteinase activated receptor

PyMT: Polyoma middle T antigen

SCID: Severe combined immunodeficient

SEM: Standard Error of the Mean

siRNA: Small interfering RNA

shRNA: Small hairpin RNA

STE: Sterile

TAK1: TGFβ activated kinase

TF: Tissue factor

TGFβ: Transforming growth factor β

TNFα: Tumor necrosis factor α

Tpl2: Tumor progression locus 2

α: Alpha

β: Beta

μM: micromolar

μL: microliter

I. Introduction

Cancer is the second leading cause of death worldwide, causing the death of about seven million people annually (1). In cancer cells, mutations resulting from genetic insult cause uncontrolled cellular proliferation due to changes in the cellular signaling programs mediating growth and death. While many signaling pathways and genes have been implicated in cancer, work within this thesis is focused on signaling by the MAPKs, a group of signaling proteins that control both oncogenic and tumor suppressive signaling pathways in cancer.

Tumor Growth and Metastasis

Proliferation of cells is tightly regulated in the body by control of both cell growth and cell death. Development of cancer requires the acquisition of a series of mutations that not only promote cell growth but also inhibit cell death. The identification of proteins involved in cancer has led to the discovery of many novel oncogenes (such as activated forms of Ras, Src, Abl and EGFR) and tumor suppressors (such as p53, p16 and PTEN) that are either mutationally activated (oncogenes) or inactivated/deleted (tumor suppressors) from the cancer cells to promote growth (2,3). While mutation of genes such as Ras and p53 have been shown to be important in cancer development, it is currently estimated that most tumors require ~15 mutations (called driver mutations) to initiate and support the tumor (4). Many of these driver mutations have more modest

effects then genes like Ras or p53 and are likely a careful fine-tuning of oncogenic and tumor suppressive signaling pathways by the cancer cells.

Cancer cell growth is driven not only by mutational events, but also by tumor milieu. Cancer cells and surrounding stromal cells secrete many growth factors and cytokines that promote tumor growth and tumor cell survival (5-7). Many of these factors drive apoptosis in normal cells but are hijacked by cancer cells to promote cellular growth instead of apoptosis (5,7). These growth factors and cytokines also allow the tumor to recruit additional stromal cells from the host such as endothelial cells, fibroblasts, macrophages and granulocytes (7,8). These newly recruited stromal cells support the tumor by enhancing cancer cell growth, forming a functional tumor vasculature and by locally remodeling the tumor microenvironment.(9,10)

While unconstrained proliferation is an important characteristic of cancer, most cancer related death results from the metastatic spread of cancer cells to vital organs. In metastasis, cancer cells migrate out of the tumor and intravasate into the blood vessels where they can circulate throughout the body. They subsequently extravasate out of the blood vessels at a new location and seed at the site where, after a period of adaptation, they are able to grow out and form a secondary tumor (11,12). To metastasize the cancer cells must be able to remodel the local tumor environment to permit their escape and then migrate out of the primary tumor into the vasculature (11,12). This requires cancer cells to secrete a number of cellular factors including proteases such as the matrix metalloproteinases and cathepsins to break down the extracellular matrix (ECM) surrounding the tumor, remodeling of cell-cell contacts through changes in expression of adhesion molecules (such as switching from E-cadherin to N-cadherin expression and

loss of tight junction proteins), adoption of a mesenchymal morphology, and release growth factors and cytokines, such as the TGFβ family, EGF family members, and CSF family members to promote cancer cell migration and sustain the production of celluar factors required for metastasis (11-14).

It has been proposed that the changes that are required for cancer cells to metastasize are due to activation of an epithelial to mesenchymal transition (EMT) program in the cancer cells (15,16). EMT was initially characterized as a developmental program that allows epithelial cells at specific times to assume mesenchymal morphology which is needed to migrate and colonize distant locations (15). Similar to metastasis, in developmental EMT the sheets of epithelial cells lose cell-cell contacts, secrete proteases and ECM proteins and remodel their local enviroment to facilitate cell migration (15). Many of the growth factors and cytokines known to be important for tumor metastasis, such as the TGFβ family and EGF family induce EMT in many cell types (11,15,16). Gene array data has also demonstrated that metastatic cancer cells and cells undergoing EMT have similar gene expression profiles (15). Activation of the EMT program in cancer cells enhances metastatic potential (15,16). Thus the activation of the EMT program allows for coordinate activation of a series of pro-metastatic genes within the cancer cell and is crucial for cancer cell metastasis.

While tumor metastasis is one of the most detrimental occurrences with respect to clinical outcomes (as noted above, most cancer related death is due to metastasis rather than the primary tumor), little has been done in the clinic to identify drugs that inhibit metastasis. In large part, this is due to the fact that metastasis is very hard to study in the clinic. However, drugs that can inhibit tumor growth as well as metastasis may offer a

significant survival advantage over drugs that target only tumor growth. Chapter 3 in this dissertation describes our efforts to identify kinases that regulate both tumor growth and metastasis in tumor models *in vivo* that may be potential drug targets.

MAPKs, MAP3Ks and signaling

Mitogen activated protein kinase (MAPK) pathways have emerged as one of the major regulators of tumor growth and metastasis (17). MAPK pathways are signaling cascades that link extracellular stimuli (through their receptors) to intracellular responses. Specifically, MAPK pathways consist of three tiered kinase pathways in which a MAP kinase kinase kinase (MAP3K) activates a MAP kinase kinase (MAP2K), which subsequently activates a MAPK (Figure 1.1) (17). MAPKs then activate a wide array of transcription factors and additional kinases that coordinate cellular responses to the stimulus (Figure 1.1). There are four major families of MAPKs, the ERK1/2 family (consisting of ERK1 and ERK2), the JNK family (consisting of JNK1, JNK2 and JNK3), the p38 family (consisting of p38α, p38β, p38γ and p38δ) and ERK5 (18,19). Additionally, many of these MAPK genes can be alternatively spliced, generating a diverse array of MAPK isoforms (20-22). While there are four families of MAPKs, these are activated by seven MAP2Ks. The MAP2Ks are MEK1 and MEK2 that activate ERK1/2, MKK4 and MKK7 that activate JNK, MKK3, MKK4 and MKK6 that activate p38 and MEK5 that activates ERK5 (19). The seven MAP2Ks are in turn regulated by a diverse group of ~20 MAP3Ks (Figure 1.2) (21). The MAP3Ks consist of four major families based on sequence homology (21). The RAF family, originally discovered because of their homology to oncogenic v-Raf, consisting of A-Raf, B-Raf and c-Raf,

which predominantly activate ERK1/2. The Ste family, which was originally cloned due to their homology to the yeast MAP3K Ste11, consists of MEKK1-4, ASK1 and ASK2, TAK1 and Tpl2, that activate ERK1/2, JNK, p38 and ERK5 families. The TAO kinases, which are related to yeast Ste20, consist of TAO1, TAO2 and TAO3 that activate p38. Last, the mixed lineage kinase (MLK) family, consisting of MLK1-4, LZK, DLK and MLK7, predominantly activate the JNK and p38 families.

MAPK signaling has been linked to a wide range of cellular outcomes. ERK1/2 signaling has been linked canonically to cell growth and cell survival as well as to migration, cytokine and growth factor release and expression of proteases (23). By contrast, JNK signaling has been canonically associated with apoptosis, but has also been found to promote cell survival, cell proliferation, as well as inflammation, migration, protease expression and cytokine release (17). Similarly, p38 has been associated with apoptosis, although it also has been linked to cell survival, proliferation, inflammation, proangiogenic signaling, protease expression and cytokine release (17). The varied and frequently conflicting range of responses driven by MAPKs is likely the product of variations in signaling intensity and duration of MAPK activation as well as activation of specific MAPK genes and splice isoforms. The end result is a complex panoply of pro-oncogenic and anti-oncogenic functions the outcome of which likely hinges on upstream inputs into the MAPK pathways.

Given the large number of MAP3Ks and smaller numbers of MAP2Ks and MAPKs, it has been suggested that the specificity of MAPK activation is controlled by the upstream MAP3Ks (Figure 1.2) (19,21). Consistent with this hypothesis, it has been found that knockdown or knockout of specific MAP3Ks can block activation of specific

MAPKs in a stimulus dependent manner. For instance, knockdown of ZAK (also known as MLK7) has been shown to block activation of JNK and p38 by the protein sythesis inhibitor anisomycin as well as p38 activation by hyperosmolar stimuli, such as hyperosmolar NaCl (24). Tpl2 has been shown to have a specific role in Thrombin stimulated activation of ERK1/2 and JNK signaling pathways, LPS stimulated ERK1/2 activation, IL-1β stimulated ERK1/2 activation and TNFα ERK1/2 and JNK activation using knockout cell lines (25,26). However, the results with many stimuli have not been clear cut and there is controversy regarding which MAP3Ks regulate which MAPKs. For instance, no fewer then four MAP3Ks (MLK3, TAK1, ASK1 and Tpl2) have been found to regulate TNFα stimulated JNK signaling (26-29). The many MAP3Ks required for TNFα stimulation of JNK may be due to contributions of multiple MAP3Ks to the signaling event or cell type specific expression/signaling by the MAP3Ks. It may also be due to complex formation between different MAP3Ks. While heterodimeric complex formation between MAP3Ks has not been described in TNFα stimulated JNK activation, it has been described in other systems. For instance, MLK3 has been found to associate with B-Raf and c-Raf to regulate B-Raf and c-Raf activation of ERK1/2 (30). Similarly, TAK1 has been found to interact with MEKK3 and this interaction is thought to regulate the ability of MEKK3 to activate NF-κB (31). While identification of the specific MAP3Ks regulating individual MAPKs has been contentious and may involve non-kinase mechanisms, the data consistently demonstrates specificity in the signaling pathways controlled by the MAP3Ks. Research described in chapter 2 of this dissertation describes our efforts to systematically identify the MAPK responses controlled by a

group of MAP3Ks. I hypothesize that identification and targeting of MAP3K signaling will allow for selective inhibition of specific MAPK responses.

MAPK signaling and cancer in cell culture and animal models

ERK1/2 pathway

Of the four families of MAPKs, the ERK1/2 family is the group with the best known role in tumor biology. In cell culture models, ERK1 and ERK2 were originally found to be activated by mitogens, and additional work using inhibitors has determined that ERK1/2 promotes cell growth by a wide array of growth factors such as serum, EGF, LPA, FGFs and HGF. The effects of ERK1/2 on proliferation are exerted through the ability of ERK1/2 to promote cell cycle progression (such as through cyclin D expression), nucleotide synthesis (through CPSII) and protein synthesis (through Mnk1) (32,33). Further, the role of ERK1/2 signaling in growth has been confirmed with siRNA, where it has been found that the sum total of ERK1 and ERK2 levels controlled proliferation (34,35). In agreement with siRNA experiments, genetic models have also implicated sum total levels of ERK1 and ERK2 in embryonic viability (35). Whereas $ERK1^{+/-}$ mice and $ERK2^{+/-}$ mice are viable, mice heterozygous for both ERK1 and ERK2 knockout were exceedingly rare (constituting 3.4% of live births versus 50% expected for the cross) (35). In crosses of the resulting $ERK1^{+/-}ERK2^{+/-}$ mice, no mice were found to have only 1 ERK1 or ERK2 allele (35).

ERK1/2 has been found to mediate cell survival induced by a wide array of growth factors. This is accomplished through many mechanisms such as ERK1/2 phosphorylation and sequestration of the proapoptotic proteins BAD and BIM (36). The role of ERK1/2 in cell survival has been demonstrated in $ERK2^{-/-}$ embryos. Loss of

ERK2 was embryonic lethal; ERK2$^{-/-}$ embryos were markedly smaller than WT or ERK2$^{+/-}$ littermates and showed increased apoptosis, loss of mesoderm differentiation and placental defects (37). However, embryos showed roughly normal BrdU incorporation, indicating that ERK2$^{-/-}$ embryos show defects in survival rather then proliferation (37).

The upstream activators of ERK1/2, MEK1 and MEK2 show similar effects in cell survival and proliferation as ERK1/2, consistent with the fact that ERK1 and 2 are the only proteins known to be phosphorylated by MEK1/2 (38). Using animals with conditional knockout of MEK1 and MEK2 in skin, it was found that skin from MEK1/MEK2 double knockout mice had increased apoptosis and decreased proliferation (39). Furthermore, systemic MEK1$^{-/-}$ knockout mice were not viable, with death occurring around E10.5 in MEK1$^{-/-}$ embryos likely due to placental defects (40,41).

ERK1/2 signaling has been implicated not only in cancer relevant processes like cell growth and survival, but has also been directly implicated in cancer. It has been found that ERK1 and ERK2 are constitutively activated in many tumors (42). Constitutive ERK1/2 activation through introduction of a constitutively active form of MEK1/2 transforms cells and promotes both anchorage independent growth *in vitro* and tumor growth *in vivo* (43). Consistent with a role for ERK1/2 signaling in cell growth, loss of ERK1/2 signaling by inhibitors or siRNA has been shown to inhibit tumor growth in liver cancer cell xenografts (34). Loss of upstream MEK1 by siRNA also decreases liver cancer cell xenograft growth (44). The importance of ERK1/2 signaling in tumor growth has been confirmed in ERK1$^{-/-}$ mice, which show decreased tumor number and size in a two stage TPA/DMBA mouse skin cancer model (45). Similar results are seen

upstream of ERK1/2, where conditional knockout of MEK1 (but not MEK2) in skin results in reduced tumor number and size using the same TPA/DMBA model (38). Knockout of MEK1 and MEK2 in mouse skin has also been demonstrated to block epidermal hyperplasia induced by expression of oncogenic c-Raf (39). These data show that ERK1/2 is an important pro-oncogenic pathway for tumors.

JNK pathway

The JNK family of kinases was originally discovered due to their activation by cycloheximide and other cellular stresses. Compared to ERK1/2 signaling, JNK signaling is often considered to be pro-apoptotic and as such, tumor suppressive (reviewed in (46)). Apoptotic roles for JNKs have been demonstrated in $JNK1^{-/-}JNK2^{-/-}$ MEFs which were found to be resistant to apoptosis induced by anisomycin, UV, and methyl methanesulfonate (47). Work with JNK inhibitors and JNK siRNA have also linked JNK to apoptosis by numerous cellular factors and cell stresses (48-50). Apoptosis induction by JNK is known to be mediated by JNK dependent transcription of proapoptotic factors such as Fas-L and Bak (51,52). JNK can also phosphorylate and regulate mediators of the mitochondrial apoptotic pathway including Bcl2, Bad and Bim (53-56). While JNK is an important mediator of apoptosis, other studies have demonstrated a role for JNK in other pathways such as cell growth and survival. The JNK pathway is activated by many growth stimuli such as serum, EGF and LPA (57,58). JNK activation by growth stimuli is frequently necessary for cell growth in response to these growth factors (57,59). Furthermore, downstream targets of JNK such as the transcription factor c-Jun, have been found to promote cell proliferation and survival

(60,61). JNK knockout MEFs offer further confirmation of the role of JNK in growth, JNK1$^{-/-}$ MEFs show a decreased rate of proliferation (62). Paradoxically, JNK2$^{-/-}$ MEFs show increased proliferation; however, this has been proposed to be due to a compensatory increase in JNK1 and c-jun levels in JNK2$^{-/-}$ MEFs (62). Similarly, using inhibitors it has been found that JNK promotes cell growth in many cell types such as smooth muscle cells, fibroblasts and leukemia cells (63-65). Interestingly, it appears that the varied roles of JNK signaling in apoptosis, cell growth, and cell survival may be due to kinetics of signaling. MEFs stimulated with TNFα show a biphasic activation of JNK. Using a chemical genomics approach, it was shown that late phase JNK activation promoted cell death whereas early phase JNK activation promoted cell survival (66). Thus the varied roles of JNK signaling are likely a product of varying spatial and temporal activation of JNK as well as the profile of JNK isoforms activated by the stimulus.

In vivo, JNK signaling has been found to be both pro- and anti-oncogenic. Potential activating mutations have been identified in JNK1, JNK2 and the upstream kinase MKK7 in tumor samples, indicating a potential oncogenic role for JNK signaling in human tumors (17). This is corroborated by the identification of a role for JNK1 in hepatocellular carcinoma (HCC). Elevated JNK1 activation has been demonstrated in tumor samples from human patients with HCC (67). The oncogenic role of JNK1 was demonstrated by JNK1 knockdown in HCC cell lines which resulted in reduced cell proliferation and tumor growth in xenografts *in vivo*, while JNK2 knockdown had no effect (67). Using both JNK1$^{-/-}$ mice and a peptide based JNK inhibitor, it was also demonstrated that JNK1 was necessary for liver tumor proliferation in the

diethylnitrosamine (DEN) liver tumor model (67,68). Oncogenic roles for JNK1 signaling have been demonstrated in other experimental cancer models such as the *N*-methyl-*N*-nitrosourea induced stomach cancer model (69). Elevated JNK activation has been demonstrated in cohorts of human patients as well. Elevated JNK phosphorylation has been found in malignant effusions from ovarian cancer patients and in basal like and triple negative patient breast tumor samples (70,71). JNK signaling has also been implicated in oncogenic ILK signaling in human rhabdomyosarcomas (72). Downstream of JNK, it has been found that blocking JNK phosphorylation of c-jun can inhibit intestinal tumors formed in mice engineered to express mutant APC (73). However, skin cancer models demonstrate varied roles of JNK proteins in pro- and anti-oncogenic signaling. Consistent with an oncogenic role for JNK signaling, $JNK2^{-/-}$ mice were found to have a decreased rate of papilloma formation in a DMBA/TPA model of skin cancer (74). However, using the same model, $JNK1^{-/-}$ mice were found to have increased papilloma formation, implying a role for JNK1 in tumor suppression (75). JNK1 has also been demonstrated to have a tumor suppressive role in intestinal cancer. Contrary to findings in APC mice, in which JNK1 knockout blocked tumor formation by APC mutants, $JNK1^{-/-}$ mice are predisposed to develop spontaneous intestinal tumors due to increased proliferation and decreased differentiation of intestinal cells. These results demonstrate that JNK signaling has varied roles in tumor outcome that are dependent on the upstream activators of JNK signaling, the JNK isoforms involved in the signaling and the cell types involved in the cancer.

p38 pathway

Similar to JNK, p38 has been considered a stress activated kinase and is known to be activated by many cellular stresses such as hyperosmolarity, UV and γ-irradiation, exposure to bacterial products and inflammatory cytokines (19,76). However, p38 has been demonstrated to be activated by mitogens as well including EGF, HGF and lipid signals such as lysophosphatidic acid and sphinogosine 1-phosphate (77-80). Consistent with stress induced p38 signaling, p38 has been demonstrated to have tumor suppressive functions *in vitro* through its control of apoptosis and cell cycle regulation (81,82). This tumor suppressive effect of p38 signaling is mediated by p38 regulation of proteins such as cyclins, death receptors, Bcl-2 family proteins and p53 (83-86). p38 signaling has also been demonstrated to inhibit cell proliferation through p38 dependent suppression of JNK signaling and c-Jun activation (87). However, a growing body of data has also demonstrated that p38 can promote oncogenesis as well. Inhibitor studies as well as siRNA and dominant negative approaches have shown that p38 regulates cell proliferation, particularly in p53 null cell lines (88). p38 has also been demonstrated to promote cellular survival through regulation of autophagy and inactivation of GSK3β (89,90). p38 has also been implicated in the release of many cytokines, proteases and growth factors such as VEGF, MMPs, IL-6 and IL-8 and that are critical regulators of tumor growth, metastasis and vascularization (91-94).

Similar to *in vitro* studies, *in vivo* studies have demonstrated both oncogenic and tumor suppressive roles of p38, although tumor suppressive roles have been most extensively documented for p38α. Disruption of p38α or upstream MKK3/6 has been demonstrated to enhance tumor growth of transformed MEFs (95). Tumor suppressive roles of p38 have been corroborated in cancer models. Conditional knockout of p38α

lead to increased tumor size and number in liver tumors induced using a DEN/Phenobarbital protocol correlating with increased JNK activation (87). p38 signaling has found to be tumor suppressive in lung as well. Conditional knockout of p38α in mouse lung has demonstrated that loss of p38 enhances lung tumorigenesis caused by expression of $Kras^{G12V}$ (96). Specifically, lung tumors in $Kras^{G12V}p38\alpha^{-/-}$ were markedly larger and correlated with much earlier mortality in $p38\alpha^{-/-}$ mice (96). Similarly, deletion of the p38 phosphatase Wip1 inhibited tumor growth in mouse mammary tumor virus (MMTV)-Her2 and MMTV-Hras driven mammary tumors (97). Oncogenic roles for p38 have also been demonstrated, predominantly with p38δ. Using the H-ras driven TPA/DBA skin cancer model and the K-ras driven $Kras^{G12V}$ lung cancer model, it was demonstrated that knockout of p38δ resulted in reduced tumor number and volume in these Ras driven models (98). Activation of p38 has also been demonstrated in human breast cancer patients with pleural effusions, where p38 phosphorylation is a prognostic marker for disease outcome (99).

ERK5 pathway

Of the four MAPK pathways, the ERK5 pathway is the least characterized. In cell culture, ERK5 has been shown to promote EGF dependent proliferation in specific cell lines (100). ERK5 has also been demonstrated to promote cellular survival in multiple cell types, including neurons and MEFs (101,102). A role for ERK5 signaling in survival was demonstrated in TNFα resistant MCF-7 cells, in which TNFα resistance was mediated through the ERK5 pathway by overexpression of the MAP2K MEK5 (103). ERK5 has also been demonstrated to be important in survival and transformation

mediated by the tyrosine kinase Abl and oncogenic BCR/Abl (104). A potential role for ERK5 signaling in tumor growth and progression has been demonstrated *in vivo* in prostate cancer. Specifically, it was found that expression of miR-143, a microRNA that regulates ERK5 levels, decreased with prostate cancer progression (105). Expression of miR-143 could inhibit cell growth *in vitro* and tumor growth *in vivo* and knockdown of ERK5 resulted in a similar inhibition of cell growth *in vitro* as was observed in miR-143 overexpressing cell lines (105).

ERK5 has been demonstrated to regulate levels of pro-metastatic factors such as the transcription factor Slug, MMP-9 and IL-6 (106-108). Consistent with a role in metastasis, ERK5 signaling has been demonstrated to regulate actin reorganization and migration *in vitro* (106,109). Metastatic functions of ERK5 have also been demonstrated *in vivo*. ERK5 was found to be overexpressed in human breast cancer patients. In these patients, overexpression of ERK5 was correlated with decreased survival (110). Similarly, overexpression of MEK5 was demonstrated in prostate cancer with MEK5 expression levels correlating with bony metastases and with decreased survival in prostate cancer patients (107). These results demonstrate that ERK5 signaling may be an important mediator of tumor progression and metastasis.

MAP3K Signaling and Cancer

Raf Family

Of the MAP3Ks, the Raf family, consisting of A-Raf, B-Raf and c-Raf, has been best characterized in cancer. The Raf family was originally cloned based on its homology to the mouse sarcoma virus gene product v-Raf. Oncogenic mutations of the kinases have

been found that result in constitutive activation of ERK1/2 signaling (111). Of the three family members, B-Raf has the strongest transforming potential followed by c-Raf, while A-Raf has minimal transforming potential (112). The variations in transforming potential within the Raf family appear to be due to differences in the ability of individual Raf family members to activate ERK1/2. In terms of activation of ERK1/2 signaling by Raf isoforms, B-Raf > c-Raf > A-Raf consistent with the relative transforming ability of each Raf gene (112). In agreement with findings on Raf transforming activity in cell lines, sequencing of Raf family members in tumor cells have found similar patterns of Raf mutations in tumors. As the most transforming of Raf family members, B-Raf has been found to be mutated in many cancers, particularly in melanomas. Large scale sequencing of B-Raf mutations in melanoma has found that up to 60% of melanomas and ~7% of all tumors express a B-Raf^{V600E} mutation that results in constitutive B-Raf activation (111). By contrast c-Raf mutations have been found much more sporadically in cancer. Mutations of the final Raf family member, A-Raf are extremely rare in cancer and are not thought to be drivers of cancer.

Although B-Raf^{V600E} mutations are common in melanoma, the role of B-Raf^{V600E} in melanoma has been questioned, as B-Raf^{V600E} mutations have been found in benign nevi in human patients (113). This corroborates with mouse findings in which B-Raf^{V600E} mutation in the absence of secondary mutations can only promote melanocytic hyperplasia (114). However, when combined with deletion of a tumor suppressor, such as PTEN, B-Raf^{V600E} can cause rapid formation of metastatic melanomas in mice (114). Furthermore, the importance of B-Raf^{V600E} mutation has been demonstrated using inducible shRNA in melanoma cell lines; induction of B-Raf shRNA in B-Raf^{V600E} cell

lines inhibited cell growth *in vitro* and caused rapid tumor regression *in vivo* accompanied with loss of ERK1/2 phosphorylation (115). PLX4032, a drug that specifically targets B-Raf^{V600E} has shown impressive efficacy in xenografts as well as in phase I clinical trials, in which patients with the B-Raf^{V600E} mutation showed an 80% response rate to the drug (116-118).

STE Family

The STE family of MAP3Ks, originally cloned because of their homology to yeast Ste11, consists of MEKK1-4, ASK1 and ASK2, TAK1 and Tpl2. These kinases regulate either ERK1/2 and JNK (MEKK1, Tpl2), JNK and p38 (MEKK4, ASK1, ASK2 and TAK1), JNK and ERK5 (MEKK2) or p38 and ERK5 (MEKK3). Many of these kinases have been implicated in cancer relevant processes *in vitro* in processes such as migration, invasion and cell growth. However, data on the roles of these kinases in tumors *in vivo* has been limited.

MEKK1 has been demonstrated to regulate the expression of the pro-metastatic protease uPA. Mice deficient for MEKK1 displayed reduced metastasis in an MMTV-polyoma middle T antigen (PyMT) model of breast cancer, a model in which metastasis has been demonstrated to be uPA dependent. While metastasis was reduced in the MMTV-PyMT model, tumor growth remained unchanged, demonstrating selective decoupling of metastasis from tumor growth (119).

Imaging mass spectrometry on prostate cancer tissue and surrounding uninvolved tissue identified a single MEKK2 peptide as the sole peptide differentiating between cancer and normal tissue. It was further demonstrated that MEKK2 was upregulated in

prostate cancer four fold relative to benign tissue, implying a role for MEKK2 in cancer progression (120). However, other work also demonstrates a tumor suppressive role for MEKK2. MEKK2 has been demonstrated to be downregulated by the microRNA miR-26a, a microRNA that can promote cell transformation (121). It was further demonstrated that MEKK2 knockdown could inhibit JNK dependent apoptosis in response to chemotherapeutics, thus implying a pro-apoptotic role MEKK2 at least in response to chemotherapeutics.

MEKK3, which is very closely related to MEKK2, has been found to be overexpressed in ovarian cancer relative to surrounding tissue and correlated with increased cell survival *in vitro* upon treatment with chemotherapeutics (122). However, experiments using a teratoma model formed by injection of MEKK3$^{-/-}$ ES cells found that MEKK3 deficiency had no effects on teratoma growth (123).

The closely related ASK1 and ASK2 are two MAP3Ks that regulate cellular response to reactive oxygen species (ROS). ROS signaling has been demonstrated to promote and inhibit tumor growth depending on context. While ROS signaling can have both oncogenic and tumor suppressive roles, data using the DBA/TPA induced skin cancer model in ASK1$^{-/-}$ and ASK2$^{-/-}$ mice show that both ASK knockout mice have elevated tumor formation, demonstrating a tumor suppressive role for ASK1 and ASK2 (124). The tumor suppressive role of ASK1 has been further demonstrated with ASK1$^{-/-}$ animals using a colitis induced cancer model, in which ASK1$^{-/-}$ mice have increased numbers and size of colitis induced colon tumors relative to wild type mice (125). The increased tumor burden in ASK1$^{-/-}$ mice in the colitis induced tumor model is accompanied by a decreased survival in tumor bearing ASK1$^{-/-}$ mice relative to wild type.

Tpl2 was originally cloned as a tumor progression locus that was truncated by Moloney murine leukemia virus (MoMuLV) insertion in MoMuLV dependent lymphoma formation in rats (126). These truncations were found to enhance basal activity of Tpl2 and promote activation of ERK1/2 and JNK (127). Furthermore, it was found that transgenic mice with thymocyte specific expression of truncated Tpl2, but not full length Tpl2, readily developed lymphomas (127). Consistent with a role for Tpl2 in lymphoma, in a small cohort of human patients, elevated Tpl2 expression has been detected in a subset of T-cell malignancies (128). More recently, in a small scale study, Tpl2 has been found to be overexpressed in 40% of breast tumors. Tpl2 mutations were also found at elevated rates in basal like breast cancer tumor relative to non-tumor tissue and the mutation rate of Tpl2 was further elevated in a metastasis from the tumor.

MLK family

The mixed lineage kinase, or MLK family, was originally cloned and named based on the resemblance of family members to both serine/threonine kinases and tyrosine kinases. Subsequent work has demonstrated that all known MLK family members are serine/threonine kinases rather then tyrosine kinases. This family consists of MLK1-4, LZK, DLK and MLK7. However, of the three families of MAP3Ks, the MLK family has the least understood role in cancer. *In vitro*, the MLK family has been demonstrated to mediate apoptosis through both JNK and p38 signaling. This MLK family role in apoptosis conflicts with studies that demonstrated that MLK3 overexpression promoted anchorage independent growth in fibroblasts and MLK7 overexpression promoted tumor formation by fibroblasts (129,130). MLK3 has also been demonstrated to mediate

transformation by activated Rac isoforms (131). In human patients, MLK3 mutations have been identified as potential driver mutations in mismatch repair deficient gastrointestinal tumors (132). These mutations occurr outside of the kinase domain and are hypothesized to alter protein-protein interactions in the mutant (132). *In vivo* tumor formation in fibroblasts expressing MLK3 mutants was greatly accelerated relative to fibroblasts expressing wild type MLK3 (132).

MAPKs as Drug Targets

MAPKs have been an active target for drug development for cancer based on their roles in many cancer processes and for treatment of other diseases of dysregulated MAPK signaling such as inflammatory disease and Alzheimer's disease. However, to date, none of the MAPK inhibitors developed have made it through clinical trials (17). The failure of MAPK inhibitors is due to multiple factors including lack of clinical efficacy, lack of inhibitor specificity, and toxicity effects from the inhibitors. The lack of clinical efficacy of MAPK inhibitors may be due to broad inhibition of both oncogenic and tumor suppressive functions of the MAPKs. The toxicity of the drugs has been problematic as well; inhibitors of ERK1/2 have had ocular toxicity side effects and p38α inhibitors have been frequently plagued by liver toxicity (17). However, whether these effects are specific for ERK1/2 and p38α or represent common off target effects for these inhibitors has yet to be confirmed. These results demonstrate that while MAPKs are high priority targets for novel cancer therapeutics, direct targeting of MAPKs may not offer either the necessary efficacy or clinical safety required of therapeutics. Instead, targeting

of upstream MAP3Ks may allow us to selectively inhibit oncogenic MAPK signaling with fewer side effects.

Untargeted Kinases in the Cancer Kinome

The multiple mutations required for cancer development mean that many tumors show different spectrums of mutation. This is further complicated by the genetic diversity of the individual the tumor is derived from. The wide spectrum of genetic changes in tumors has made individual cancers difficult to treat, as drugs that are promising in one patient may be less effective in another. Furthermore, tumors rapidly adapt to drug regimens due to the high mutational frequency within the tumors. Therefore, there is a clinical need for novel anticancer drugs to treat non-responding tumors and tumors that have become resistant to chemotherapeutic regimens.

Research on the cancer kinome has focused almost exclusively on the most studied 1-5% of genes (133). However, genetic approaches assessing driver mutations in the kinome have demonstrated that the driver mutations required for cancer are spread through many kinase genes, and driver mutations are no more common in the most studied subset of genes than elsewhere in the kinome (133). Similarly, siRNA experiments measuring cell growth *in vitro* have demonstrated that many of the kinases required for cellular growth are outside of the most studied groups of kinases. These results demonstrate the need for new drugs targeting kinases outside of the widely studied kinases (133).

In our work, we screen MAP3Ks for their contribution to tumor growth and metastasis. Outside of B-Raf, the MAP3Ks have been largely ignored by the cancer

research community despite the fact that MAP3K signaling controls the oncogenic and tumor suppressive effects of MAPKs, a group of proteins that has been extensively characterized in cancer research and has been targeted repeatedly (and at high cost) with many drugs and by many drug companies. By determining the roles for MAP3Ks in tumor growth and metastasis, we hope to identify MAP3Ks that are required for oncogenic MAPK signaling while leaving the tumor suppressive effects of MAPK signaling intact. MAP3Ks that fit these criteria will be high quality therapeutic targets for the development of a new generation of drugs that function through MAPK network regulation.

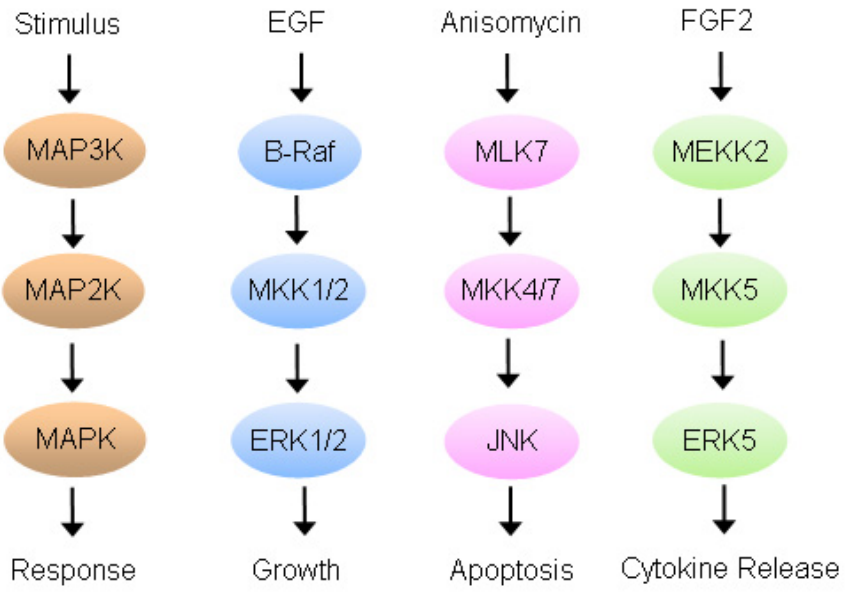

Figure 1.1. Generalized MAPK signaling and known MAPK pathways.

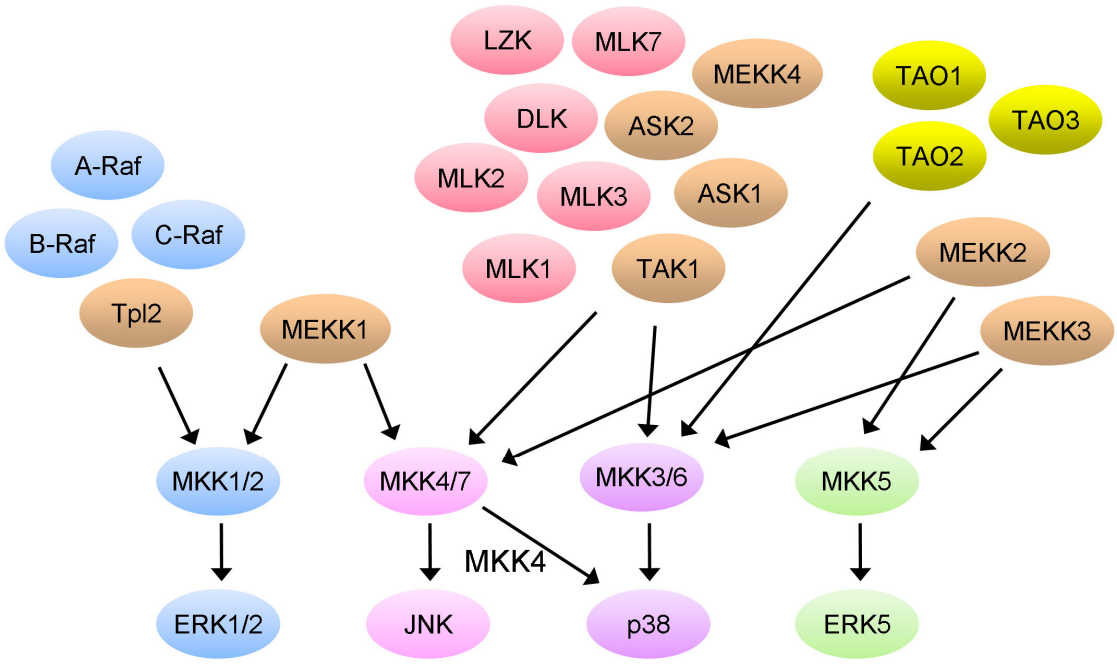

Figure 1.2. The Diversity of MAP3K signaling in the MAPK network. Families of MAP3Ks are shown in identical colors. Raf family is blue, STE family is tan, MLK family in red and TAO family in yellow. Most MAP3Ks regulate multiple MAPK pathways.

II. Systematic Screening of MAP3Ks to Identify MAP3K Regulated Activation of the MAPK Network

Introduction

Altered cell signaling through MAPK pathways frequently underlies pathologic conditions including neurological and inflammatory diseases and cancer. MAPK pathways are three tiered kinase relays in which a stimulus causes a MAP3K to activate a MAP2K that activates a MAPK (18). The MAPKs, consisting of the ERK1/2, JNK, p38 and ERK5 families, subsequently coordinate a cellular response to the stimulus by phosphorylating and activating additional cellular factors including other kinases and transcription factors (18). Through regulation of downstream targets, MAPKs are able to regulate diverse cellular processes such as proliferation, cell death and survival, secretion of cytokines and cell migration. Phosphorylation of these MAPKs is regulated in a spatial and temporal manner, with different patterns of MAPK activation leading to diverse cellular responses. This was elegantly demonstrated in mouse embryo fibroblasts (MEFs) where using a chemical genomics method it was shown that acute phase JNK activation promoted cell survival whereas persistent JNK activation promoted cell death (66).

Given the physiological importance of MAPK pathways, their activation must be tightly controlled *in vivo*. Control of spatial and temporal MAPK signaling has been suggested to occur at the level of the MAP3Ks, due to their position upstream of the MAPKs and the large number of MAP3Ks encoded in the genome (19). While there are

~20 MAP3Ks, these signal to only 7 MAP2Ks which regulate only four families of MAPKs (19). Each of the MAPK families is regulated by multiple MAP3Ks; however, individual MAP3Ks do not appear to be highly redundant. Evidence from knockdown and knockout experiments have demonstrated that inactivation of an individual MAP3K results in unique MAPK signaling defects (25-27). The lack of redundancy in MAP3K signaling has also been demonstrated physiologically; MAP3K knockout mice have been made for many MAP3Ks demonstrating phenotypes ranging from minor decreases in skin thickness in the MLK3 knockout mice, to neural tube defects and skeletal abnormalities in MEKK4 knockout mice (27,134).

To date, studies on the regulation of MAPK pathways by MAP3Ks have focused on relatively small numbers of stimuli in a range of cell types. Furthermore, although recent data has demonstrated that MAP3Ks can act as negative regulators of MAPK activation through many mechanisms, such as direct competition for common cellular factors and heterodimerization between MAP3Ks, most of the data to date has focused on MAP3Ks as positive regulators of MAPK signaling (31). A more complete understanding of these MAPK signaling networks and their regulation by MAP3Ks may allow us to selectively decouple the deleterious effects of MAPK signaling from beneficial MAPK signaling events. However, the systematic studies of MAP3Ks and their effects on MAPK networks that would allow the targeting of these deleterious MAPK effects have not been done.

We sought a screening method that would allow us to rapidly identify the MAP3Ks that control stimulus induced MAPK activation. Use of double stranded siRNA molecules has emerged as a tool that allows for the rapid study of classes of genes

(135). We therefore designed a screen using siRNA to selectively knock down 11 MAP3Ks and screened for changes in MAPK activation by immunofluorescence in response to seven different stimuli. Using this screen, we were able to identify subsets of MAP3Ks that are positive and negative regulators of MAPK signaling. The effect of individual MAP3K knockdowns varied depending on which stimulus was used and which MAPK pathway was assayed. Classification of the seven stimuli used in the screen into three broad groups (growth factors, cytokines and cell stresses) demonstrated that specific MAP3Ks regulated MAPK activation by multiple stimuli of a group. These results indicate that the cell uses discrete MAP3K-MAPK modules to regulate cellular responses of groups of similar stimuli.

Methods

Cell lines, cell culture, general reagents

All chemicals, including thrombin, sorbitol and anisomycin were from Sigma-Aldrich unless noted. EGF and HGF were from Peprotech, TNFα was from R&D systems. siRNA siGENOME SMART pools against the MAP3Ks were from Dharmacon. Media and fetal calf serum (FCS) were from Invitrogen. HeLa cell lines stably expressing PAR1 were a generous gift from JoAnn Trejo (University of California at San Diego). HeLa cell lines were grown in DMEM with 10% FCS, with 100 units/mL of penicillin and streptomycin and 250 μg/mL hygromycin (to maintain PAR1 expression). HeLa cells expressing PAR1 and JNK1α1 were obtained by infecting HeLa cells expressing PAR1 with retroviruses containing an HA tagged JNK1α1 and selecting on 500 μg/mL G418.

Western blotting

Media was removed and cells were washed once with 1 x ice cold PBS. Cells were lysed by adding lysis buffer to the cells (1% Triton X-100, 150 mM NaCl, 10 mM Tris pH 7.5) supplemented with complete protease inhibitors (Roche), PMSF and $NaVO_4$. Lysates were clarified by centrifugation and protein concentrations were quantitated using Bradford reagent. Equal quantities were loaded on a polyacrylamide gel, separated and transferred. After blocking in milk, blots were incubated overnight with polyclonal rabbit anti-phospho-ERK1/2 antibody (Cell Signaling) or monoclonal mouse anti-γ-tubulin antibodies (clone GTU-88, Sigma) to detect loading. Blots were washed, incubated with fluorescent anti-rabbit Cy3 or anti-mouse Cy5 secondary antibodies (GE Healthcare) and detected using a Typhoon 9400 variable mode imager (GE Healthcare).

MAP3K screening

96 well glass imaging bottom plates (Nunc) were coated with fibronectin for 1 hr. After coating, wells were washed once with PBS and 20μL of serum free DMEM containing siRNA precomplexed with Dharmafect 1 was added to each well. Each MAP3K siRNA was assayed in triplicate. A trypsinized cell suspension of 4 x 10^3 HeLa cells in 80 μL of complete media was added to each well. siRNA was used such that the final concentration of siRNA was 50 nM in 100 μL. After 5 hours of transfection, media was changed to fresh complete media and incubated overnight. The next day, media was removed and cells were serum starved overnight in DMEM/0.5% FCS. Except as noted, cells were stimulated with the indicated ligands for either 5 min (thrombin stimulated

ERK1/2 activation), 10 min (serum), 20 min (EGF, HGF, TNFα and thrombin stimulated JNK activation) or 60 min (anisomycin, sorbitol). Ligand concentrations were 10 ng/mL (EGF and HGF), 20 ng/mL (HGF), 10 nM (thrombin), 10 μg/mL (anisomycin), 0.2 M (sorbitol) and 4% (serum). After stimulation, cells were fixed for 14 min in 3% paraformaldehyde/sucrose, washed and permeabilized with 0.2% Triton X-100 for 7 min. Cells were blocked in goat serum and stained overnight with either monoclonal phospho-ERK1/2 antibody (Cell Signaling, clone 197G2), polyclonal phospho-JNK antibody (Cell Signaling) or monoclonal phospho-p38 (Cell Signaling, clone 12F8). After staining, wells were washed and incubated for 90 min with DAPI, AlexaFluor 647 conjugated wheat germ agglutinin and AlexaFluor488 anti-rabbit secondary antibodies. Wells were washed and subsequently imaged by epifluorescent imaging. Background subtraction, masking and quantitation of phospho-MAPK immunostaining was performed using the Slidebook software package (3i).

Real time PCR of siRNA transfected HeLa cells in screening conditions

Cells were transfected in 96 well glass bottom plates under screening conditions. For each siRNA, 5 wells of siRNA transfected cells were lysed and pooled and total RNA was extracted from the cell lines using an RNeasy mini kit (Qiagen). 1 μg of total RNA was reverse transcribed using the High Capacity cDNA Reverse Transcription kit (Applied Biosystems). Resulting cDNAs were diluted and Realtime PCR was performed with inventoried Taqman gene expression assays (Applied Biosystems) on a Applied Biosystems 7500 Fast real-time PCR system using the standard 3 step denaturing,

annealing and elongation process. Results for all targets were normalized using human β-actin message as a calibrator.

Results

Screening Method to Identify MAPK Activation by MAP3Ks

Stimulus evoked MAPK pathway activation is mediated through activation of upstream MAP3Ks. However, to date, the involvement of MAP3Ks in MAPK pathway activation has been poorly studied. To identify MAP3Ks that regulate the MAPK network, we designed a 96 well siRNA based screening approach that enables the rapid discovery of MAP3Ks regulating ERK1/2, JNK and p38 signaling in cell culture. This screening approach utilized immunofluorescent staining of activated MAPKs by phospho specific antibodies to enable detection of changes in MAPK signaling. Specifically, individual MAP3K siRNA pools were reverse transfected into a HeLa cell line that stably expressed the PAR1 receptor, to enable the stimulation of cells with thrombin, and JNK1α1 to enhance the very modest JNK activation seen in wild type cells. Twenty four hours after transfection, the cells were serum starved for 24 hours and stimulated, fixed, and stained for MAPK activation using phosphorylation specific antibodies for either ERK1/2, JNK or p38. Cells were counterstained to detect the nucleus and whole cell volume to identify and mask the nucleus, whole cell volume and the cytoplasm (by subtraction of the nuclear mask from the whole cell mask) (Figure 2.1A). Images were background subtracted and MAPK activation was quantified in the masked regions by measuring the average phospho-MAPK staining intensity within the mask.

Using these methods, activation of all three MAPKs could be determined in response to a stimulus. Interestingly, measurement of all three MAPK responses to a stimulus (e.g. anisomycin) demonstrated differing kinetics and magnitude of activation between the three pathways, indicating that phosphorylation specific ERK1/2, JNK and p38 antibodies do not cross-react with other MAPK species (Figure 2.1B). Furthermore, the relative activation of each MAPK was different in each subcellular location. ERK1/2 and p38 activation changes were most pronounced in the nucleus and either modestly reduced in the cytoplasm (ERK1/2) or greatly reduced in the cytoplasm (p38). JNK activation by contrast was most pronounced in the cytoplasm and decreased in the nucleus. The differing kinetics, location and strength of activation of individual MAPKs was observed in response to multiple stimuli and demonstrated specificity in detecting the activation of individual MAPKs. MAPK activation detected by phospho-specific MAPK immunofluorescence showed similar kinetics of activation as was seen by western blot with phospho-specific antibodies, further indicating the specificity of the immunofluorescent approach (Figure 2.1C). The slightly more sustained activation of ERK1/2 seen in the immunofluorescent staining at 10 minutes is likely due to the improved time resolution in immunofluorescence experiments because of the rapidity of fixing cells relative to the detergent based lysis used for western blotting. While fold changes observed with phospho-specific immunofluorescence were more modest than observed by western blot this is likely due to increased signal to noise ratio in western blot because the proteins are separated by size, minimizing the detection of other proteins bound non-specifically by the antibody. Furthermore, stimulation induced ERK1/2

activation by immunofluorescence could be readily blocked by pretreating the cells with the MEK1/2 inhibitor U0126 (Figure 2.1C, bottom panel).

Our screening approach was predicated on successful knockdown of our target MAP3Ks with siRNA. Thus we sought to determine our siRNA transfection efficiency under screening conditions.. Using an optimized transfection protocol, siRNA transfection efficiency was determined by transfecting the JNK1α1 containing HeLa screening line with JNK1 siRNA and using immunofluorescence to monitor the knockdown of the stably expressed HA tagged JNK1α1 isoform. Using our transfection conditions, we were able to knockdown stably expressed JNK1α1 in substantially all cells (Figure 2.1D). A set of siRNA pools targeting 11 MAP3Ks was used for screening. Real time PCR verified the knockdown obtained by these siRNA pools under screening conditions (Figure 2.1E). We found that with the exception of MEKK3, MEKK4, Tpl2 and B-Raf, all siRNA pools inhibited their target MAP3Ks to greater then 80% at the RNA level. By contrast, knockdown of MEKK3, MEKK4 and B-Raf were all greater then 60% (67%, 75% and 65% respectively) while Tpl2 knockdown had a modest effect, knocking down Tpl2 ~40% at the RNA level. These siRNAs were used to probe the changes in ERK1/2, JNK and p38 signaling in response to three groups of stimuli consisting of either growth factors (EGF, HGF, Thrombin and serum), cell stresses (anisomycin and hyperosmolar sorbitol) or cytokines (TNFα).

Growth Factor Induced ERK1/2 and JNK activation

Stimulation of cells with growth factors (EGF, HGF, Thrombin and serum) rapidly induced activation of ERK1/2 and JNK in all cases except for serum that induced

only minor JNK activation. However, none of the growth factors induced detectable levels of p38 phosphorylation by immunofluorescence. This was corroborated in western blots, where p38 phosphorylation was very modest and likely below the detectable threshold for immunofluorescence (data not shown). Knockdown of Tpl2 inhibited ERK1/2 activation by multiple growth factors, demonstrating that Tpl2 was required for maximal activation of ERK1/2 by growth factors (Figure 2.2A-C, left panels). While the effects of Tpl2 on ERK1/2 activation were relatively modest (only about 20-40% of the stimulated ERK1/2 activation was lost), Tpl2 siRNA achieved only 40% knockdown indicating that more complete Tpl2 knockdown would likely have a stronger effect on ERK1/2 signaling (Figure 2.1E and 2.2A-C, left panel). Our finding that Tpl2 is required for thrombin induced ERK1/2 activity was corroborated in $Tpl2^{-/-}$ MEFs (25). c-Raf knockdown also modestly diminished ERK1/2 signaling by EGF and HGF consistent with the published role of c-Raf in ERK1/2 activation, while thrombin stimulation of ERK1/2 activation did not require c-Raf (136). Interestingly, ERK1/2 activation by serum required MEKK2, a kinase without a known role in ERK1/2 activation (Figure 2.2D). Screening also identified several MAP3Ks that were negative regulators of ERK1/2 activation by growth factors. Knockdown of the MAP3Ks MEKK1 and MEKK4 resulted in increased ERK1/2 signaling in response to HGF, thrombin and serum (Figure 2.2A-D). Interestingly, MEKK1 and MEKK4 knockdown in EGF stimulated cells also showed a trend towards increased ERK1/2 activation, although the change was not statistically significant. These results indicate that MEKK1 and MEKK4 are negative regulators of ERK1/2 signaling.

Growth factor dependent JNK activation showed similar dependence on a small number of genes. Knockdown of MEKK2 inhibited JNK activation by EGF, HGF and thrombin. In all three cases, stimulus dependent JNK activation was inhibited by 70-80% by MEKK2 knockdown while knockdown of other MAP3Ks had little effect on JNK activation (Figure 2.2A-D right panel). These results demonstrate that MEKK2 regulates JNK activation by multiple growth factors in HeLa cells. Consistent with our findings in HeLa cells, a role for MEKK2 in growth factor mediated JNK activation has been demonstrated in fibroblasts stimulated with FGF-2 as well (108). We also identified MEKK1, TAK1 and B-Raf as negative regulators of EGF induced JNK signaling, TAK1 and MLK3 as negative regulators of HGF induced JNK signaling and ASK1 and Tpl2 as negative regulators of thrombin induced JNK signaling.

Cell Stress Stimulated JNK and p38 activation

Cell stress induced by either protein synthesis inhibition with anisomycin or hyperosmolar stress induced with hyperosmolar sorbitol caused robust activation of JNK and p38, while ERK1/2 activation was more difficult to detect. Using MAP3K siRNAs, we found that MLK7 was a major regulator of anisomycin and hyperosmolar sorbitol induced JNK and p38 activation, with MLK7 knockdown blocking between 85-95% of stimulated p38 and JNK activation depending on the stimulus and MAPK (Figure 2.3A and B). This is consistent with findings in MEFs demonstrating that MLK7 controls JNK and p38 activation by anisomycin and p38 activation by hyperosmolar NaCl (24). However, contrary to earlier findings indicating that hyperosmolar JNK activation is MLK7 independent, we found that hyperosmolar JNK activation was MLK7 dependent.

Knockdown of MLK3 demonstrated that MLK3 has modest effects on p38 activation by anisomycin and sorbitol (reducing p38 activation by ~25%), while MLK3 knockdown had modest to no effect on JNK activation (Figure 2.3A and B). These results demonstrate that stress induced MLK3 activation preferentially controls p38 phosphorylation rather then JNK phosphorylation. We also found that TAK1 knockdown partially inhibited p38 activation by anisomycin but had no effect on sorbitol induced p38 activation, indicating that multiple kinases are required for full activation of p38 by anisomycin. We identified several MAP3Ks that enhanced JNK and p38 activation when knocked down by siRNA. MEKK1 and MEKK4 knockdown enhanced p38 signaling by cell stress stimuli. We also found that c-Raf knockdown increased JNK activation by anisomycin while Tpl2 and TAK1 knockdown enhanced JNK activation by sorbitol. The identification of two kinases, Tpl2 and c-Raf, that were identified as major regulators of growth factor induced ERK1/2 activation, implied that crosstalk between ERK1/2 and JNK signaling could regulate JNK activation by stress stimuli.

TNFα Stimulated JNK and p38 Activation

Stimulation of cells with the cytokine TNFα induced rapid JNK and p38 activation, but ERK1/2 activation by TNFα was below the threshold of detection. To date, identification of the MAP3K(s) responsible for TNFα induced JNK and p38 activation have been contentious. Previous work has identified no less then five MAP3Ks that control TNFα induced JNK and/or p38, including MEKK3, ASK1, TAK1, Tpl2 and MLK3 (26-29,93). Our screen found that only TAK1 regulated JNK and p38 activation by TNFα in HeLa cells while MEKK3, ASK1 and MLK3 knockdown had no

effect on TNFα induced JNK and p38 or, in the case of MEKK3 knockdown, enhanced TNFα stimulated JNK activation (Figure 2.4). Thus our results corroborate earlier findings demonstrating a role for TAK1 in TNFα stimulated JNK and p38 activation that is independent of MEKK3, ASK1 and MLK3. While MEKK3, ASK1 and MLK3 do not appear to be involved in TNFα stimulated JNK and p38 activation in HeLa cells, it is possible that they contribute to TNFα stimulated JNK and p38 activation in other cell types. Interestingly, TAK1 knockdown only inhibited TNFα stimulated JNK and p38 activation by ~55% and ~45% respectively despite ~90% knockdown of TAK1 at the RNA level. It is possible that another, as of yet uncharacterized, MAP3K participates in this pathway. However, the partial loss of JNK and p38 signaling in TAK1 knockdowns may also be due to less robust knockdown of TAK1 at the protein level relative to RNA or that the remaining pool of TAK1 protein is highly processive in activating JNK and p38. Additionally, we also identify MEKK1 as a negative regulator of JNK and p38 activation by TNFα.

Discussion

The MAPK network is composed of a large group of kinases that signal in response to diverse stimuli including cytokines, growth factors, cell stresses, DNA damage, heat and cold. Response to these diverse stimuli is coordinated by MAP3Ks which behave as signaling nodes, integrating incoming cellular signals and relaying them to the terminal MAPKs that coordinate cellular responses to the stimuli. While downstream MAPKs have been extensively studied in cellular response to stimuli, the critical upstream MAP3Ks that regulate MAPK induction are frequently unknown, or

contentious. By more completely understanding the MAPK network, we will be better able to target the MAPK network to selectively regulate cellular responses. To identify the MAP3Ks that control MAPK activation in response to an array of stimuli, we designed an immunofluorescence based screening approach that enables the rapid detection of stimulus induced ERK1/2, JNK and p38 activation. In comparison to previous screens, our screen allows for the direct detection of MAPK activity rather then detection of downstream outcomes such as c-Jun phosphorylation by JNK or MAPKAPK2 nuclear translocation for p38 (137). Direct observation of MAPK phosphorylation enables the specific quantification of changes in MAPK signaling and also eliminates potential complicating effects of measuring downstream effectors such as changes in their stability or expression (e.g. c-Jun transcriptional regulation by other MAPK families). This screening approach is amenable to larger scale screening efforts as well. Indeed, two screens using similar approaches in Drosophila cells were performed to identify genome wide regulators of ERK1/2 and JNK signaling in response to a small group of stimuli (138,139).

For many stimuli, the MAP3Ks that control MAPK activation are either unknown or contentious. Using our screening method we screened a group of 11 MAP3Ks for their roles in growth factor, cell stress and cytokine induced ERK1/2, JNK and p38 signaling. We were able to identify known positive regulators of growth factor, cytokine and cell stress induced ERK1/2, JNK and p38, including identifying the requirement of c-Raf for EGF and HGF induced ERK1/2, TAK1 as a positive regulator of TNFα stimulated JNK and p38 signaling and the role of MLK7 in anisomycin stimulated JNK and p38 and sorbitol stimulated p38 (28,136,140). We were also able to discover novel

positive regulators of growth factor and cell stress induced ERK1/2, JNK and p38 signaling. We identified Tpl2 and MEKK2 as positive regulators of growth factor induced ERK1/2 and JNK. MLK3 and TAK1 as positive regulators of anisomycin stimulated p38 and MLK3 as a positive regulator of sorbitol induced p38.

To date, most research on growth factor induced ERK1/2 activation has centered on the Raf family of proteins. However, multiple MAP3Ks outside of the Raf family activate ERK1/2. While we do identify c-Raf as a positive regulator of ERK1/2 activation by EGF and HGF, we also find that ERK1/2 activation by growth factors requires Tpl2. These results demonstrate that MAP3Ks outside of canonical Raf family members are required for ERK1/2 activation by growth factors. Interestingly Raf was required for ERK1/2 activation by EGF and HGF, both of which signal through receptor tyrosine kinases. However, thrombin signaling mediated through the G-protein coupled receptor (GPCR) PAR1 did not require c-Raf for maximal ERK1/2 activation. Therefore, c-Raf appears to selectively control tyrosine kinase ERK1/2 activation but not GPCR mediated ERK1/2 activation. Thus, contrary to the established roles of Raf family members in ERK1/2 activation, targeting of Tpl2 may be a better method to selectively inhibit ERK1/2 activation in response to a wide array of stimuli. We also identified a role for MEKK2 in regulating growth factor induced JNK activation. JNK activation by growth factors has been implicated in many of the physiological outcomes of growth factor stimulation, such as cell proliferation, migration, secretion of growth factors and proteases and survival (108,141-144). Thus our results indicate that MEKK2, through JNK activation, likely regulates many of the physiological outcomes of growth factor stimulation.

Previous work has suggested that MAP3Ks can also negatively regulate activation of other MAPK pathways. However, no studies have been undertaken to systematically identify MAP3Ks that behave as negative regulators. Using our screening method, we were able to identify MAP3Ks that negatively regulate MAPK activation as well. The negative effects of these MAP3Ks may proceed through many mechanisms including MAPK crosstalk, effects on receptors and MAP3K heterodimer formation. Several of the MAP3Ks identified as negative regulators in our screen may fit into these categories. For instance, enhanced thrombin stimulated JNK signaling in Tpl2 knockdown cells may be due to diminished ERK1/2 signaling in these cells and loss of ERK1/2 negative feedback of JNK activation. Enhanced JNK signaling in EGF stimulated TAK1 knockdown cell lines is consistent with findings demonstrating that TAK1 can inhibit EGFR signaling through p38 dependent EGFR internalization (145). Increased JNK signaling seen in HGF stimulated TAK1 knockdown cells may be due to similar mechanisms, with TAK1 induced p38 mediating internalization of the HGF receptor c-Met. By contrast, enhanced JNK activation in TNFα stimulated MEKK3 siRNA treated cells may be due to complex formation between MEKK3 and TAK1. Unphosphorylated MEKK3 and TAK1 have been demonstrated to form a complex, thus knockdown of MEKK3 may block formation of the inhibitory complex and promote JNK activation through increased TAK1 activity (31). We also identified MEKK1 as a negative regulator of ERK1/2 activation by growth factors. Enhanced ERK1/2 signaling in MEKK1 siRNA treated cells is consistent with findings demonstrating that MEKK1 can promote ERK1/2 turnover through its RING domain (146). Thus MAPK signaling networks are highly dynamic and knockdown of

seemingly unrelated MAP3Ks can perturb signaling responses through diverse interactions within the MAPK network.

MAPK signaling and its physiological outcomes are important to many diseases including cancer, neurological disease and chronic inflammation. These MAPK networks control cellular responses to many stimuli, with magnitude, duration, and location of MAPK signaling as well as cell type and cell environment controlling the physiological outcome of MAPK signaling. Thus targeting of pathogenic MAPK signaling requires a high degree of selectivity in targeting the pathogenic MAPK signaling in affected cell type(s). Identification of MAP3Ks that are positive and negative regulators of induced MAPK signals and the targeting of these MAP3Ks with small molecules will enable us to selectively block pathogenic MAPK signals and enable the development of novel therapeutics for diseases in which MAPK signaling is dysregulated.

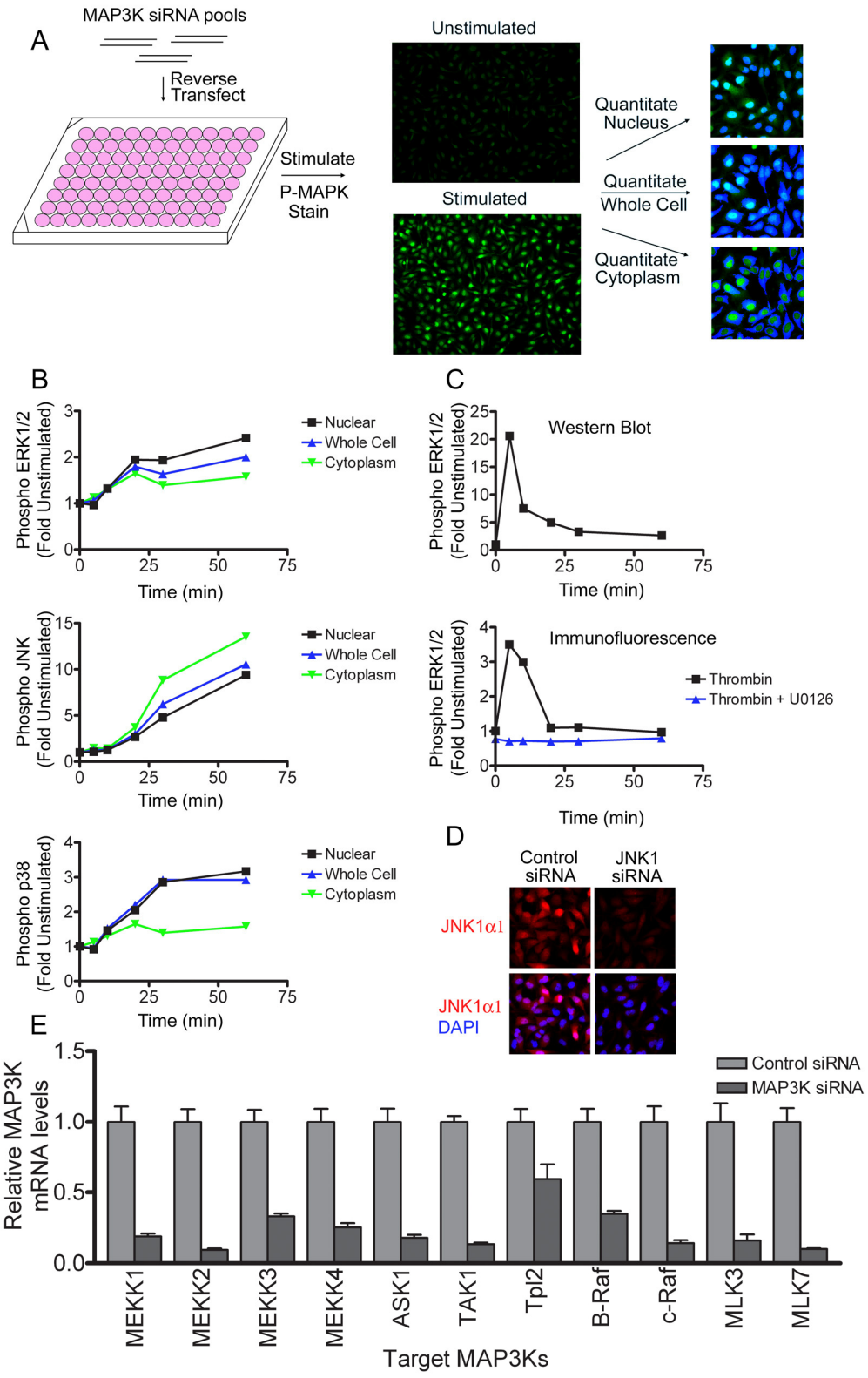

Figure 2.1. Design of a High Throughput MAPK Activation screen for MAP3K Screening. A) Scheme demonstrating the work flow of the MAPK screen. B)

Phospho-MAPK activation by anisomycin (10 μg/mL) for ERK1/2, JNK and p38 activation in all three cellular locations showing distinct kinetics and magnitude of activation by all three MAPKs. C) Comparison of ERK1/2 activation by 10 nM Thrombin detected by phospho-ERK1/2 detection by western blot (top panel) or immunofluorescence (bottom panel). Pretreatment of cells with 10 μM U0126 inhibited ERK1/2 activation detected by immunofluorescence (bottom panel). D) Transfection of HeLa cell lines under screening conditions with siRNA. HeLa cells under screening conditions were transfected with JNK1 siRNA pool targeting stability expressed HA JNK1α1. Knockdown of JNK1α1 was detected by anti-HA immunofluorescence, demonstrating near complete loss of HA staining in JNK1 siRNA transfected cells. E) Knockdown of MAP3Ks under screening conditions with MAP3K siRNAs. HeLa cells were transfected under screening conditions with siRNAs against MAP3Ks. MAP3K knockdown was detected by real time PCR of MAP3K message and normalized to control message, demonstrating knockdown of all 11 MAP3Ks screened with this assay.

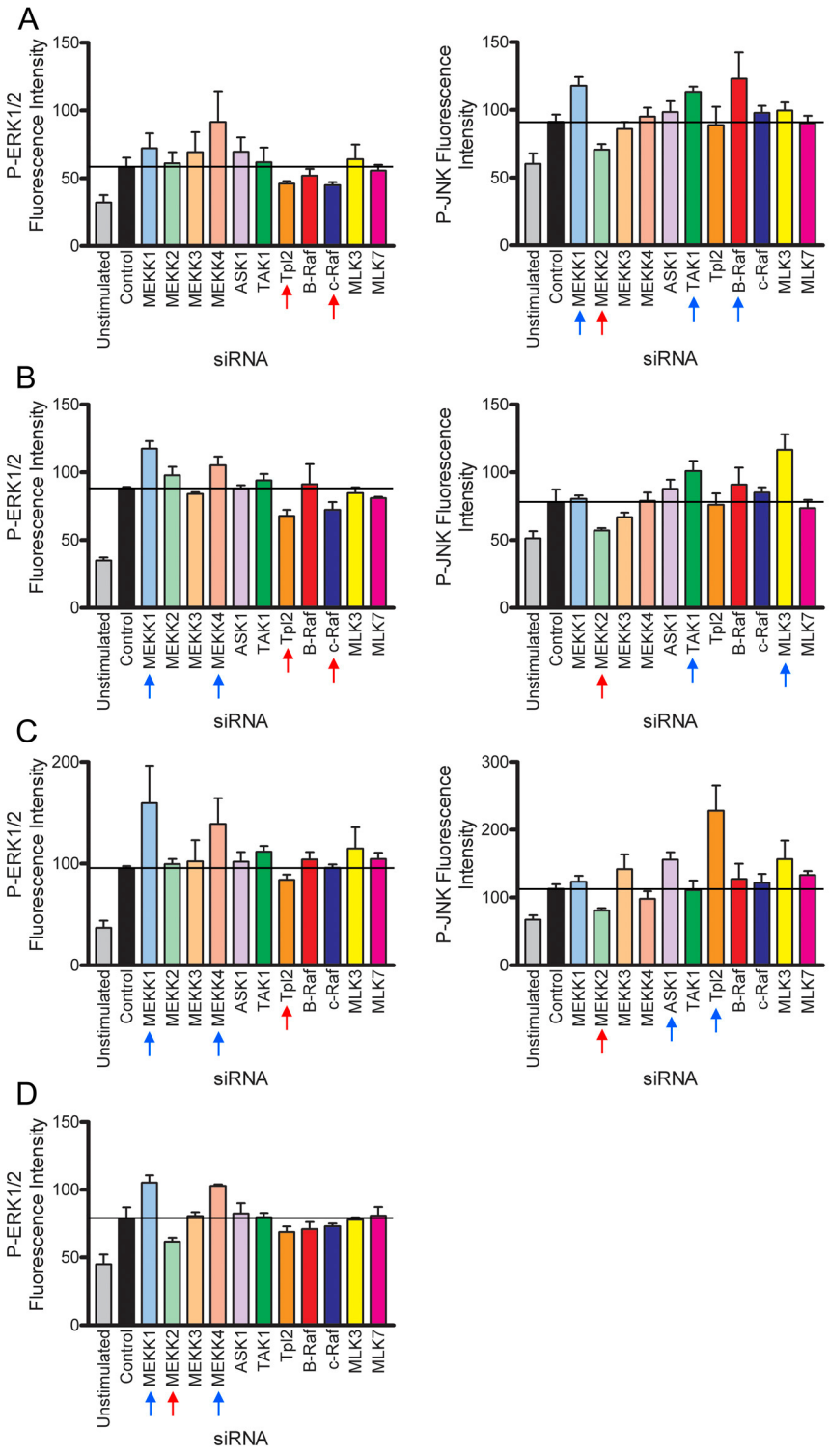

Figure 2.2. Tpl2 and MEKK2 regulate ERK1/2 and JNK activation by growth factors. HeLa cells were transfected with MAP3K siRNAs in triplicate, stimulated with either A) 10 ng/mL EGF for 20 min, B) 20 ng/mL HGF for 20 min, C) 10 nM Thrombin for 5 min (ERK1/2) or 20 min (JNK) or D) 4% serum 10 min, fixed and immunostained

for phospho-ERK1/2 (left panels) or phospho-JNK (right panels). Average nuclear fluorescence was determined for each MAP3K siRNA line and is graphed as mean ± standard deviation. MAP3K siRNAs that caused a statistically significant increase in MAPK activation (as indicated by two-tailed t-tests against control cells) are indicated by blue arrows and MAP3K siRNAs that caused a statistically significant decrease in MAPK activation are indicated by red arrows.

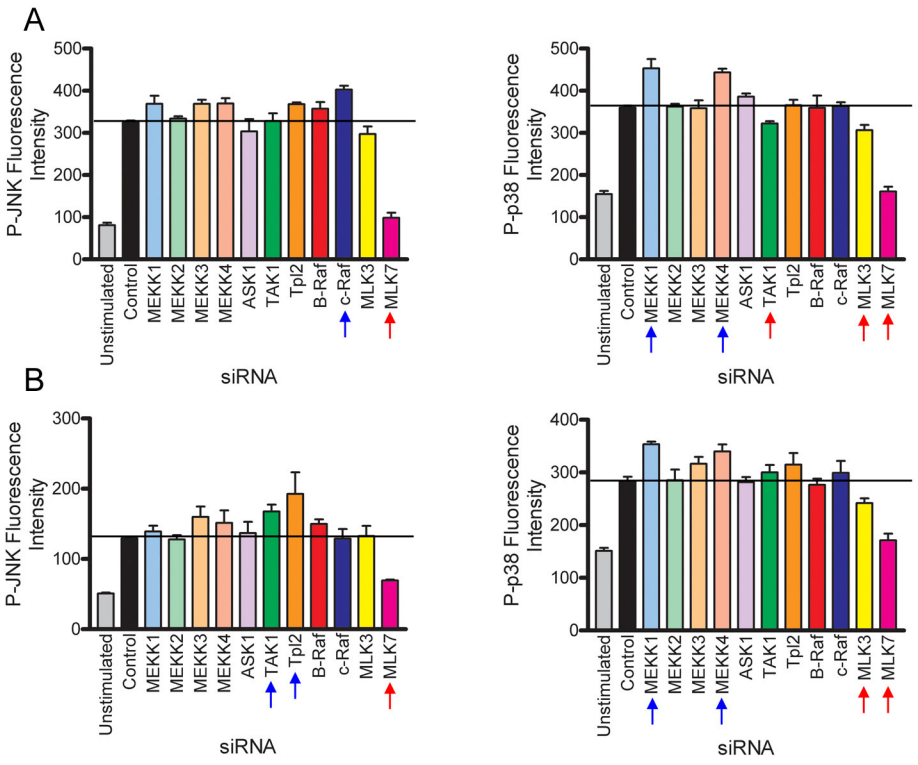

Figure 2.3. MLK3 and MLK7 regulate stress induced JNK and p38 activation. HeLa cells were transfected with MAP3K siRNAs in triplicate, stimulated with either A) 10 μg/mL anisomycin for 60 min or B) 0.2 M sorbitol for 60 min, fixed and immunostained for phospho-JNK (left panels) or phospho-p38 (right panels). Average nuclear fluorescence was determined for each MAP3K siRNA line and is graphed as mean ± standard deviation. MAP3K siRNAs that caused a statistically significant increase in MAPK activation (as indicated by two-tailed t-tests against control cells) are indicated by blue arrows and MAP3K siRNAs that caused a statistically significant decrease in MAPK activation are indicated by red arrows.

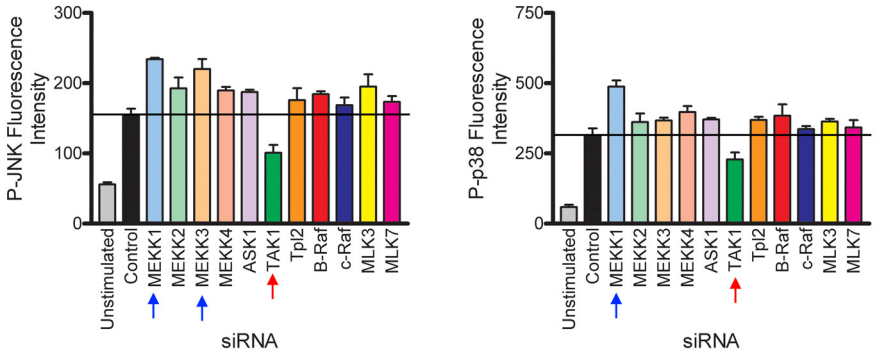

Figure 2.4. TAK1 regulates TNFα induced JNK and p38 activation. HeLa cells were transfected with MAP3K siRNAs in triplicate, stimulated with 10 ng/mL TNFα for 20 min, fixed and immunostained for phospho-JNK (left panels) or phospho-p38 (right panels). Average nuclear fluorescence was determined for each MAP3K siRNA line and is graphed as mean ± standard deviation. MAP3K siRNAs that caused a statistically significant increase in MAPK activation (as indicated by two-tailed t-tests against control cells) are indicated by blue arrows and MAP3K siRNAs that caused a statistically significant decrease in MAPK activation are indicated by red arrows.

III. In Vivo RNAi Screen Defines a Cooperative MAP3Kinase Network Controlling Tumor Growth and Metastasis

Introduction

Within the defined MAPK network there are approximately 50 kinases comprising almost 10% of the human kinome. Thus, it is not surprising that members of the MAPK signaling network are frequently amplified, overexpressed and activated in breast cancer. For example, components of the MAPK network are overrepresented in genomic and proteomic analysis of genes amplified and overexpressed in metaplastic breast cancer (147). In addition, high levels of phosphorylated JNK and p38 correlate with highly invasive, poor prognosis breast cancers (99). Phosphorylated p38 has also been proposed as a prognostic marker for patients with breast cancer pleural effusions, and proved to be a much more statistically significant marker for disease outcome in patients with pleural effusions than phosphorylated ERK1/2 (99). Twenty per cent of breast cancer patients have ERK5 overexpression, which correlates with shortened disease-free survival times (110). ERK5 is also overexpressed in squamous cell carcinoma correlating with metastasis of the disease, and is amplified in hepatocellular carcinoma (148,149). The MAPK network is dysregulated upstream of the MAPKs as well. The MAP3K Tpl2, which activates ERK1/2 and JNK, has been shown to be amplified and overexpressed in 40% of human breast cancers (150). Activating mutations of B-Raf are found in ~7% of all tumors and about 60% of melanomas,

resulting in constitutive activation of ERK1/2 (111). In these tumors, activating B-Raf mutations correlate with poor survival, recurrence and resistance to chemotherapy (36,151,152). Despite the overwhelming evidence from the analysis of patient tumor samples that the MAPK signaling network is significantly dysregulated in cancer, there is little definitive understanding of the actual in vivo function of the MAPK signaling network in regulating tumor growth and metastasis. The exception is activated B-Raf that constitutively activates MKK1/2 leading to ERK1/2 activation and increased cell proliferation (111). It could be argued that the focus on activation of ERK1/2-dependent cell proliferation by mutant B-Raf has in some ways hindered the conceptual understanding of the behavior of the MAPK signaling network in cancer. The control of the MAPK signaling network by MAP3Ks other than the Raf family is never restricted to a single MAPK pathway. Most MAP3Ks regulate at least two different MAPKs such as JNK and p38 (e.g., MLK3), ERK5 and JNK (e.g., MEKK2) or p38 and ERK5 (e.g., MEKK3) (21). Also, unlike the model of the B-Raf-MKK1/2-ERK1/2 pathway, all MAPK pathways are activated by multiple MAP3Ks. Beyond B-Raf, MAP3Ks including c-Raf, Tpl2 and MEKK1 have been shown to regulate ERK1/2 activity in genetically engineered mouse models and by RNAi (26,136,153). Thus the MAPK signaling network should be viewed not simply as multiple pathways but as a cooperative network involving many MAP3Ks that dynamically integrate different cellular stimuli to coordinately activate ERK1/2, JNK, p38 and ERK5 (21). Attempts to target these cooperative MAPK signaling networks with drugs inhibiting MAPK activation have failed due to toxicity and lack of efficacy. The difficulties in targeting MAPK directly are likely due to the physiological importance of MAPKs and because signaling by

individual MAPKs has been demonstrated to be oncogenic or tumor suppressive depending on cellular context. By contrast, selective targeting of MAP3Ks within the MAPK signaling network may allow for the selective targeting of oncogenic versus tumor suppressive MAPK signaling and bypass of toxicity effects due to greater selectivity.

Our goal was to develop a practical and reasonably rapid *in vivo* assay to define functional roles of the MAP3K signaling network in tumor growth and metastasis. By necessity, this required *in vivo* tumor models because *in vitro* cell culture systems have limited ability to predict *in vivo* effects on tumor growth and metastasis. The claudin-low MDA-MB-231 breast adenomacarcinoma cell line was used for these studies because of its high metastatic potential in orthotopic breast xenografts (154). We utilized stable shRNA knockdown of nine MAP3Ks as well as ERK5 to define the properties of the MAPK signaling network in the control of tumor cell growth and metastasis. The *in vivo* assay proved successful in demonstrating that the MAP3Ks function in a cooperative manner to control both tumor growth and metastasis. The findings demonstrate the utility of *in vivo* screens of previously untargeted or poorly characterized protein kinases in discovering new cancer relevant regulatory networks and potential new targets for cancer therapy.

Methods

Reagents and Cell culture

Recombinant TGF-β1 and EGF were purchased from peprotech. U0126, SP600125, SB203580, Dasatinib and Lapatinib were purchased from LC Labs. Other chemicals

were purchased from Sigma unless noted. Cell culture media was purchased from Sigma and Invitrogen. BT474 and HEK293 cells were from ATCC. MDA-MB-231 cells were from Patrick Casey's lab (Duke University). For bioluminescent imaging, cells were transfected with retroviruses containing the luciferase gene and selected on 800 μg/mL G418. MDA-MB-231 cells were maintained in DMEM/10% FBS with 100 units/mL of penicillin and streptomycin. BT474 cells were maintained in DMEM:F12 (1:1) containing 10% FBS and 100 units/mL of penicillin and streptomycin.

Knockdown of MAP3Ks in cell lines

shRNA constructs from the Open Biosystems TRCN collection were cotransfected into HEK293 cells along with pMD2.G and psPAX2 (Addgene, Addgene plasmid 12259 and 12260, originally from Trono lab) to produce lentiviral shRNA particles. Lentiviruses containing shRNAs were infected into target cells, and 3 days post infection, cells positive for shRNA expression were selected with 2 μg/mL puromycin (Clontech). Individual TRCN clone numbers used for mouse injection experiments are indicated in Figure S1.

Tumor Xenografts

Mouse experiments were performed in accordance with the UNC Institutional Care and Use Committee (IACUC) and national guidelines. shRNA knockdown of target proteins was confirmed in all cell lines before injection into mice. Cell lines were split immediately prior to injection to ensure that cell lines were healthy and actively growing. Tumor xenografts were established by injecting either 2 x 10^6 MDA-MB-231 cells or 4 x 10^6 BT474 cells in a 50:50 mix of SFM:matrigel into the inguinal fat pad or flank of 8 week old SCID mice as indicated. For BT474 cells estrogen pellets were implanted in

the mice to facilitate growth. Estrogen pellets were made as in (155). Tumor size was measured by either calipers or ultrasound imaging using a Vevo 770 (Visualsonics) every week from week four on. Tumor length and width were converted to tumor volume using the equation Volume = Length x ($Width^2/2$). Metastasis was measured by injecting mice intraperitoneally with 100 μL of luciferin (50 mg/mL, Gold Biosciences) and imaging the mice using a Xenogen IVIS 100 (Caliper Lifesciences). Photon flux from bioluminescent images was quantitated by drawing a region of interest around the tumor and quantitating photons using Living Image software (Caliper Lifesciences). Depending on tumor burden, mice were sacrificed at 7 or 8 weeks post injection (MDA-MB-231 cells) or 12 weeks post injection (BT474 cells) and the primary tumor and lymph node metastases were removed. Primary tumors were fixed in 4% paraformaldehyde/sucrose for subsequent histology studies and metastases were placed in RNAlater (Qiagen) and frozen for subsequent extraction of RNA.

Cell Viability Assays

For each shRNA/condition 1 x 10^3 MDA-231 cells were plated in quadruplicate in five 96 well plates. Cells were allowed to adhere overnight. If cells were treated with drugs, drugs were added 18 hours after plating. On each day, one 96 well plate was assayed using CellTiter-Glo assay reagents (Promega) according to the manufacturer's protocol. Briefly, resuspended CellTiter-Glo reagent was added 1:1 to each well, plate was rocked and luminescence was measured on a Pherastar microplate reader (BMG Labtech). All luminescent readings were normalized to day 0 luminescent measurements.

Western Blotting

Media was removed and cells were washed once with 1 x ice cold PBS. Cells were lysed by adding lysis buffer to the cells (1% Triton X-100, 150 mM NaCl, 10 mM Tris pH 7.5) supplemented with complete protease inhibitors (Roche), PMSF, $NaVO_4$ and NaF. Insoluble debris were removed from the lysate by centrifugation and the protein concentration of the resulting lysates was quantified using Bradford reagent. Equal quantities of protein were separated on polyacrylamide gels, transferred to nitrocellulose and were probed with antibodies as noted. Antibodies against MEKK1, B-raf, c-raf and Tpl2 were from Santa Cruz Biotech. The antibody against MEKK2 has been previously published (108). The MEKK3 antibody was from BD Transduction labs. The TAK1, Src family phospho-Y416, EGFR phospho-Y1068 (clone D7A5), phospho-ERK1/2, phospho-JNK1/2 and phospho-p38 antibodies were from Cell Signaling. The ERK5, γ-Tubulin (GTU-88) and actin (AC-40) antibodies were from Sigma.

Realtime PCR of cell line RNA

Total RNA from cell lines was extracted using an RNeasy kit (Qiagen). 3μg total RNA was reverse transcribed using the High Capacity cDNA Reverse Transcription kit (Applied Biosystems). Resulting cDNAs were diluted and Realtime PCR was performed with inventoried Taqman gene expression assays (Applied Biosystems) on a Applied Biosystems 7500 Fast real-time PCR system using the standard 3 step denaturing, annealing and elongation process. Results for all targets were normalized using human β-actin message as a calibrator.

Immunofluorescent Staining of Tissue Sections

Tumors were removed from animals and fixed overnight in 4% paraformaldehyde/sucrose. After fixing, tumors were equilibrated in sucrose, frozen in OCT and 10 μM tissue sections were cut using a microtome. Sections were permeabilized with 0.2% Triton X-100, blocked in 10% goat serum and stained with antibodies against F4/80 (clone BM8, Santa Cruz Biotechnology) for 1 hr. Primary antibodies were detected using biotinylated secondary antibodies and Cy3 streptavidin (Jackson Immunoresearch).

Immunofluorescent Analysis of Cells

MDA-MB-231 cells were plated in 96 well imaging plates (Grenier) and serum starved overnight. After overnight starvation, cells were fixed with 3% paraformaldehyde/sucrose, permeablized with 0.2% Triton X-100 and blocked with 10% goat serum. After blocking, cells were incubated overnight with phospho-ERK1/2 antibodies (clone D13.D14.4E, Cell Signaling). Cells were washed and incubated with Alexa 555 secondary (Invitrogen), DAPI and Alexa 488-phalloidin (Invitrogen) for 1 hr. Cells were imaged using a 20x objective on a BD Pathway microscope.

Analysis of Secreted Proteins

8×10^4 MDA-MB-231 cells were plated in 6 well plates and allowed to attach overnight. After attachment, media was changed to serum free DMEM and cells were incubated for 3 days. Media was removed and spun to remove cellular debris and frozen at -80°C. Supernatant samples were sent to Rules Based Medicine (Austin, TX) for multiplex cytokine analysis using the HumanMAP array.

Real time PCR of lymph nodes for presence of tumor cells and MAP3K knockdown

Total RNA was isolated from RNALater-stabilized murine lymph nodes using the Micro RNeasy Kit (Qiagen). cDNA from each knockdown (lymph nodes containing MAP3K shRNA MDA-MB-231 cells) and its corresponding control samples (lymph nodes containing control MDA-MB-231) were generated using the High Capacity Reverse Transcription Kit (Applied Biosystems). Real-time quantitative PCR was done in triplicate for each lymph node sample to determine message levels of the human MAP3K and B-actin. A standard curve was generated from the control samples by graphing the average threshold values (C_T) for the human MAP3K versus those for human b-actin. The corresponding knockdown samples were graphed similarly; continued knockdown of the MAP3K in the lymph nodes containing MAP3K shRNA MDA-MB-231 cells was indicated if these data points fell above the control lymph node standard curve. All TaqMan assays (Applied Biosystems) used in these experiments were determined empirically to detect only human and not murine cDNA.

Results

An *in vivo* Screen of MAP3K function in Tumor Growth and Metastasis

Previously, we have determined that expression of MEKK1 is required for efficient metastasis in an MMTV-PyMT transgene model of breast cancer through the ability of MEKK1 to control uPA activity (119). We sought a method by which we could determine the contribution of other MAP3Ks to tumor growth and metastasis in an unbiased way. Genetic models were not amenable to a screening approach as knockouts for a number of the MAP3Ks are embryonic lethal. Additionally, use of genetic mouse

models of cancer with MAP3K knockout mice does not allow the dissection of the contributions of MAP3K signaling in the stroma from those of MAP3K signaling in the tumor. To screen multiple MAP3Ks, it was necessary that the model be both amenable to genetic manipulation to ablate targeted MAP3Ks and enable us to directly observe the contributions of the MAP3K to tumor growth and metastasis. To these ends, an orthotopic xenograft model with injection of tumor cells into the inguinal fat pad was amenable to screening and resulted in tumors in their native milieu. Stable expression of MAP3K shRNAs from the RNAi consortium library enabled efficient silencing of target MAP3Ks in this model. For xenografts, we used MDA-MB-231 cells because, unlike many cell lines, they are readily metastatic *in vivo*. MDA-MB-231 cells carry B-Raf^{G464V}, Kras^{G13V} and have a mutationally inactivated p53 gene (88,156). Further, we stably expressed luciferase in our screening MDA-MB-231 line to enable *in vivo* tracking of the cells, thus allowing us to longitudinally track tumor growth by ultrasound imaging and spontaneous metastasis from the fat pad by bioluminescent imaging (Figure 3.1B).

To confirm the validity of our screening approach, we used shRNAs to knock down MEKK1 in our MDA-MB-231 screening line. We reasoned that we should observe a loss of metastasis, but no change in tumor growth in our xenografts, consistent with our previous observations in MMTV-PyMT mouse models. We injected the resulting cell lines into the inguinal fat pad of SCID mice. We found that while shRNA targeting MEKK1 blocked tumor metastasis, tumor growth was the same in tumors formed from either MEKK1 shRNA expressing cells or control cells (Figure 3.1C-E). These results indicate that our xenograft model could recapitulate the results of a genetically engineered mouse cancer model.

Having confirmed the veracity of our xenograft model for MEKK1, we sought to identify potential MAP3Ks to target in our screen. Using our screening cell lines we found that, consistent with previous findings, inhibitors of ERK1/2, JNK and p38 MAPKs all reduced cell growth *in vitro* (Figure 3.1F). Based on literature and our cell growth findings *in vitro*, we determined that it was important to target MAP3Ks that regulate all four MAPK pathways. To parse the contribution of each MAPK pathway to tumor outcome, we chose MAP3Ks that can signal through either ERK1/2 (B-Raf, c-Raf, Tpl2), JNK and p38 (TAK1, MLK3 and MLK7) or JNK and ERK5 (MEKK2) and p38 and ERK5 (MEKK3) (Figure 3.1A). For each target MAP3K, the cell lines containing the two shRNAs with the best knockdown of the MAP3K were injected into separate sets of mice and tumor growth and metastasis were compared against a control vector containing cell line to determine the effect of MAP3K knockdown (Figure 3.1B). For each MAP3K, the phenotypes of the two shRNAs were compared to determine the effect of knocking down the target MAP3K. Cases in which the two shRNAs had divergent effects were considered to be due to off-target effects of one of the shRNAs and as the true phenotype was ambiguous we considered knockdown of the MAP3K to have a discordant phenotype.

MAP3Ks Controlling ERK1/2 Signaling Regulate Tumor Growth but not Metastasis

Of the four MAPK families in humans, the ERK1/2 family is perhaps the pathway best linked to cancer. We screened three MAP3Ks that control the ERK1/2 pathway, B-Raf, c-Raf and Tpl2. While B-Raf and the constitutively activated B-Raf^{V600E} mutant

forms have been extensively characterized in melanoma tumor growth, we decided to study the role of B-Raf in our breast cancer model system for several reasons: i) the role of B-Raf in metastasis *in vivo* has not been well characterized; ii) while B-Raf^{V600E} has been studied in cancers such as melanoma and papillary thyroid carcinoma, less is known about B-Raf in breast cancer; iii) MDA-MB-231 cells express a rare B-Raf^{G464V} mutant rather then B-Raf^{V600E} in combination with a rare Kras^{G13V} mutation (156). Of the library shRNAs, the two best shRNAs resulted in 60% and 90% knockdown of B-Raf for shRNA 1 and shRNA 2 respectively (Figure 3.2A). We found that cell lines expressing B-Raf shRNAs developed tumors that were 20% and 15% of control tumor size respectively (Figures 3.3A and 3.3C). Diminished tumor size in B-Raf shRNA cell lines correlated with decreased growth of B-Raf knockdown lines *in vitro*. Since mutationally activated B-Raf regulates cell growth through constitutive ERK1/2 activation, we sought to determine whether B-Raf knockdown inhibited ERK1/2 activation in the background of KRAS mutation. Using B-Raf shRNA 1 and shRNA 2 cell lines, we were able to confirm that that B-Raf^{G464V} could promote ERK1/2 activation in the background of a KRAS^{G13V} mutation (Figure 3.3F-3.3H) by both western blot and immunofluorescence. Despite diminished ERK1/2 activation in culture and the greatly reduced tumor size in B-Raf knockdown tumors, we find that B-Raf knockdown tumors metastasize to the lymph node at near normal rates (Figures 3.3B and 3.3D). Lymph node metastases were removed and real time PCR was used to analyze knockdown of B-Raf in the lymph node. Real time PCR confirmed the continued knockdown of B-Raf in lymph node metastases (Figure 3.10A).

While c-Raf was originally cloned as the cellular homolog of oncogenic viral v-Raf, mutation of c-Raf is much less common than B-Raf and is not thought to be a major driver of tumors (112). Using shRNAs targeting c-Raf, we were able to knockdown c-Raf by 99% at the protein level with either shRNA 1 or shRNA 2 (Figure 3.2B). Subsequent mammary fat pad injection of these shRNA containing cell lines gave rise to tumors of discordant size. Cell lines containing c-Raf shRNA 1 gave rise to tumors that were roughly 30% control size while cell lines containing c-Raf shRNA 2 gave rise to tumors that were nearly identical in size to control cell lines (Figure 3.3I). As each shRNA had similar levels of knockdown, the phenotype was considered to be a discordant phenotype. While the shRNAs gave rise to tumors of different size, both shRNAs had wild type levels of metastasis indicating that c-Raf did not regulate tumor cell metastasis (Figure 3.3J).

Tpl2 targeting shRNAs gave knockdown of 91% and 96% for Tpl2 shRNA 1 and shRNA 2 respectively (Figure 3.2C). Relative to the p52 form of Tpl2, the p58 form proved to be somewhat refractory to shRNA. Cell lines expressing either Tpl2 shRNA 1 or shRNA2 both showed decreased tumor growth, giving rise to tumors that were 30% and 50% of control tumor size (Figures 3.3K and 3.3L). While truncated versions of Tpl2 have been shown to behave as oncogenes, this demonstrates that full length Tpl2 is necessary for efficient tumor growth *in vivo*. Metastasis data for Tpl2 was discordant, potentially indicating off target effects of one of the shRNAs, with shRNA 1 showing diminished metastasis and shRNA 2 showing control levels of metastasis despite similar levels of knockdown between the two shRNAs (Figure 3.3M). Real time PCR of the lymph node metastases demonstrated continued knockdown of Tpl2 in these metastases,

confirming that the differences in metastasis between cell lines were not due to selective loss of expression of one shRNA in metastatic cells (Figure 3.10C).

MAP3Ks targeting JNK and p38 Regulate Tumor Growth and Metastasis

While ERK1/2 signaling has been characterized extensively in tumor growth, the contributions of JNK and p38 signaling to tumor growth and metastasis have remained much more ambiguous. We targeted three MAP3Ks that activate JNK and p38 signaling, TAK1, MLK3 and MLK7. Using MLK3 shRNAs, we were able to knockdown MLK3 with two MLK3 shRNAs by 90% at the RNA level (Figure 3.2E). Both shRNAs markedly inhibited tumor growth as assessed by ultrasound volume measurements or final tumor weight (Figures 3.4A and 3.4C). Furthermore, both of these shRNAs strongly inhibited tumor metastasis (Figures 3.4B and 3.4E). Only a single mouse out of 14 mice injected with MLK3 shRNAs developed a lymph node metastasis, while 9 of 14 control mice were positive for metastasis. Real time PCR of the single lymph node metastasis from MLK3 shRNA expressing cells demonstrated that MLK3 was still knocked down in the lymph node metastasis, indicating that cells deficient for MLK3 can undergo low level metastasis (Figure 3.10E). The effects of MLK3 knockdown on tumor growth were recapitulated in a second experiment with either MLK3 shRNA 1 or a third shRNA against MLK3 showing an identical decrease in tumor growth and metastasis (Figure 3.5A and 3.5B).

The simplest explanation for diminished tumor growth in MLK3 knockdown tumors was decreased proliferation of MLK3 knockdown cell lines *in vitro*. We therefore measured cell growth of MLK3 knockdown cells *in vitro*. Cell growth assays

demonstrated that MLK3 knockdown resulted in decreased proliferation of MLK3 knockdown cells (Figure 3.4E). We sought to identify changes in signaling that may account for the loss of tumor growth and metastasis in MLK3 knockdown cell lines. Previous reports had determined that MLK3 was responsible for JNK phosphorylation in response to free fatty acids in MEFs (157). We reasoned that high local levels of free fatty acids in the mammary fat pad may signal through MLK3, contributing to the defects in tumor growth and metastasis observed in MLK3 deficient cell lines. We tested whether MLK3 is required for free fatty acid stimulated JNK in MDA-MB-231 cells by assessing JNK activation in control and MLK3 knockdown cells treated with palmitate. In agreement with studies in mouse embryonic fibroblasts, we found that MLK3 knockdown abrogated JNK activation by palmitate (Figure 3.4F). To test whether the milieu of the fat pad was affecting MLK3 tumor growth and metastasis, we assayed MLK3 shRNA cell line growth and metastasis in the flank rather then the fat pad. We injected control cells and three cell lines each expressing a different shRNA against MLK3 into the flanks of SCID mice. However, all three MLK3 shRNA containing cell lines showed the same phenotype (diminished tumor growth and metastasis) in the flank as we observed in the fat pad (Figure 3.5C and 3.5D). These results indicate that while MLK3 knockdown regulates free fatty acid induced JNK activation, the diminished tumor growth and metastasis of MLK3 knockdown cell lines *in vivo* is not due to altered free fatty acid signaling in the mammary fat pad.

Recent data has demonstrated that p38 signaling promotes proliferation of p53 mutant cell lines such as MDA-MB-231 cells (88). As MLK3 cells have decreased proliferation and MLK3 is known to activate p38, we determined whether p38 signaling

was inhibited in MLK3 knockdown cells. We assessed activation of p38 in serum starved, TGFβ stimulated control and MLK3 knockdown cells. We found that MLK3 knockdown cells expressing two different MLK3 shRNAs showed a loss of basal and TGFβ stimulated p38 signaling (Figure 3.4G). This loss of p38 signaling in the absence of MLK3 may contribute to the decreased proliferation phenotype seen in MLK3 knockdown cells.

Secreted proteins such as growth factors, proteases, cytokines and chemokines control many cancer related processes such as tumor growth and metastasis. We sought to determine whether the reduced tumor size and metastasis of MLK3 knockdown cells is due to alterations in secreted proteins in MLK3 knockdown cells. To further characterize MLK3 knockdown cell lines, cell culture supernatants from MLK3 knockdown lines were analyzed for levels of 88 secreted factors using multiplex bead assays. Increased secretion of the macrophage stimulatory factor RANTES was found in cell culture supernatants from MLK3 knockdown cells (data not shown). We therefore probed MLK3 knockdown tumors for the presence of macrophages by immunofluorescent staining of F4/80. While macrophages were detected only intermittently in control tumors, MLK3 knockdown tumors were permeated throughout with macrophages (Figure 3.6). Furthermore, this increase was specific for MLK3 knockdown and not due to diminished tumor growth in MLK3 knockdown tumors. Other MAP3K knockdown tumors such as MEKK2 and B-Raf with diminished tumor growth showed normal levels of macrophage infiltration into the tumor (Figure 3.6 and not shown). This increase may be due to recognition of MLK3 knockdown tumors by the innate immune system and the resulting phagocytosis of tumor cells. In total, these results demonstrate a role for

MLK3 in tumor growth and metastasis *in vivo*, independent of local fat levels. We find that MLK3 knockdown inhibits tumor growth *in vivo* and cell proliferation *in vitro*. MLK3 knockdown cells show loss of basal and simulated p38, which is known to promote proliferation in p53 mutant lines and MLK3 knockdown tumors have increased recognition by the innate immune system.

Knockdown of MLK7 was achieved with two shRNAs with ~95% and 85% knockdown for shRNA 1 and shRNA 2 by RNA levels (Figure 3.2F). Injection of cell lines containing the two MLK7 shRNAs gave strikingly discordant phenotypes in tumor growth, with MLK7 shRNA 1 containing cell lines resulting in barely detectable tumors and MLK7 shRNA 2 containing cell lines resulting in tumors that were ~4 fold larger than control tumors (Figures 3.4H and 3.4J). The large tumors formed by cells containing MLK7 shRNA 2 are more consistent with previous results that find MLK7 controls cell stress induced death. Despite the discordance in tumor size, both of the MLK7 shRNAs blocked metastasis, this was particularly striking for MLK7 shRNA 2 where despite markedly increased tumor size there was no evidence of metastasis (Figures 3.4I and 3.4K). We assayed MLK7 knockdown cell lines for cell signaling deficiencies and found the MLK7 cell lines had defects in JNK and p38 activation by both anisomycin and hyperosmolar sorbitol, in agreement with previous findings with MEFs (Figure 3.4L and 3.4M) (24).

Knockdown of TAK1 was readily achieved, with two shRNAs each giving 99% knockdown at the protein level (Figure 3.2D). Tumors formed from cell lines containing either TAK1 shRNA showed either no defect in tumor growth or modestly increased tumor growth (Figures 3.4N). Similarly, neither TAK1 shRNA had any effect on

spontaneous metastasis from the fat pad (Figures 3.4O). Real time PCR confirmed that metastases from TAK1 shRNA containing cell lines still retained TAK1 knockdown (Figure 3.10D), indicating that TAK1 does not control either tumor growth or metastasis.

MAP3Ks that Control JNK and ERK5 or p38 and ERK5 Regulate Tumor Growth and Metastasis

ERK5 has recently emerged as an important MAPK controlling cell proliferation and has also been linked to survival and metastasis in human patient samples (100,107,110). Only two MAP3Ks are predicted to activate ERK5, MEKK2 and MEKK3 which both contain N-terminal PB1 domains that mediate their interaction with MEK5, the MAP2K for ERK5. Both MEKK2 and MEKK3 activate additional MAPK pathways, MEKK2 has been shown to activate JNK pathways, while MEKK3 has been demonstrated to activate p38 signaling. Two shRNAs for MEKK3 were identified that resulted in cell lines with MEKK3 knockdown of 98% and 99% (Figure 3.2H). When injected into mice, these cell lines resulted in diminished tumor growth; MEKK3 shRNA 1 and shRNA 2 tumors were ~50% and 5% of control tumor size (Figures 3.7A and 3.7C). Despite reduced tumor growth, MEKK3 knockdown cell lines showed near normal metastasis rates (Figures 3.7B and 3.7D). Real time PCR of metastases demonstrated continued MEKK3 knockdown in the population of cells that metastasized, indicating that loss of shRNA expression was not responsible for normal levels of metastasis (Figure 3.10G). These results demonstrate that while MEKK3 knockdown inhibits tumor growth, metastasis does not require MEKK3.

Testing the available MEKK2 shRNAs identified two shRNAs that knocked down MEKK2 by either 99% or 77% at the protein level (Figure 3.2G). Injection of the resulting MEKK2 knockdown cell lines showed diminished tumor growth, resulting in tumors that were ~33% and 10% the size of control tumors respectively (Figures 3.7E and 3.7G). Furthermore, cell lines knocked down for MEKK2 showed a decreased propensity for metastasis, with metastasis detected in only one of 12 mice injected with MEKK2 shRNAs while metastasis was detected in 7 of 13 mice injected with control cells (Figures 3.7F and 3.7H). MEKK2 knockdown tumors were allowed to grow until the tumors metastasized. We found that metastasis in MEKK2 knockdown tumors was delayed five weeks relative to controls (7 weeks in controls vs. 12 weeks in MEKK2 shRNA). While metastasis was much delayed, metastases from MEKK2 shRNA tumors still retained knockdown of MEKK2 indicating that MEKK2 delayed but did not completely abrogate metastasis (Figure 3.10F). These effects of MEKK2 on tumor growth and metastasis were verified with a second independent set of injections (Figure 3.8A and 3.8B). These results verify that MEKK2 is required for tumor growth and metastasis.

As MEKK2 has been found to regulate ERK5, we assessed whether loss of MEKK2 expression inhibited ERK5 activation in response to the potent metastatic stimulus EGF. We and others have observed that the currently available phospho-ERK5 antibodies have poor sensitivity (158). Therefore, we assessed ERK5 activation by supershift, detecting the slower moving phosphorylated ERK5 band using total ERK5 antibodies. We found both MEKK2 shRNAs block activation of ERK5 by EGF in MDA-MB-231 cells (Figures 3.7I and 3.8C). In contrast to ERK5 signaling, ERK1/2 and

JNK1 activation was unchanged while there was a decrease in JNK2 signaling (Figure 3.7I). Similar results were seen with the second shRNA against MEKK2, with loss of ERK5 activation, unchanged ERK1/2 and JNK1 signaling while JNK2 activation was increased (Figure 3.8C). While ERK5 has been implicated in proliferation, we found no difference between control and MEKK2 shRNA cell line proliferation *in vitro* (Figure 3.8D).

As MEKK2-ERK5 signaling may be an important regulator of metastasis, we sought to characterize upstream cellular factors required to activate MEKK2. Previous experiments have determined that MEKK2 activates ERK5 in a Src dependent fashion in mink lung endothelial cell lines (159). We therefore tested whether Src was required for EGF stimulated ERK5 activation in MDA-MB-231 cells, using the Src family inhibitors PP2 and Dasatinib, the inactive inhibitor PP3 and the EGFR/Her2 inhibitor Lapatinib. As expected, EGF induced ERK5 activation was inhibited by EGFR inhibition with Lapatinib (Figure 3.7J). However, we found that while ERK5 activation by EGF was sensitive to PP2, it was insensitive to Dasatinib (Figure 3.7J). Differences in the activity of the two inhibitors could be explained by a more modest inhibitory effect of Dasatinib or by differences in the Src family kinases inhibited by the two drugs. However, western blots detecting Src family autophosphorylation at Y416, found that Dasatinib had a much more profound effect of Src family autophosphorylation than PP2 (Figure 3.7J). PP2 has also been found to inhibit EGFR with a modest K_D, however, blotting for the EGFR autophosphorylation site Y840 found that while EGFR autophosphorylation was readily inhibited by Lapatinib, PP2 did not affect EGFR autophosphorylation (Figure 3.7J). However, given the ability of Dasatinib to inhibit Src activity without altering ERK5

phosphorylation, it seems likely that the effects of PP2 on ERK5 activation are due to off-target effects of the drug. Thus, MEKK2 activation is Src independent but requires EGFR receptor activation.

We sought to identify potential downstream targets of MEKK2-ERK5 signaling. As cancer cells secrete many factors that promote tumor growth and metastasis, we used a luminex bead based assay to identify proteins that were differentially secreted between control and MEKK2 knockdown cell lines. Profiling of 88 secreted proteins in the MEKK2 shRNA cell lines demonstrated selective loss of tissue factor (TF) expression in MEKK2 shRNA cell lines (Figure 3.8E). TF has been demonstrated to promote tumor growth and metastasis through interactions with factor VII and activation of the PAR2 receptor (160,161). Using TF specific real time PCR primers we found that tissue factor expression was lost at RNA level as well as at the protein level (Figure 3.8F). Interestingly, at the level of both protein and RNA, the effect of MEKK2 shRNA 2 is more modest then shRNA 1, consistent with the relative levels of knockdown achieved with MEKK2 shRNA 1 and MEKK2 shRNA 2. These results identify a target of MEKK2, TF, which may be an important mediator of MEKK2 oncogenic and metastatic signaling.

The EGFR family member Her2/ERBB2 is frequently overexpressed in breast cancer and is associated with poor prognosis. Overexpressed Her2 is known to result in constitutive activation of ERK5, which promotes cell proliferation. As MEKK2 was required for ERK5 activation by MEKK2, we investigated whether MEKK2 mediated ERK5 activation in HER2 overexpressing breast cancer cell lines. We expressed MEKK2 shRNA in the HER2 overexpressing cell line BT474 and found that MEKK2

knockdown blocked constitutive activation of ERK5 in BT474 cells. While ERK5 was almost completely in the phosphorylated active form in control cells, ERK5 was almost completely in the inactive dephosphorylated form in MEKK2 shRNA cells (Figure 3.7K). This was accompanied by an increase in JNK phosphorylation, perhaps because of loss of ERK5 prosurvival effects, but ERK1/2 activation remained unchanged (Figure 3.7K). As ERK5 has been implicated in proliferation in HER2 overexpressing cells, we injected the control and MEKK2 shRNA cell lines into the flanks of SCID mice and measured tumor growth. By bioluminescent imaging, we found that control vector containing tumors were markedly larger then tumors formed from MEKK2 shRNA containing BT474 cells (Figure 3.7L). Quantitation of the resulting luciferase signal demonstrated a 12 fold decrease in photon flux in MEKK2 shRNA tumors relative to control vector expressing tumors (Figure 3.7M). These results implicate MEKK2 in tumor growth and metastasis and demonstrate the existence of an ERBB family member-MEKK2-ERK5 signaling axis that contributes to tumor signaling. Furthermore, our results identify tissue factor as a potential target by which MEKK2 may regulate tumor growth and metastasis.

Knockdown of ERK5 blocks metastasis in MDA-MB-231 cells

We find that MEKK2 regulates ERK5 and controls tumor growth and metastasis. Previous work has demonstrated roles for ERK5 in proliferation *in vitro* and in regulation of metastasis and survival in human breast cancer patients (107,110). We wanted to assess directly whether knockdown of ERK5 in MDA-MB-231 cells would show similar tumor growth and metastasis phenotypes as we saw in MEKK2 knockdown cells. Two different shRNAs against ERK5 resulted in knockdown of ERK5 levels (Figure 3.9A).

Cell lines expressing control vector and ERK5 shRNAs were xenografted into the mammary fat pad and tumor growth and metastasis of the two knockdown cell lines was compared to control cell lines. While neither of these cell lines had altered tumor growth relative to control cells, ERK5 knockdown correlated with reduced metastasis (Figures 3.9B-D). In our experiments, only one of 10 animals injected with ERK5 shRNA cell lines had lymph node metastasis. Thus while tumor growth in MDA-MB-231 cells is ERK5 independent, efficient metastasis of MDA-MB-231 cells requires ERK5 expression. These results demonstrate the requirement of MEKK2-ERK5 signaling in tumor metastasis.

Discussion

Our goal in this study was to use shRNA screens to define the function of the MAPK signaling network in controlling breast cancer tumor growth and metastasis. Rationale for the screen was based on the overwhelming evidence that the MAPK signaling network is significantly amplified, overexpressed and activated in breast cancer, suggesting the signaling network has a major influence on driving the breast cancer phenotype. Numerous studies have characterized loss of function and chemical inhibition of MAPK network proteins in cancer cells in vitro (55,84,88,106). Also, MAPK network proteins such as B-Raf, JNK, ERK1/2 and ERK5 have been studied *in vivo* in xenograft models as individual targets (67,115,162). A more comprehensive screen to define the cooperative behavior of the MAPK network had not been completed. MAP3Ks were targeted for shRNA knockdown for the screen, because it is the diversity of MAP3Ks and their different protein-protein interactions and modifications that integrate the MAPK

network in the cellular response to different stimuli involving GTPases, additional kinases and receptors (108,131,134,153). Thus, MAP3Ks function as signaling hubs for integration of the MAPK network with the physiological response of cells to their environment.

The MAP3Ks we targeted differentially regulate ERK1/2, JNK, p38 and ERK5. Seven of the nine targeted MAP3Ks had a pronounced inhibition of either tumor growth and/or metastasis. The findings demonstrate that MAP3Ks and their selective and differential activation of the four primary MAPK families have significant regulatory functions in controlling in vivo tumor growth and metastasis. Based on the literature, our data enables us to parse the roles played by different MAPK pathways in tumor growth *in vivo* (Figure 3.9E). We find, consistent with the known role of ERK1/2 in cell proliferation, two MAP3Ks, B-Raf and Tpl2, that regulate ERK1/2 activation control tumor growth *in vivo*. Interestingly, despite their effects on tumor growth, neither B-Raf nor Tpl2 has reproducible effects on metastasis, indicating that ERK1/2 signaling regulates tumor growth but not metastasis. By contrast, MEKK1, MEKK2, MEKK3, MLK3 and MLK7, MAP3Ks regulating JNK and/or p38 variously inhibit tumor growth and metastasis, demonstrating that JNK and p38 signaling are critical to both tumor growth and metastatic spread. MEKK2 and MEKK3 also regulate ERK5, thus we knocked down ERK5 directly to assess its role in tumor outcome. Knocking down ERK5 demonstrated that ERK5 was required for metastasis. The array of MAP3Ks whose loss of expression had a measureable phenotype mapped to the control of ERK1/2, JNK, p38 and ERK5. Thus, the collective family of MAP3Ks, MAP2Ks MAPKs, functions to drive the tumor phenotype. Interestingly, ERK1/2, JNK, p38 and ERK5 signaling pathways

were all required for tumor growth and metastasis in the background of a cell line containing activating mutations of B-Raf and Ras. This is particularly interesting given the central role accorded to Ras, B-Raf-MKK1/2-ERK1/2 signaling and more generally, ERK1/2 signaling in tumor outcome. The findings demonstrate the importance of the entire MAPK network, not simply specific drivers such as mutant B-Raf, in contributing to tumor phenotype and explain why so many members of the MAPK network are overexpressed and/or activated in breast cancer. The screen results show loss of individual MAP3Ks by shRNA knockdown can significantly compromise the network such that tumor growth and/or metastasis are inhibited. Only loss of TAK1 and c-Raf expression failed to have a measurable and reproducible inhibition of either tumor growth or metastasis by two independent shRNAs. For c-Raf there was discordance in the two shRNAs in regards to tumor growth. The fact that one c-Raf shRNA did not inhibit tumor growth, and the presence of an activating B-Raf mutation to drive constitutive ERK1/2 activation and proliferation in the MDA-MB-231 cells, suggests the second shRNA for c-Raf had an off-target response in its inhibition of tumor growth. TAK1 knockdown, if anything, enhanced tumor growth.

Of the MAP3Ks studied in our experiments, most have been linked to cancer in a relatively limited fashion. Despite their limited provenance in cancer, we find that many of these MAP3Ks that have potent effects on tumor growth and/or metastasis. Two of the top-scoring MAP3Ks were MLK3 and MEKK2, which both have potent effects on both tumor growth and metastasis. MLK3 is activated by the small GTPases Rac and Cdc42 and has been extensively studied for its role in mediating neuronal apoptosis (131,163). As MLK3 was required for growth in our experiments, apoptosis is clearly not the

function of MLK3 in the MDA-MB-231 tumor system. Instead, knockdown of MLK3 in MDA-MB-231 cells resulted in loss of JNK activation in response to fatty acids and p38 activation in response to TGFβ. In vitro, loss of MLK3 expression resulted in an inhibition of cell growth, potentially due to loss of the p38 dependent cell proliferation that has been demonstrated in p53 null cell lines. Based on our data, it would be expected that MLK3 overexpression would promote proliferation of p53 mutant cell lines. Interestingly, searches of a public database of gene expression data (www.oncomine.org) demonstrated that MLK3 was found to be overexpressed in multiple studies on Barrett's esophagus and esophageal adenocarcinoma samples from human patients. p53 mutations are common in esophageal adenocarcinoma and progression of normal esophagus to Barrett's esophagus to esophageal adenocarcinoma is dependent on p53 mutation in many cases. Furthermore, MLK3 knockdown tumors were extensively infiltrated with macrophages while we saw little evidence of increased macrophage infiltration in MEKK2 knockdown tumors that also showed reduced growth. The altered immune response in MLK3 knockdown tumors may result in scavenging of MLK3 knockdown tumor cells contributing to the diminished tumor growth in MLK3 knockdown tumors.

The role of MEKK2 in tumor growth and metastasis has not been systematically studied but there is the beginning of a linkage for its role in cancer. In one study linking MEKK2 to cancer, 11 prostate cancer tissue samples were compared to uninvolved prostate tissue using imaging mass spectrometry (120). One peptide was found to discriminate cancer from uninvolved tissue and this peptide was a fragment of MEKK2. In confirmation of the MS data, MEKK2 was expressed at 4.4-fold higher level in

prostate cancer tissue versus benign tissue using western blotting. Even higher levels of MEKK2 expression were observed in LNCaP, Du145 and PC3 prostate cell lines (120). Our current study shows that MEKK2 is required for activation of ERK5 by ERBB family members. Specifically, we find that MEKK2 mediates ERK5 activation by EGF stimulated EGFR activity in MDA-MB-231 cells and by constitutive ERK5 activation induced by Her2 overexpression in BT474 cells. MEKK2 is also in a complex that can be co-immunoprecipitated with the EGFR (our unpublished observation). ERK5 knockdown experiments demonstrated that MEKK2 regulates tumor growth in an ERK5 independent manner, consistent with MEKK2 regulation of JNK signaling. This regulation of tumor growth by MEKK2 occurs in multiple breast cancer subtypes as MEKK2 knockdown inhibits growth of Her2 positive BT474 xenografts as well. While regulation of tumor growth in MDA-MB-231 cells by MEKK2 is ERK5 independent, both MEKK2 and ERK5 shRNA-mediated knockdown inhibited metastasis of MDA-MB-231 cells demonstrating a role for MEKK2 mediated ERK5 activation in metastasis. This finding corroborates with the recent finding that ERK5 expression levels correlate with disease free survival time in human breast cancer patients (110). Further, our findings implicating a MEKK2-ERK5 signaling axis in breast cancer suggest that overexpression of MEKK2 in prostate cancer may promote prostate cancer progression through ERK5 activation. Recent findings have demonstrated a role for ERK5 activation in prostate cancer. In a study done in prostate cancer, ERK5 expression was significantly increased in high-grade prostate cancer compared to benign prostatic hyperplasia (162). Analysis of ERK5 expression in samples taken before and after hormone relapse showed a correlation with ERK5 nuclear localization (indicating ERK5 activation) and hormone-

insensitive disease (162). ERK5 overexpression in PC3 cells resulted in more efficient tumor formation in mice (162). In a recent study, miR-143 was shown to be a tumor suppressor in prostate cancer using a mouse model (105). One of the mechanisms of miR-143 appears to be suppression of ERK5 protein expression (105). The MAP2K of the ERK5 pathway, MKK5 has also been implicated in tumor development. It was found that overexpression of MKK5 correlated with bone metastasis and poor prognosis in a cohort of 127 cases of prostate cancer and 20 cases of benign prostatic hypertrophy (107). Thus the MEKK2-MKK5-ERK5 signaling pathway we identified in breast cancer may be conserved in multiple tumor types and suggest that targeting of the MEKK2-MKK5-ERK5 pathway is of therapeutic value in both breast and prostate cancer.

Kinases are probably the most important target class today for oncology drug discovery, with nine inhibitors currently approved for different cancers (133). Identification of multiple MAP3Ks that are required for proper function and dynamics of the MAPK network has revealed several kinases within the untargeted cancer kinome required for tumor growth and metastasis (133). Our shRNA screens have shown it is possible to target a signaling network commonly activated in cancer and identify kinases whose loss of expression inhibits the cancer phenotype. Similar RNAi screens for other commonly activated signaling networks will undoubtedly define kinases whose function in tumor progression has not been recognized. Such studies will define the cooperative nature of kinase networks and identify previously unrecognized kinases involved in cancer and other human diseases that can be therapeutically targeted.

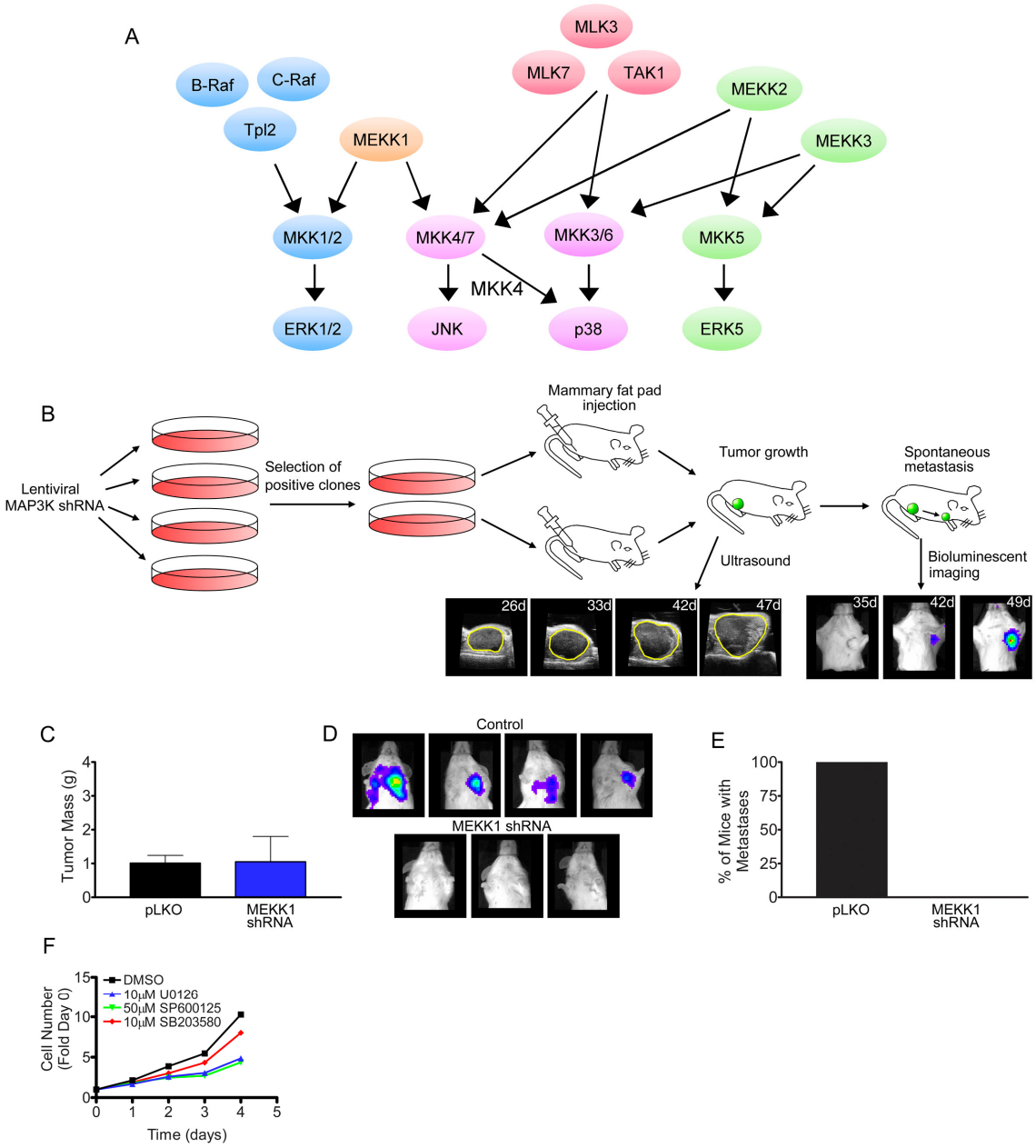

Figure 3.1. Methodology for RNAi Screening of MAP3K Function in Tumor Growth and Metastasis and Validation *in vivo*

(A) Model illustrating the MAPK signaling networks regulated by each of the MAP3Ks screened in this paper. (B) Schematic demonstrating the workflow of the screen and readouts of tumor growth and metastasis by ultrasound and bioluminescent imaging. (C) MEKK1 does not inhibit tumor growth. Tumor mass of tumors formed from control cells and MEKK1 shRNA cells. Data is presented as mean ± standard error of the mean (SEM). (D) Loss of metastasis in tumors with MEKK1 knockdown. Bioluminescent imaging of metastases from tumors formed from either control cells or MEKK1 shRNA cells demonstrating reduced metastasis from MEKK1 knockdown tumors. (E) Quantitation of results from bioluminescent imaging. Metastasis expressed as percent of animals metastasis positive in control and MEKK1 knockdown tumors. (F) Inhibition of

multiple MAPK pathways reduces cell proliferation. MDA-MB-231 cells were grown in the presence of either DMSO (control) 10 μM U0126 (MEK1/2 inhibitor), 50 μM SP600125 (JNK inhibitor), or 10 μM SB203580 (p38 inhibitor) for the times indicated. Data at each time point is presented as mean ± SEM for each condition assayed in quadruplicate. Tumor experiments were done in collaboration with Nancy Johnson and Bruce Cuevas.

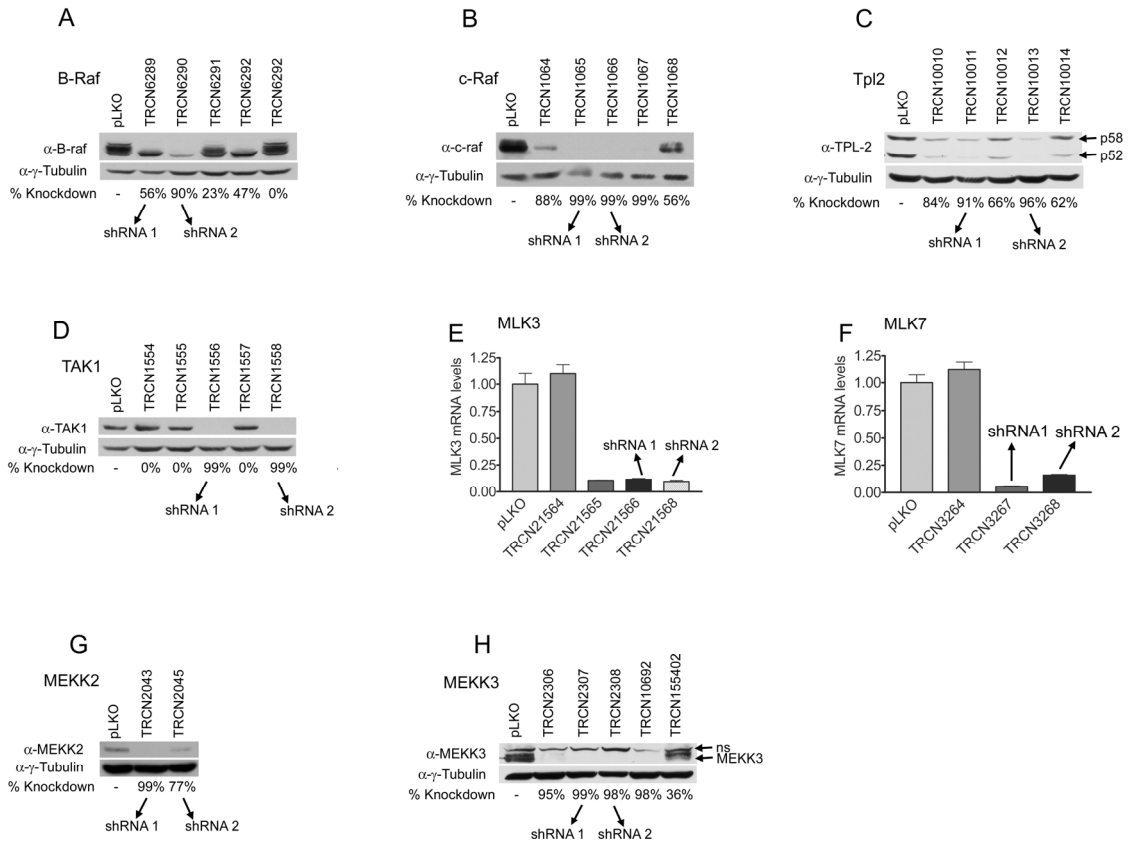

Figure 3.2. Knockdown of MAP3Ks by TRCN shRNAs.
(A, B, C, D, G and H) Western blots demonstrating knockdown of specific MAP3Ks by TRCN shRNAs. γ-Tubulin was used as a loading control. For each MAP3K shRNA, the TRCN sequence number is listed and the percentage knockdown as determined by densitometry of the MAP3K relative to control is indicated below the blots. MAP3Ks targeted are (A) B-Raf. (B) c-Raf. (C) Tpl2. (D) TAK1. (G) MEKK2. (H) MEKK3. (E and F) Real time PCR demonstrating knockdown of MLK3 and MLK7 by TRCN shRNAs. For each shRNA, RNA levels were normalized to β-actin signal as an endogenous calibrator and MAP3K RNA levels were quantitated relative to control cells. MAP3Ks analyzed are (E) MLK3 and (F) MLK7. These experiments were done in collaboration with Jing Yang.

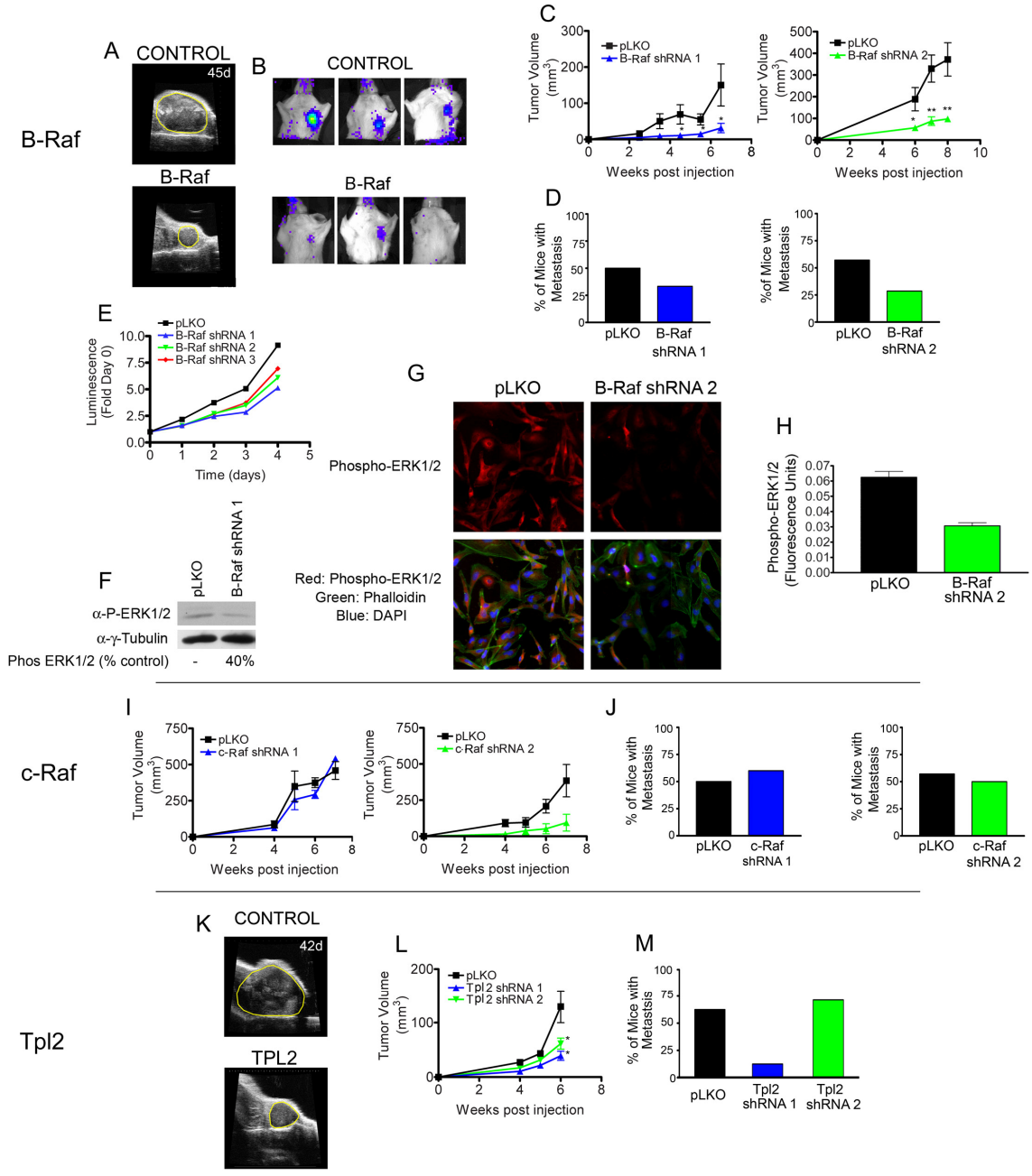

Figure 3.3. Knockdown of MAP3Ks Regulating ERK1/2 Signaling Results in Defects in Tumor Growth

(A) B-Raf knockdown inhibits tumor growth. Representative ultrasound images of control and B-Raf knockdown tumors at 45 days post injection. Extent of tumors is denoted in yellow. (B) B-Raf knockdown has modest effects on metastasis. Representative bioluminescent images of control and B-Raf tumors at time of sacrifice demonstrating that metastasis is largely unchanged in B-Raf knockdown tumors. (C) Quantitation of tumor volume in control and multiple B-Raf shRNA tumors demonstrating inhibition of tumor growth with multiple B-Raf shRNAs. For each time point, data is presented as mean ± SEM, n = 6 (Control and B-Raf shRNA 1) or n = 8 (Control and B-raf shRNA 2), * $p < 0.05$, ** $p < 0.01$. (D) Quantitation of mice

determined to be metastasis positive at time of sacrifice in mice with control and multiple B-Raf knockdown tumors. (E) B-Raf knockdown inhibits cell growth *in vitro*. B-Raf knockdown cell lines were grown for 4 days post plating and viability was assessed in quadruplicate on each day using an ATP based viability assay. Data is presented as mean ± SEM for each time point. (F) Loss of ERK1/2 signaling by western blot in B-Raf shRNA 1 containing cells. Cells were blotted for either phospho-ERK1/2 or gamma tubulin as a loading control. Densitometry was used to quantitate phospho-ERK1/2 levels relative to control. (G) Loss of ERK1/2 signaling by immunofluorescence in B-Raf shRNA 2 containing cells. Control and B-Raf shRNA cells were stained for either phospho-ERK1/2 (Red), actin (green) or nuclei (blue). (H) Quantitation of phospho-ERK1/2 staining in control and B-Raf shRNA cells. Whole cells were masked using actin staining to denote the cells. Phospho-ERK1/2 staining within the mask was quantitated for control and B-Raf shRNA cells. (I) c-Raf knockdown has discordant effects on tumor growth. Tumor volume of tumors formed from control and c-Raf knockdown cells determined by ultrasound. Volumes are expressed as mean ± SEM for each point, n = 7 and 6 (Control and c-Raf shRNA 1) or n = 6 and 5 (Control and c-Raf shRNA 2). (J) c-Raf knockdown has no effect on metastasis. Metastasis positive mice were quantitated at time of sacrifice and expressed as percentage of mice metastasis positive in mice with control or c-Raf knockdown tumors. (K) Tpl2 knockdown inhibits tumor growth. Representative ultrasound images of control and Tpl2 knockdown tumors, tumor area is denoted with yellow lines. (L) Quantitation of tumor volume in control and Tpl2 knockdown cell lines demonstrating decreased tumor growth in multiple Tpl2 knockdown cell lines. For each time point, data is presented as mean ± SEM, n = 8 (Control and Tpl2 shRNA 1) or n = 7 (Tpl2 shRNA 2), * $p < 0.05$. (M) Knockdown of Tpl2 has discordant effects on metastasis with two Tpl2 shRNAs. Quantitation of metastasis positive mice at time of sacrifice in mice with control and Tpl2 knockdown tumors. Tumor experiments were done in collaboration with Nancy Johnson.

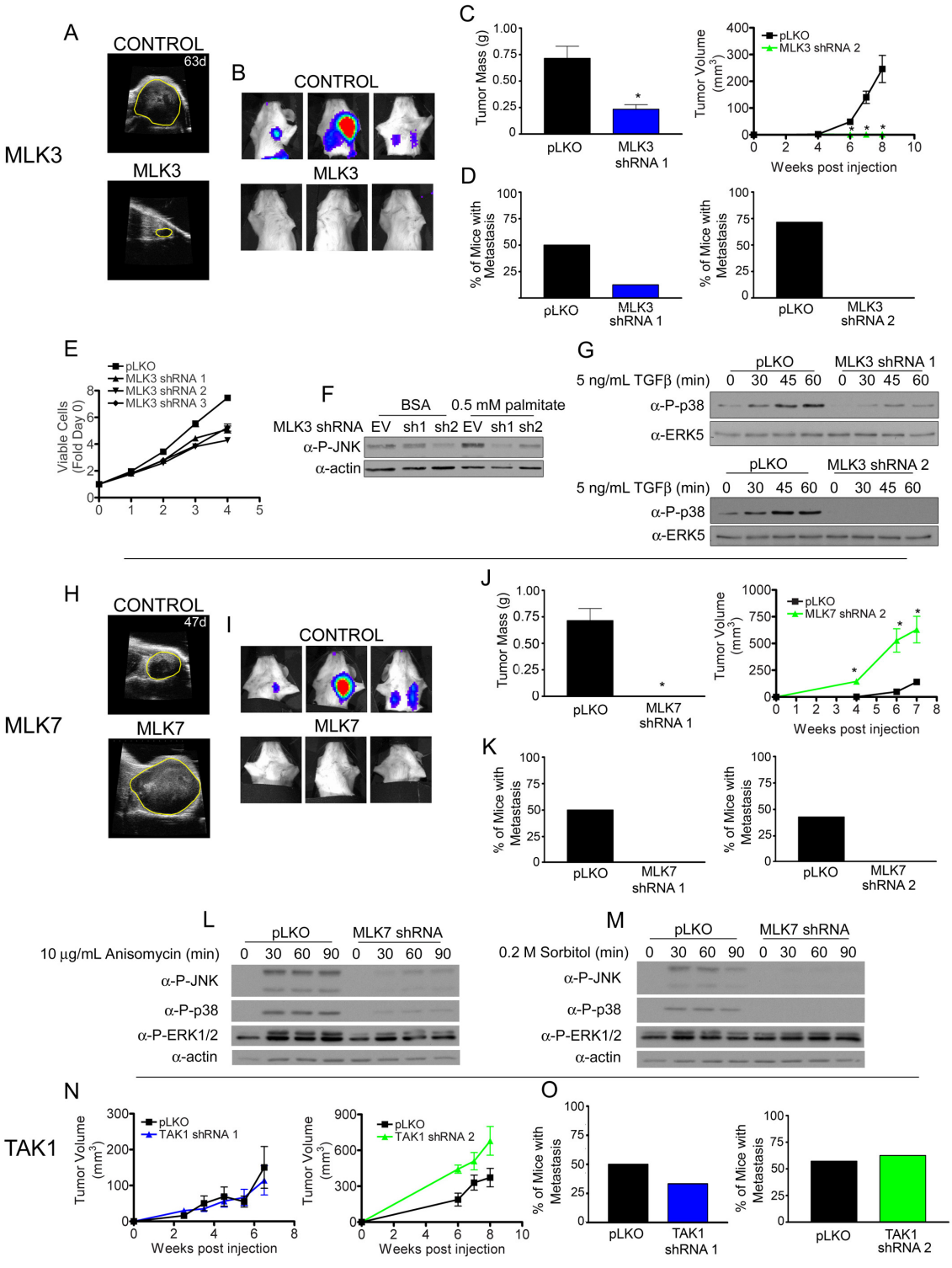

Figure 3.4. Knockdown of MAP3Ks Regulating JNK and p38 Signaling Results in Defects in Tumor Growth

(A) MLK3 knockdown inhibits tumor growth. Ultrasound images of control and MLK3 knockdown tumors 63 days post injection. Margins of tumor are indicated by yellow

line. (B) MLK3 knockdown inhibits metastasis. Representative bioluminescent images at time of sacrifice to detect metastases from control and MLK3 knockdown tumors. (C) Quantitation of differences in tumor size by either final tumor weight for MLK3 shRNA 1 or tumor volume over time for MLK3 shRNA 2. Each data point is presented as mean ± SEM, n = 6 (MLK3 shRNA 1) or n = 5 (MLK3 shRNA 2). (D) Quantitation of percentage of mice metastasis positive at time of sacrifice in mice injected with control and MLK3 knockdown cell lines. (E) MLK3 knockdown inhibits cell growth. Control and MLK3 knockdown cell lines were plated in 96 well plates and allowed to grow for 4 days. At each day, viable cells were measured using an ATP based viability assay and normalized to day 0 signal. (F) MLK3 knockdown inhibits JNK activation by free fatty acid. Control, MLK3 shRNA 1 and MLK3 shRNA 2 cell lines were treated with either 0.5% fatty acid free BSA or 0.5 mM palmitate in 0.5% fatty acid free BSA for 18 hrs and lysates were blotted for either phospho-JNK or actin. (G) MLK3 knockdown inhibits TGFβ stimulated p38 activation. Control, MLK3 shRNA 1 and MLK3 shRNA 2 cell lines were serum starved and treated with 5 ng/mL TGFβ for the times indicated and blotted for either phospho-p38 or total ERK5 as a loading control. (H) MLK7 knockdown enhances tumor growth. Representative ultrasound images of control and MLK7 shRNA 2 tumors. Extent of tumors is indicated in yellow. (I) MLK7 knockdown inhibits metastasis. Representative bioluminescent images of control and MLK7 knockdown injected mice. (J) MLK7 knockdown results in discordant tumor growth phenotype. Quantitation of tumor size of control and MLK7 knockdown tumors measured by ultrasound or tumor mass. For each data point, tumor size is indicated as mean ± SEM for n = 7 and 8 (Control and MLK7 shRNA 1 or Control and MLK7 shRNA 2). (K) Quantitation of metastasis in control and MLK7 knockdown cell lines expressed as percentage of mice positive for metastasis at time of sacrifice. (L and M) Knockdown of MLK7 inhibits JNK and p38 in response to anisomycin and hyperosmolar sorbitol. Cells were serum starved and treated with 10 μg/mL anisomycin or 0.2 M sorbitol for the indicated times. Lysates were blotted for phospho-JNK, phospho-p38, phospho-ERK1/2 and actin as a loading control. (N) TAK1 knockdown has no effect on tumor growth. Quantitation of tumor growth in control and TAK1 shRNA tumors. For each time point, data is presented as mean ± SEM, n = 6 (Control and TAK1 shRNA 1) or n = 8 (Control and TAK1 shRNA 2). (O) Quantitation of metastases from control and TAK1 knockdown tumors demonstrating similar levels of metastasis in control and multiple TAK1 shRNA cell lines. Tumor experiments were done in collaboration with Nancy Johnson.

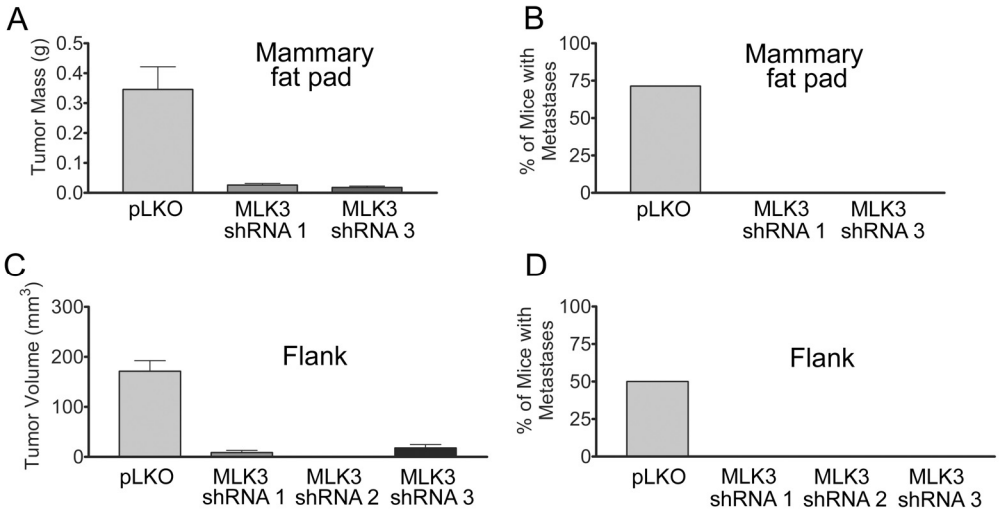

Figure 3.5. MLK3 knockdown by multiple shRNAs Regulates Tumor Growth and Metastasis at Multiple Sites of Implantation.
(A and B) Cell lines expressing either an MLK3 shRNA used in the screen (MLK3 shRNA 1) or a third independent shRNA against MLK3 (MLK3 shRNA 3) have decreased tumor growth and metastasis *in vivo*. (A) Tumor growth assessed by tumor weight at time of sacrifice in control and MLK3 shRNA cell lines. Data represent mean ± SEM of n = 7 (Control and MLK3 shRNA 3) or n = 8 (MLK3 shRNA 1). (B) Metastasis assessed as percentage of animals metastasis positive in control and MLK3 knockdown tumors. (C and D) Cell lines with MLK3 knockdown have similarly decreased tumor growth and metastasis when implanted in the flank. Control cell lines or cell lines expressing three different MLK3 shRNAs were injected into the flanks of SCID animals. (C) Tumor growth was assessed by tumor weight at time of sacrifice in control and MLK3 shRNA cell lines. Mice injected with MLK3 shRNA cell lines show similar decreases in tumor growth as was seen in the mammary fat pad. Bars represent mean ± SEM, n = 6 (Control, MLK3 shRNA 2 and MLK3 shRNA 3) or n = 5 (MLK3 shRNA 1). (D) Metastasis quantitated as percentage of mice metastasis positive at time of sacrifice. MLK3 knockdown lines show a similar loss of metastasis to what is seen in mammary fat pad injections of MLK3 knockdown cells. Tumor experiments were done in collaboration with Nancy Johnson.

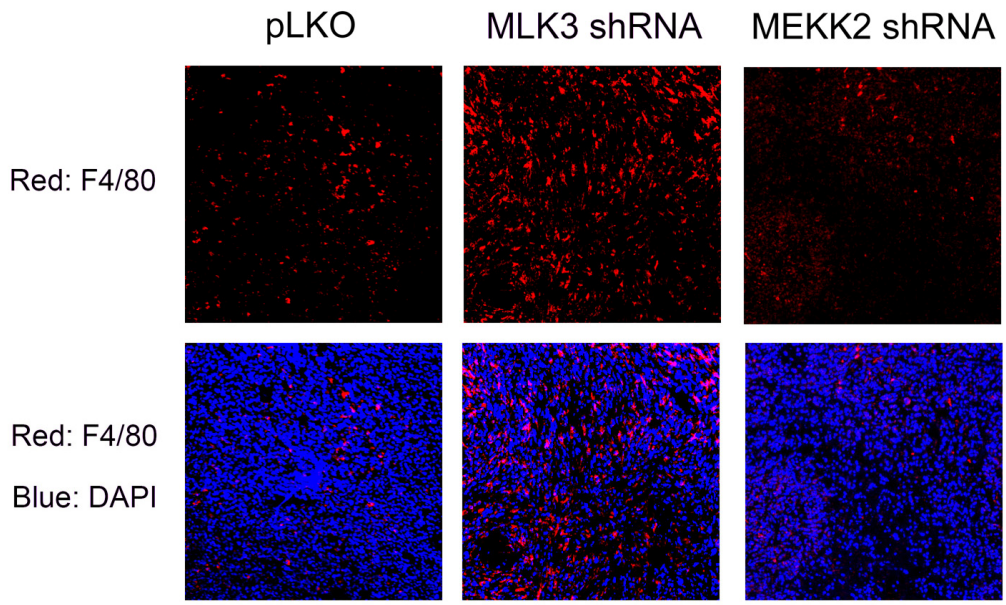

Figure 3.6. Increased macrophage infiltration of MLK3 knockdown tumors. Control, MLK3 and MEKK2 knockdown tumors were fixed and stained for the macrophage marker F4/80 (red) and nuclei (DAPI, blue). This experiment was done in collaboration with Nancy Johnson

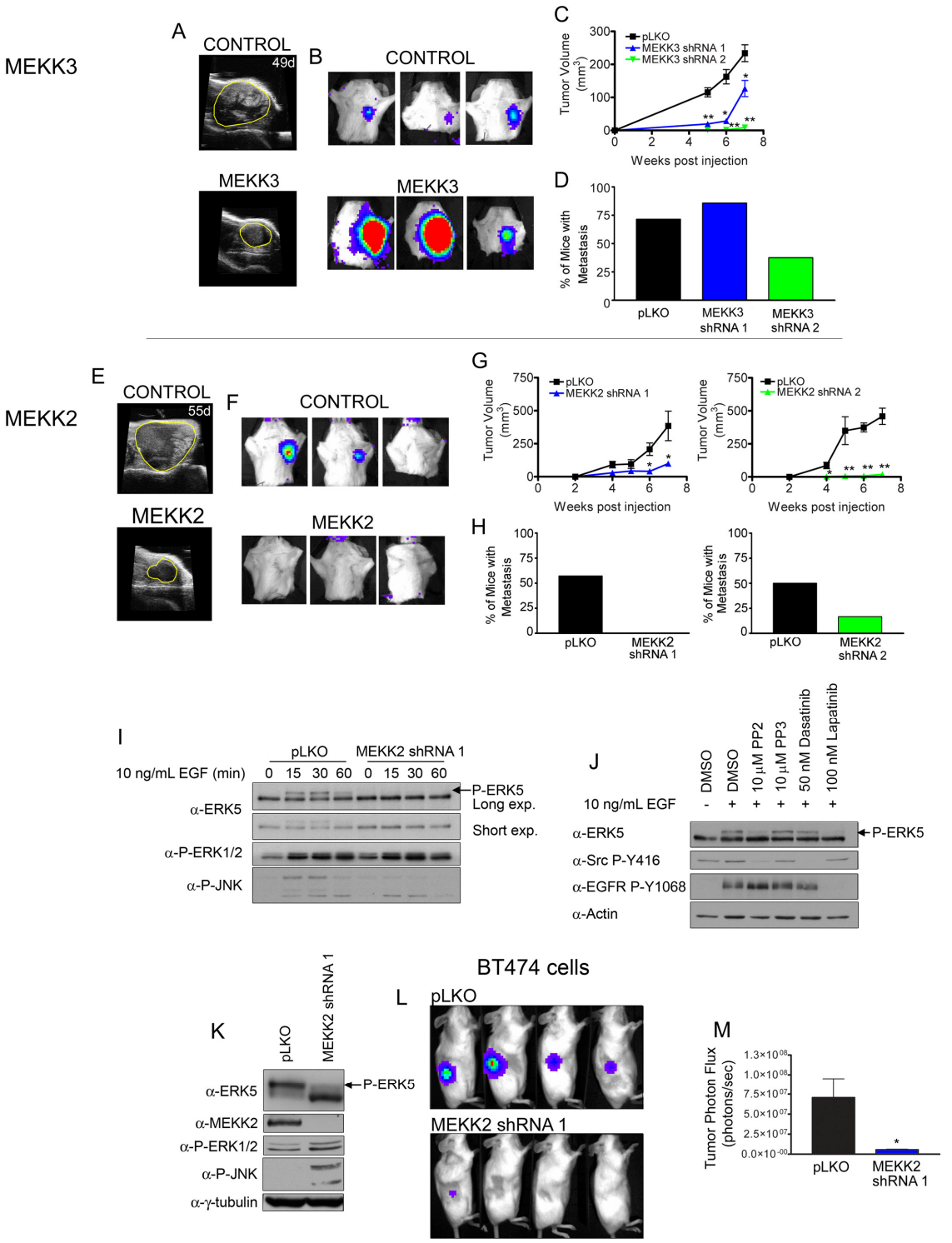

Figure 3.7. Knockdown of MAP3Ks regulating either ERK5 and JNK or ERK5 and p38 inhibit tumor growth and metastasis.

(A) MEKK3 knockdown inhibits tumor growth. Representative ultrasound images of control and MEKK3 knockdown tumors. Extent of tumors is indicated by the yellow lines. (B) MEKK3 knockdown does not affect tumor metastasis. Representative

bioluminescent images of metastases from control and MEKK3 knockdown tumors at time of sacrifice. (C) Quantitation of control and MEKK3 knockdown tumor volume as determined by ultrasound imaging. For each point, data is presented as mean ± SEM for n = 7 (Control and MEKK3 shRNA 1) or n = 8 (MEKK3 shRNA 2), * $p < 0.05$, ** $p < 0.01$. (D) Quantitation of metastasis in control and MEKK3 knockdown tumors as determined by bioluminescent imaging expressed as percentage of mice metastasis positive at time of sacrifice. (E) MEKK2 knockdown inhibits tumor growth. Ultrasound images of control and MEKK2 knockdown tumors 55 days post injection. Extent of tumors is denoted in yellow. (F) MEKK2 knockdown inhibits tumor metastasis. Bioluminescent images detecting presence or absence of metastases from control and MEKK2 knockdown tumors at time of sacrifice. (G) Quantitation of tumor volume in control and MEKK2 knockdown determined by ultrasound imaging. For each data point, data is presented as mean ± SEM for n = 7 and 6 (Control and MEKK2 shRNA 1) or n = 6 (Control and MEKK2 shRNA 2), * $p < 0.05$, * $p < 0.01$. (H) Quantitation of metastases from control and MEKK2 knockdown tumors as determined by bioluminescent imaging and expressed as percentage of mice positive for metastasis at time of sacrifice. (I) MEKK2 knockdown inhibits ERK5 activation by EGF stimulation. Cells were stimulated with 10 ng/mL EGF for the indicated times and blotted for ERK5, phospho-ERK1/2 and phospho-JNK. For ERK5 blots, long exposures were performed to identify the supershifted phosphorylated active form of ERK5 indicated with arrows, while shorter exposures were performed to demonstrate equal loading of samples. (J) ERK5 activation by EGF is Src independent and EGFR dependent. Cells were serum starved and treated with DMSO control, PP2, PP3, Dasatinib or Lapatinib for 15 minutes prior to stimulation with 10 ng/mL EGF for 15 minutes. Cells were lysed and blotted for either total ERK5, Src family Y416-phospho, EGFR Y1068-phospho or actin as a loading control. (K) Knockdown of MEKK2 inhibits constitutive ERK5 activation in BT474 cells. Control BT474 cells or BT474 cells expressing MEKK2 shRNA were lysed and blotted for either ERK5, MEKK2, phospho-ERK1/2, phospho JNK or γ-tubulin as a loading control. MEKK2 knockdown was accompanied by a marked loss of the supershifted phosphorylated form of ERK5. (L) MEKK2 knockdown inhibits tumor growth in BT474 cells. Bioluminescent images of tumors from mice flank injected with either control or MEKK2 knockdown BT474 cells 6 weeks post injection. (M) Regions of interest were drawn around bioluminescent tumor images of BT474 control and MEKK2 knockdown tumors and tumor photon flux was measured. Bars represent mean ± SEM for each cell type, n = 12 (control) n = 10 (MEKK2 shRNA 1), * $p < 0.05$. Tumor experiments were done in collaboration with Nancy Johnson.

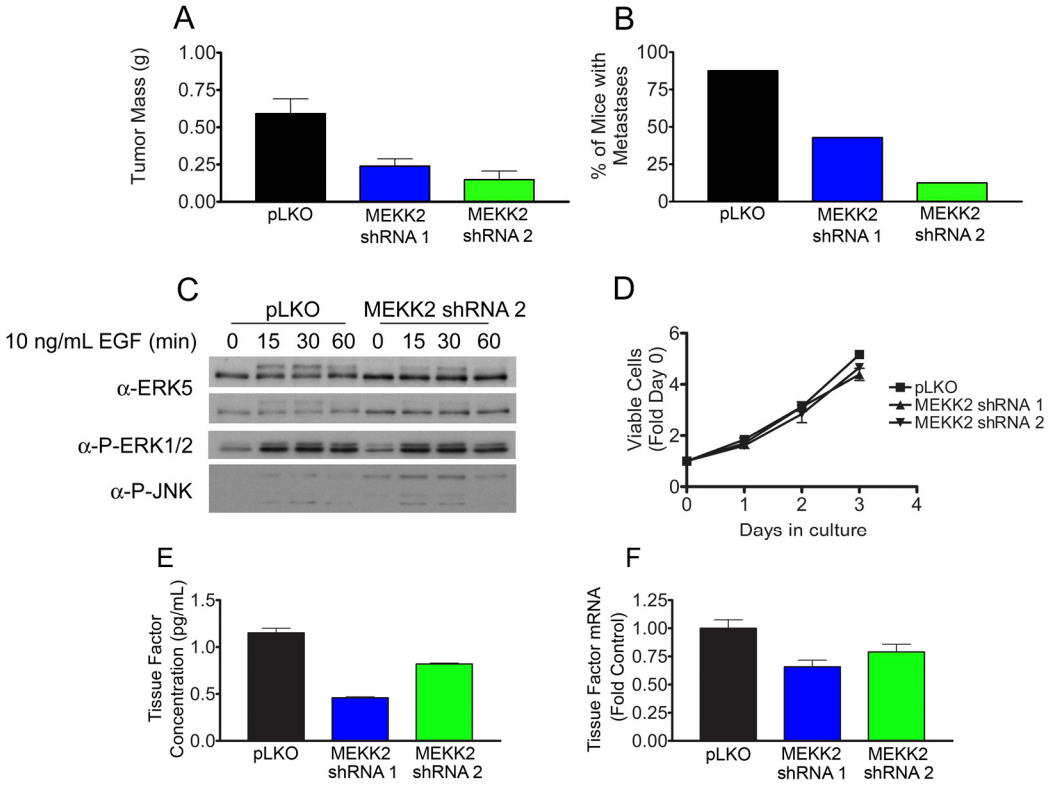

Figure 3.8. MEKK2 knockdown has reproducible effects in a second set of injections and on ERK5 activation and tissue factor expression.
(A and B) Effects of MEKK2 knockdown on tumor growth and metastasis recapitulate in a second independent set of injections. Control cell lines and cell lines expressing MEKK2 shRNA 1 and shRNA 2 were injected into the mammary fat pad of SCID mice. (A) Mice injected with MEKK2 shRNAs show decreased tumor size relative to control. Quantitation of tumor size by weight at time of sacrifice. Bars represent mean ± SEM of n = 8 (Control and MEKK2 shRNA 2) or n = 7 (MEKK2 shRNA 1). (B) Tumors formed from a second set of MEKK2 shRNA cell line injections had diminished metastasis. Quantitation of metastasis as percentage of mice metastasis positive by bioluminescent imaging in control and MEKK2 shRNA cell line injected mice. (C) Knockdown of MEKK2 with a second shRNA results in reduced ERK5 activation in response to EGF. Lysates from EGF stimulated control and MEKK2 shRNA 2 knockdown cell lines were blotted for ERK5, phospho-ERK1/2, phospho-JNK or for γ-Tubulin as a loading control. (D) MEKK2 knockdown does not alter cell growth *in vitro*. Control and MEKK2 knockdown cell lines were plated in 96 well plates and viability was assessed by ATP viability assay. (E) MEKK2 knockdown decreases tissue factor secretion. Control and MEKK2 knockdown cell lines were grown in serum free media for three days and tissue factor secretion in the supernatant was assessed using a bead based cytokine assay. (F) MEKK2 knockdown decreases tissue factor mRNA levels in cells. mRNA was isolated from control and MEKK2 shRNA cell lines and tissue factor

message level in MEKK2 knockdown cell lines was quantitated relative to tissue factor levels in control cell lines. RNA levels were normalized using β-actin levels as a calibrator. Tumor experiments were done in collaboration with Nancy Johnson.

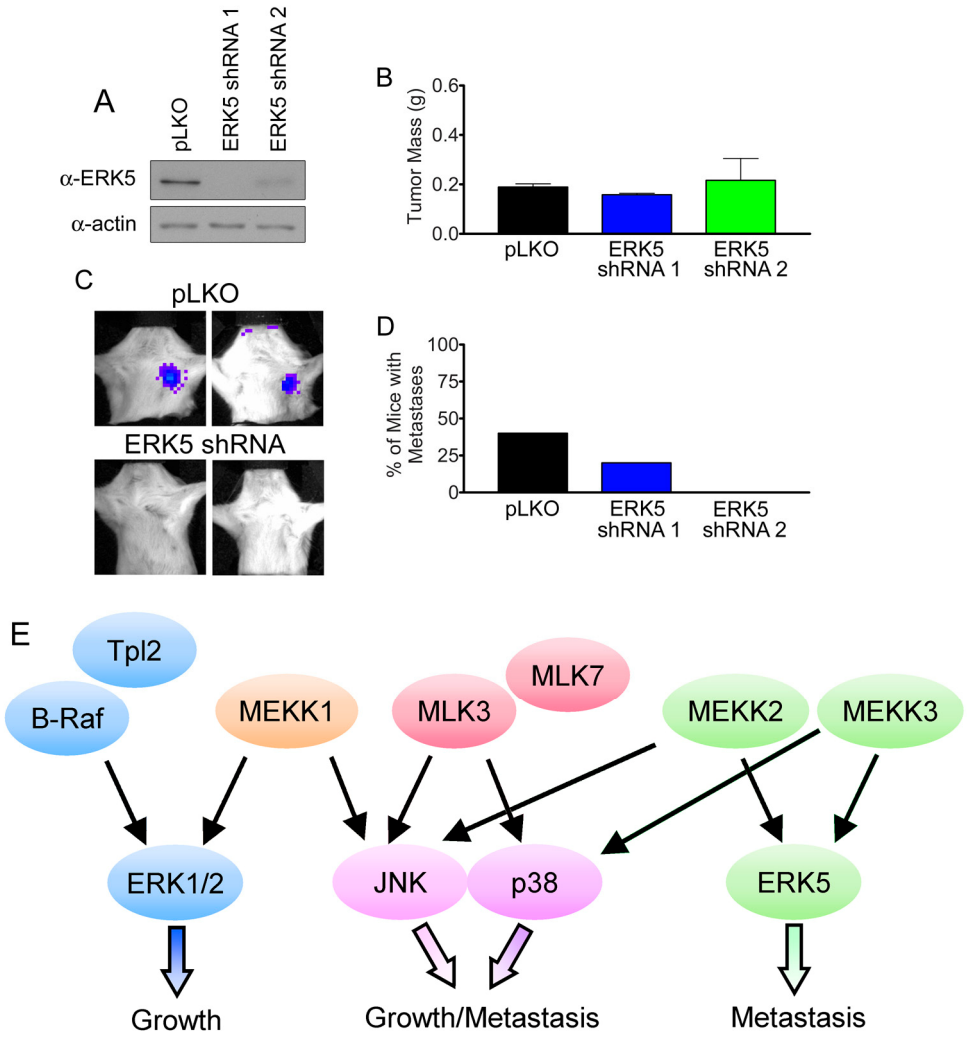

Figure 3.9. ERK5 Knockdown Inhibits Metastasis but not Tumor Growth.
(A) ERK5 knockdown with ERK5 shRNAs. Control and ERK5 shRNA MDA-MB-231 stable cell lines were lysed and blotted for ERK5 levels and actin levels as a loading control. (B) ERK5 knockdown does not alter tumor growth. Control and ERK5 shRNA cell lines were injected into SCID mice and mice were sacrificed 8 weeks post injection. Tumor size was measured by weight. Bars represent mean ± SEM, n = 5 for each cell line. (C) Representative bioluminescent images showing the presence and absence of metastasis in control and ERK5 shRNA cell lines. (D) Quantitation of percentage of mice that were found to be metastasis positive in control and ERK5 knockdown lines at time of sacrifice. (E) Model of MAP3K signaling network members identified as regulating either tumor growth or metastasis, downstream MAPK pathways and tumor outcomes determined from MAP3K knockdown experiments. Tumor experiments were done in collaboration with Nancy Johnson.

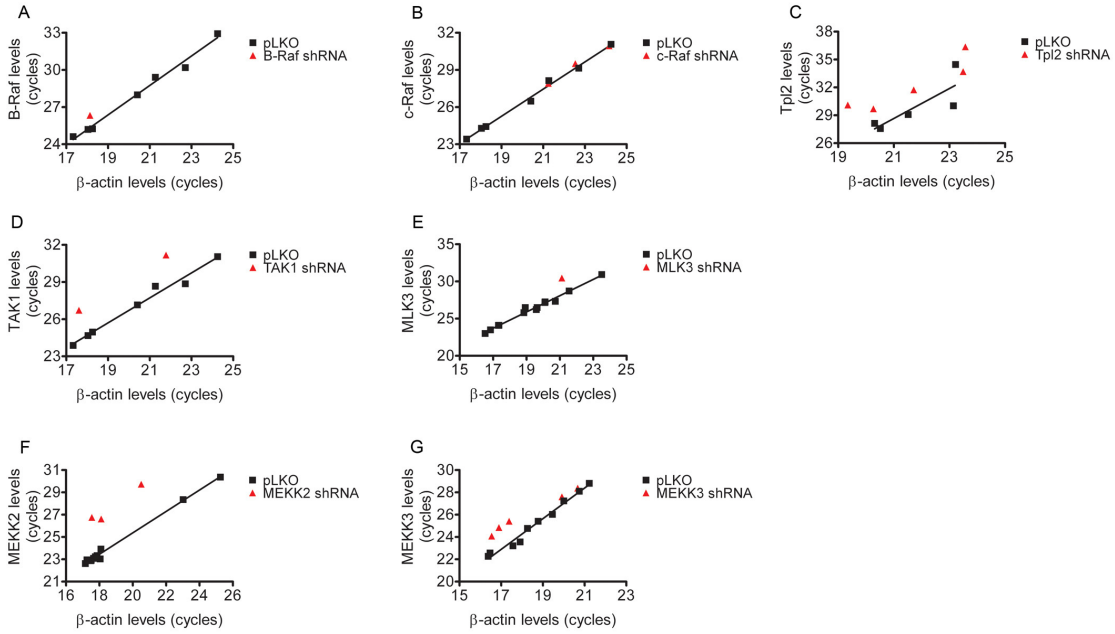

Figure 3.10. Knockdown of MAP3Ks in lymph node metastases from MAP3K knockdown cell lines.
MAP3K knockdown was assessed in lymph node metastases from MAP3K knockdown cell lines. For each MAP3K target, knockdown was assessed relative to MAP3K levels in lymph node metastases from control tumors. Deflection of samples from MAP3K knockdown cell lines above the standard curve created by control lymph node metastases indicated continued knockdown of the MAP3K in the metastasized cells. Knockdown was assessed in metastases from cell lines knocked down for either (A) B-Raf. (B) c-Raf. (C) Tpl2. (D) TAK1. (E) MLK3. (F) MEKK2. (G) MEKK3. These experiments were done with Debbie Granger.

IV. Conclusion

MAPK networks are dysregulated in many diseases resulting in pathological signaling events. Upstream MAP3Ks control the magnitude, duration and location of MAPK activation which regulate the physiological outcome of MAPK signaling. MAPK signaling has been extensively studied in cancer, a disease in which MAPK signaling is frequently dysregulated and promotes tumor growth and metastasis. However, with the exception of B-Raf, the upstream MAP3Ks that control the pathogenic MAPK signaling have been scarcely studied. I have used screening methods to identify the MAPK pathways activated by MAP3Ks in response to an array of stimuli. I also screened a group of nine MAP3Ks in an *in vivo* tumor xenograft assay to identify MAP3Ks that functionally control tumor growth and/or metastasis *in vivo*.

Regulation of MAPK Signaling by MAP3Ks in Cell Culture

The individual MAPKs are organized into dynamic networks. These networks are controlled through the actions of their upstream MAP2Ks and MAP3Ks. MAP2Ks have been well characterized and with the exception of MKK4, appear to regulate only one MAPK family, by contrast, the MAP3Ks can regulate multiple families of MAPKs but their roles in signaling have been poorly characterized. While MAP3Ks are traditionally positive regulators of MAPK signaling, emerging data has demonstrated that MAP3Ks can also behave as negative regulators of MAPK signaling through cross-talk between individual MAP3Ks as well as between MAPKs and MAP3Ks (31,145).

To explore how MAP3K activation can regulate spatial and temporal activation of MAPKs by a diverse array of stimuli, I created an immunofluorescent screening method that can rapidly detect activation of ERK1/2, JNK and p38 activation in multiple regions of the cell. This screen was combined with a MAP3K siRNA library to determine how knockdown of individual MAP3Ks can alter the dynamics of the MAPK network. My screen identified MAP3Ks that were positive and negative regulators of MAPK signaling, demonstrating that disruption of MAP3Ks can perturb the MAPK network in a multitude of ways. Many of these MAP3Ks that positively and negatively regulate MAPK signaling are novel regulatory interactions. Furthermore, even in well established pathways such as growth factor stimulated ERK1/2 activation, we are able to identify novel MAP3Ks that regulate ERK1/2 activation, demonstrating that our current knowledge of the MAPK network is still very incomplete. While downstream MAPK activation and physiological outcome is frequently known for a given stimulus, my screening approach allows for the rapid characterization of proteins that lie upstream of the MAPK, including MAP2Ks, MAP3Ks, adapter proteins and receptors. Selective targeting of these upstream regulators will enable the prevention of undesired or pathological MAPK signaling events.

This siRNA screening method is readily adaptable to whole genome screens as has been done in Drosophila cells or to selectively target groups of genes that have few characterized roles in MAPK signaling (138,139). For instance, given the known role of ubiquitination in the MAPK network, this screen could be used to screen siRNA libraries of E3 ubiquitinating enzymes and deubiquitinating enzymes to identify novel components of the ubiquitination machinery that alter MAPK signaling (146,164,165). Similarly,

crosstalk has been described between some members of the cell cycle and checkpoint machinery and MAPK pathways, thus my screen could be used to rapidly identify novel mechanisms of crosstalk between the cell cycle and checkpoint kinase pathways and MAPKs and the proteins involved in it (166,167).

Interestingly, kinase mediated effects have been demonstrated to be highly cell type specific. Data from siRNA screens has demonstrated that kinases required for specific cell lines are highly varied with well over half of all kinases predicted to be essential in at least one cancer cell line (168,169). While work in this dissertation focused on only HeLa cells, similar immunofluorescence techniques could be used to rapidly characterize the MAPK network in a range of cell types. Limited efforts by myself and others in the lab have been able to measure activation ERK1/2, JNK and p38 activation in other cell types including MEFs and MDA-MB-231 cells. Interestingly, preliminary results using MDA-MB-231 cells expressing MAP3K shRNAs indicated that contrary to our results in HeLa cells, MDA-MB-231 cells required TAK1 in addition to MLK7 for JNK and p38 activation by sorbitol (data not shown). Thus the screening techniques in this dissertation allow for rapid characterization of the MAPK network, allowing us to identify cell type specific signaling differences. A large number of the essential kinases found by siRNA are either MAPK network components or upstream kinases known to activate the MAPK pathways (168,169). Using immunofluorescent MAPK activation detection, it would be interesting to determine whether knockdown of these essential kinases result in reproducible changes in MAPK activation and whether these signaling differences lead to different physiological outcomes.

MAP3K regulation of Tumor Growth and Metastasis *in vivo*

MAPK networks are frequently dysregulated in cancer, wherein dysregulated MAPK signaling can promote tumor growth and metastasis by a wide array of mechanisms. While companies have made many efforts at great cost to directly target the MAPKs, to date, these efforts have not made it through clinical trials. MAPK inhibitors have disappointed in the clinic because of either lack of efficacy or side effects. As an alternative to direct inhibition of MAPKs, targeting the MAP3Ks may enable selective targeting of oncogenic MAPK responses with high specificity. To identify specific roles for individual MAP3Ks in the tumor program, we used an shRNA screening approach coupled to orthotopic xenografts to assess the function of MAP3Ks in breast cancer *in vivo*.

As we enter this era of personalized medicine, in which array based detection of gene amplification in tumors and sequencing of tumor transcriptomes and genomes are medically feasible, we need to identify the genes that are required for tumor growth and metastasis to interpret data gleaned from these sources. While functional genomics has recently bloomed and has significantly contributed to our knowledge of cancer, *in vitro* and *in vivo* data are needed to guide genomic findings and drug target selection; genomics can identify the driver genes that are mutated in a given cancer, but they do not identify why that mutation contributes to cancer. The absence of knowledge about why a mutation drives cancer is one of the limitations of genomic efforts. Proteins that are required for function of the cancer driver but are not mutated remain, from a cancer genetics standpoint, invisible. For instance, it has been demonstrated that mutational activation of B-Raf predicts sensitivity of cancer cells to MEK1/2 inhibitors (170). Based

on established data demonstrating that B-Raf activates ERK1/2 through MEK1/2, we can readily predict the role of MEK1/2 inhibition in B-Raf mutant cells, however, these conclusions would be impossible if we were studying this system *de novo* based solely on the genetic data about B-Raf mutations. Furthermore, due to the role of MAP3Ks in transmitting oncogenic signals, MAP3Ks may be required for tumor growth and metastasis but are likely not to be mutated or overexpressed, consistent with large scale sequencing results that have identified many driver mutations in B-Raf but few driver mutations in other MAP3Ks (111,171,172). Thus the cancer specific roles of MAP3Ks may be refractory to genomic approaches, requiring screening efforts such as mine to determine their function. My data provides answers to which of these MAP3Ks are important for tumor growth and metastasis and may serve as a blueprint for further studies seeking to understand the roles of proteins that are similarly refractory to genomic studies. Similar techniques could also be used to screen genes with driver mutations found by genomic efforts. It seems unlikely that all driver mutations were created equal, and xenograft studies such as these will allow us to compare the relative strength of different driver mutations.

Based on my work, I was able to identify two MAP3Ks, MLK3 and MEKK2 that have pronounced effects on tumor growth and metastasis. Interestingly, despite the potent effects of MLK3 and MEKK2 knockdown on tumors, neither MLK3 nor MEKK2 are essential in mice; both MLK3 and MEKK2 knockout mice are viable and result in normal, fertile adults. Thus drugs targeting MLK3 and MEKK2 may have potent tumor effects, but, based on mouse data, are unlikely to have the toxicity effects that have plagued other inhibitors of MAPK signaling, making them excellent potential drug

targets (27,173). I also identify several other kinases (Tpl2, MEKK3, potentially MLK7) that may be successful drug targets based on their effects on tumor growth.

Based on the previously reported specificity of these MAP3Ks I was able to broadly identify tumor outcomes associated with specific MAPK pathways. I demonstrate that all four MAPK pathways can potentially alter either tumor growth or metastasis. While clinical testing on tumor samples has focused on measuring specific prognostic proteins and tumor markers such as estrogen receptor status, HER2 expression, EGFR expression and uPA/PAI-1 levels, my results suggest that detection of MAPK pathway activation may be an important diagnostic guideline in cancer, consistent with published results (70,71,99,110). My data suggests that JNK, p38 and ERK5 activation, rather than canonical ERK1/2 activation will be important markers of long term survival based on the roles of these pathways in metastasis. Furthermore, as this age of personalized medicine dawns, it is interesting (although perhaps rash) to speculate whether further prognostic and diagnostic gains could be made by isolating primary tumor cells and profiling the activation of primary tumor cell MAPK networks by a range of stimuli using screening approaches such as the immunofluorescent MAPK activation screen characterized here.

Concluding Remarks

In this dissertation, I have used screening approaches targeting the MAP3Ks to determine where and when they activate MAPK pathways. Using an *in vivo* screening approach, I have also characterized the role of a diverse group of MAP3Ks in tumor growth and metastasis. Importantly, these screening efforts use either *in vitro* or *in vivo*

phenotype to guide our work rather then expectation; to date, screening and genomic efforts have demonstrated that, in large part, cancer relevant signaling is mediated by previously uncharacterized kinases (133,168). Discovering these kinases demands that phenotype drive target selection. Using these screening approaches, I was able to identify novel regulators of well characterized pathways (such as growth factor induced signaling) and identify five MAP3Ks with limited provenance in cancer as regulators of tumor growth and metastasis *in vivo*. Targeting of these MAP3Ks involved in cancer may allow the development of novel cancer therapeutics with better efficacy and fewer side effects. While these screening efforts widen our understanding of MAP3K function *in vitro* and *in vivo*, MAP3K signaling is all too often considered a "black box" and remains considerably understudied. The methods I design in this dissertation and the results I obtain with them give researchers better tools to study MAP3Ks and more reason to study them which I hope will promote further study of the MAP3Ks.

References

1. *ACS Global Cancer Facts and Figures 2007* http://www.cancer.org/downloads/STT/Global_Facts_and_Figures_2007_rev2.pdf

2. Negrini, S., Gorgoulis, V. G., and Halazonetis, T. D. (2010) *Nat Rev Mol Cell Biol* **11**, 220-228

3. Vogelstein, B., and Kinzler, K. W. (2004) *Nat Med* **10**, 789-799

4. Wood, L. D., Parsons, D. W., Jones, S., Lin, J., Sjoblom, T., Leary, R. J., Shen, D., Boca, S. M., Barber, T., Ptak, J., Silliman, N., Szabo, S., Dezso, Z., Ustyanksky, V., Nikolskaya, T., Nikolsky, Y., Karchin, R., Wilson, P. A., Kaminker, J. S., Zhang, Z., Croshaw, R., Willis, J., Dawson, D., Shipitsin, M., Willson, J. K., Sukumar, S., Polyak, K., Park, B. H., Pethiyagoda, C. L., Pant, P. V., Ballinger, D. G., Sparks, A. B., Hartigan, J., Smith, D. R., Suh, E., Papadopoulos, N., Buckhaults, P., Markowitz, S. D., Parmigiani, G., Kinzler, K. W., Velculescu, V. E., and Vogelstein, B. (2007) *Science* **318**, 1108-1113

5. Diener, K. R., Need, E. F., Buchanan, G., and Hayball, J. D. (2010) *Expert Opin Ther Targets* **14**, 179-192

6. Fearon, E. R. (2009) *Cancer Cell* **16**, 366-368

7. Ali, S., and Lazennec, G. (2007) *Cancer Metastasis Rev* **26**, 401-420

8. Ganss, R. (2006) *J Cell Mol Med* **10**, 857-865

9. Bergers, G., and Benjamin, L. E. (2003) *Nat Rev Cancer* **3**, 401-410

10. Bidard, F. C., Pierga, J. Y., Vincent-Salomon, A., and Poupon, M. F. (2008) *Cancer Metastasis Rev* **27**, 5-10

11. Nguyen, D. X., Bos, P. D., and Massague, J. (2009) *Nat Rev Cancer* **9**, 274-284

12. Nguyen, D. X., and Massague, J. (2007) *Nat Rev Genet* **8**, 341-352

13. Kessenbrock, K., Plaks, V., and Werb, Z. (2010) *Cell* **141**, 52-67

14. Qian, B. Z., and Pollard, J. W. (2010) *Cell* **141**, 39-51

15. Thiery, J. P., Acloque, H., Huang, R. Y., and Nieto, M. A. (2009) *Cell* **139**, 871-890

16. Yilmaz, M., and Christofori, G. (2009) *Cancer Metastasis Rev* **28**, 15-33

17. Wagner, E. F., and Nebreda, A. R. (2009) *Nat Rev Cancer* **9**, 537-549

18. Dhanasekaran, D. N., and Johnson, G. L. (2007) *Oncogene* **26**, 3097-3099

19. Winter-Vann, A. M., and Johnson, G. L. (2007) *J Cell Biochem* **102**, 848-858

20. Gupta, S., Barrett, T., Whitmarsh, A. J., Cavanagh, J., Sluss, H. K., Derijard, B., and Davis, R. J. (1996) *Embo J* **15**, 2760-2770

21. Cuevas, B. D., Abell, A. N., and Johnson, G. L. (2007) *Oncogene* **26**, 3159-3171

22. Raman, M., Chen, W., and Cobb, M. H. (2007) *Oncogene* **26**, 3100-3112

23. Sebolt-Leopold, J. S., and Herrera, R. (2004) *Nat Rev Cancer* **4**, 937-947

24. Wang, X., Mader, M. M., Toth, J. E., Yu, X., Jin, N., Campbell, R. M., Smallwood, J. K., Christe, M. E., Chatterjee, A., Goodson, T., Jr., Vlahos, C. J., Matter, W. F., and Bloem, L. J. (2005) *J Biol Chem* **280**, 19298-19305

25. Hatziapostolou, M., Polytarchou, C., Panutsopulos, D., Covic, L., and Tsichlis, P. N. (2008) *Cancer Res* **68**, 1851-1861

26. Das, S., Cho, J., Lambertz, I., Kelliher, M. A., Eliopoulos, A. G., Du, K., and Tsichlis, P. N. (2005) *J Biol Chem* **280**, 23748-23757

27. Brancho, D., Ventura, J. J., Jaeschke, A., Doran, B., Flavell, R. A., and Davis, R. J. (2005) *Mol Cell Biol* **25**, 3670-3681

28. Sato, S., Sanjo, H., Takeda, K., Ninomiya-Tsuji, J., Yamamoto, M., Kawai, T., Matsumoto, K., Takeuchi, O., and Akira, S. (2005) *Nat Immunol* **6**, 1087-1095

29. Tobiume, K., Matsuzawa, A., Takahashi, T., Nishitoh, H., Morita, K., Takeda, K., Minowa, O., Miyazono, K., Noda, T., and Ichijo, H. (2001) *EMBO Rep* **2**, 222-228

30. Chadee, D. N., and Kyriakis, J. M. (2004) *Nat Cell Biol* **6**, 770-776

31. Di, Y., Li, S., Wang, L., Zhang, Y., and Dorf, M. E. (2008) *Cell Signal* **20**, 705-713

32. Waskiewicz, A. J., Flynn, A., Proud, C. G., and Cooper, J. A. (1997) *Embo J* **16**, 1909-1920

33. Seddighzadeh, M., Zhou, J. N., Kronenwett, U., Shoshan, M. C., Auer, G., Sten-Linder, M., Wiman, B., and Linder, S. (1999) *Clin Exp Metastasis* **17**, 649-654

34. Bessard, A., Fremin, C., Ezan, F., Fautrel, A., Gailhouste, L., and Baffet, G. (2008) *Oncogene* **27**, 5315-5325

35. Lefloch, R., Pouyssegur, J., and Lenormand, P. (2008) *Mol Cell Biol* **28**, 511-527

36. Sheridan, C., Brumatti, G., and Martin, S. J. (2008) *J Biol Chem* **283**, 22128-22135

37. Yao, Y., Li, W., Wu, J., Germann, U. A., Su, M. S., Kuida, K., and Boucher, D. M. (2003) *Proc Natl Acad Sci U S A* **100**, 12759-12764

38. Scholl, F. A., Dumesic, P. A., Barragan, D. I., Harada, K., Charron, J., and Khavari, P. A. (2009) *Cancer Res* **69**, 3772-3778

39. Scholl, F. A., Dumesic, P. A., Barragan, D. I., Harada, K., Bissonauth, V., Charron, J., and Khavari, P. A. (2007) *Dev Cell* **12**, 615-629

40. Giroux, S., Tremblay, M., Bernard, D., Cardin-Girard, J. F., Aubry, S., Larouche, L., Rousseau, S., Huot, J., Landry, J., Jeannotte, L., and Charron, J. (1999) *Curr Biol* **9**, 369-372

41. Belanger, L. F., Roy, S., Tremblay, M., Brott, B., Steff, A. M., Mourad, W., Hugo, P., Erikson, R., and Charron, J. (2003) *Mol Cell Biol* **23**, 4778-4787

42. Hoshino, R., Chatani, Y., Yamori, T., Tsuruo, T., Oka, H., Yoshida, O., Shimada, Y., Ari-i, S., Wada, H., Fujimoto, J., and Kohno, M. (1999) *Oncogene* **18**, 813-822

43. Mansour, S. J., Matten, W. T., Hermann, A. S., Candia, J. M., Rong, S., Fukasawa, K., Vande Woude, G. F., and Ahn, N. G. (1994) *Science* **265**, 966-970

44. Gailhouste, L., Ezan, F., Bessard, A., Fremin, C., Rageul, J., Langouet, S., and Baffet, G. (2010) *Int J Cancer* **126**, 1367-1377

45. Bourcier, C., Jacquel, A., Hess, J., Peyrottes, I., Angel, P., Hofman, P., Auberger, P., Pouyssegur, J., and Pages, G. (2006) *Cancer Res* **66**, 2700-2707

46. Dhanasekaran, D. N., and Reddy, E. P. (2008) *Oncogene* **27**, 6245-6251

47. Tournier, C., Hess, P., Yang, D. D., Xu, J., Turner, T. K., Nimnual, A., Bar-Sagi, D., Jones, S. N., Flavell, R. A., and Davis, R. J. (2000) *Science* **288**, 870-874

48. Jiang, H., Liang, C., Liu, X., Jiang, Q., He, Z., Wu, J., Pan, X., Ren, Y., Fan, M., Li, M., and Wu, Z. (2010) *Atherosclerosis* **210**, 71-77

49. Verma, G., and Datta, M. (2010) *Apoptosis*

50. Liu, B., Han, M., Sun, R. H., Wang, J. J., Zhang, Y. P., Zhang, D. Q., and Wen, J. K. (2010) *Breast Cancer Res* **12**, R9

51. Mansouri, A., Ridgway, L. D., Korapati, A. L., Zhang, Q., Tian, L., Wang, Y., Siddik, Z. H., Mills, G. B., and Claret, F. X. (2003) *J Biol Chem* **278**, 19245-19256

52. Fan, M., Goodwin, M. E., Birrer, M. J., and Chambers, T. C. (2001) *Cancer Res* **61**, 4450-4458

53. Lei, K., and Davis, R. J. (2003) *Proc Natl Acad Sci U S A* **100**, 2432-2437

54. Donovan, N., Becker, E. B., Konishi, Y., and Bonni, A. (2002) *J Biol Chem* **277**, 40944-40949

55. Srivastava, R. K., Mi, Q. S., Hardwick, J. M., and Longo, D. L. (1999) *Proc Natl Acad Sci U S A* **96**, 3775-3780

56. Yamamoto, K., Ichijo, H., and Korsmeyer, S. J. (1999) *Mol Cell Biol* **19**, 8469-8478

57. Weston, C. R., Wong, A., Hall, J. P., Goad, M. E., Flavell, R. A., and Davis, R. J. (2004) *Proc Natl Acad Sci U S A* **101**, 14114-14119

58. Radhika, V., Hee Ha, J., Jayaraman, M., Tsim, S. T., and Dhanasekaran, N. (2005) *Oncogene* **24**, 4597-4603

59. Choi, J., Park, S. Y., and Joo, C. K. (2004) *Invest Ophthalmol Vis Sci* **45**, 2696-2704

60. Zenz, R., Scheuch, H., Martin, P., Frank, C., Eferl, R., Kenner, L., Sibilia, M., and Wagner, E. F. (2003) *Dev Cell* **4**, 879-889

61. Ivanov, V. N., Bhoumik, A., Krasilnikov, M., Raz, R., Owen-Schaub, L. B., Levy, D., Horvath, C. M., and Ronai, Z. (2001) *Mol Cell* **7**, 517-528

62. Sabapathy, K., Hochedlinger, K., Nam, S. Y., Bauer, A., Karin, M., and Wagner, E. F. (2004) *Mol Cell* **15**, 713-725

63. Makino, T., Jinnin, M., Muchemwa, F. C., Fukushima, S., Kogushi-Nishi, H., Moriya, C., Igata, T., Fujisawa, A., Johno, T., and Ihn, H. (2009) *Br J Dermatol*

64. Cui, J., Wang, Q., Wang, J., Lv, M., Zhu, N., Li, Y., Feng, J., Shen, B., and Zhang, J. (2009) *Mol Cancer Ther* **8**, 3214-3222

65. Wei, L., Liu, Y., Kaneto, H., and Fanburg, B. L. (2010) *Am J Physiol Lung Cell Mol Physiol*

66. Ventura, J. J., Hubner, A., Zhang, C., Flavell, R. A., Shokat, K. M., and Davis, R. J. (2006) *Mol Cell* **21**, 701-710

67. Hui, L., Zatloukal, K., Scheuch, H., Stepniak, E., and Wagner, E. F. (2008) *J Clin Invest* **118**, 3943-3953

68. Sakurai, T., Maeda, S., Chang, L., and Karin, M. (2006) *Proc Natl Acad Sci U S A* **103**, 10544-10551

69. Shibata, W., Maeda, S., Hikiba, Y., Yanai, A., Sakamoto, K., Nakagawa, H., Ogura, K., Karin, M., and Omata, M. (2008) *Cancer Res* **68**, 5031-5039

70. Davidson, B., Espina, V., Steinberg, S. M., Florenes, V. A., Liotta, L. A., Kristensen, G. B., Trope, C. G., Berner, A., and Kohn, E. C. (2006) *Clin Cancer Res* **12**, 791-799

71. Wang, X., Chao, L., Li, X., Ma, G., Chen, L., Zang, Y., and Zhou, G. (2010) *Hum Pathol* **41**, 401-406

72. Durbin, A. D., Somers, G. R., Forrester, M., Pienkowska, M., Hannigan, G. E., and Malkin, D. (2009) *J Clin Invest* **119**, 1558-1570

73. Nateri, A. S., Spencer-Dene, B., and Behrens, A. (2005) *Nature* **437**, 281-285

74. Chen, N., Nomura, M., She, Q. B., Ma, W. Y., Bode, A. M., Wang, L., Flavell, R. A., and Dong, Z. (2001) *Cancer Res* **61**, 3908-3912

75. She, Q. B., Chen, N., Bode, A. M., Flavell, R. A., and Dong, Z. (2002) *Cancer Res* **62**, 1343-1348

76. Huang, Q., Yang, J., Lin, Y., Walker, C., Cheng, J., Liu, Z. G., and Su, B. (2004) *Nat Immunol* **5**, 98-103

77. Sharma, G. D., He, J., and Bazan, H. E. (2003) *J Biol Chem* **278**, 21989-21997

78. Shao, H., Wu, C., and Wells, A. (2010) *J Biol Chem* **285**, 2591-2600

79. Shimada, H., and Rajagopalan, L. E. (2010) *FEBS Lett*

80. Park, K. S., Kim, M. K., Lee, H. Y., Kim, S. D., Lee, S. Y., Kim, J. M., Ryu, S. H., and Bae, Y. S. (2007) *Biochem Biophys Res Commun* **356**, 239-244

81. Ambrosino, C., and Nebreda, A. R. (2001) *Biol Cell* **93**, 47-51

82. Shi, J., Guan, J., Jiang, B., Brenner, D. A., Del Monte, F., Ward, J. E., Connors, L. H., Sawyer, D. B., Semigran, M. J., Macgillivray, T. E., Seldin, D. C., Falk, R., and Liao, R. (2010) *Proc Natl Acad Sci U S A* **107**, 4188-4193

83. Bulavin, D. V., Demidov, O. N., Saito, S., Kauraniemi, P., Phillips, C., Amundson, S. A., Ambrosino, C., Sauter, G., Nebreda, A. R., Anderson, C. W., Kallioniemi, A., Fornace, A. J., Jr., and Appella, E. (2002) *Nat Genet* **31**, 210-215

84. Lee, B., Kim, C. H., and Moon, S. K. (2006) *FEBS Lett* **580**, 5177-5184

85. Kalra, N., and Kumar, V. (2004) *J Biol Chem* **279**, 25313-25319

86. Cai, B., Chang, S. H., Becker, E. B., Bonni, A., and Xia, Z. (2006) *J Biol Chem* **281**, 25215-25222

87. Hui, L., Bakiri, L., Mairhorfer, A., Schweifer, N., Haslinger, C., Kenner, L., Komnenovic, V., Scheuch, H., Beug, H., and Wagner, E. F. (2007) *Nat Genet* **39**, 741-749

88. Chen, L., Mayer, J. A., Krisko, T. I., Speers, C. W., Wang, T., Hilsenbeck, S. G., and Brown, P. H. (2009) *Cancer Res* **69**, 8853-8861

89. Simone, C. (2007) *Autophagy* **3**, 468-471

90. Thornton, T. M., Pedraza-Alva, G., Deng, B., Wood, C. D., Aronshtam, A., Clements, J. L., Sabio, G., Davis, R. J., Matthews, D. E., Doble, B., and Rincon, M. (2008) *Science* **320**, 667-670

91. Xu, L., Pathak, P. S., and Fukumura, D. (2004) *Clin Cancer Res* **10**, 701-707

92. Gordon, G. M., Ledee, D. R., Feuer, W. J., and Fini, M. E. (2009) *J Cell Physiol* **221**, 402-411

93. Lee, T. H., Huang, Q., Oikemus, S., Shank, J., Ventura, J. J., Cusson, N., Vaillancourt, R. R., Su, B., Davis, R. J., and Kelliher, M. A. (2003) *Mol Cell Biol* **23**, 8377-8385

94. Kawaguchi, M., Akagi, M., Gray, M. J., Liu, W., Fan, F., and Ellis, L. M. (2004) *Surgery* **136**, 686-692

95. Brancho, D., Tanaka, N., Jaeschke, A., Ventura, J. J., Kelkar, N., Tanaka, Y., Kyuuma, M., Takeshita, T., Flavell, R. A., and Davis, R. J. (2003) *Genes Dev* **17**, 1969-1978

96. Ventura, J. J., Tenbaum, S., Perdiguero, E., Huth, M., Guerra, C., Barbacid, M., Pasparakis, M., and Nebreda, A. R. (2007) *Nat Genet* **39**, 750-758

97. Bulavin, D. V., Phillips, C., Nannenga, B., Timofeev, O., Donehower, L. A., Anderson, C. W., Appella, E., and Fornace, A. J., Jr. (2004) *Nat Genet* **36**, 343-350

98. Schindler, E. M., Hindes, A., Gribben, E. L., Burns, C. J., Yin, Y., Lin, M. H., Owen, R. J., Longmore, G. D., Kissling, G. E., Arthur, J. S., and Efimova, T. (2009) *Cancer Res* **69**, 4648-4655

99. Davidson, B., Konstantinovsky, S., Kleinberg, L., Nguyen, M. T., Bassarova, A., Kvalheim, G., Nesland, J. M., and Reich, R. (2006) *Gynecol Oncol* **102**, 453-461

100. Kato, Y., Tapping, R. I., Huang, S., Watson, M. H., Ulevitch, R. J., and Lee, J. D. (1998) *Nature* **395**, 713-716

101. Finegan, K. G., Wang, X., Lee, E. J., Robinson, A. C., and Tournier, C. (2009) *Cell Death Differ* **16**, 674-683

102. Wang, X., Merritt, A. J., Seyfried, J., Guo, C., Papadakis, E. S., Finegan, K. G., Kayahara, M., Dixon, J., Boot-Handford, R. P., Cartwright, E. J., Mayer, U., and Tournier, C. (2005) *Mol Cell Biol* **25**, 336-345

103. Weldon, C. B., Scandurro, A. B., Rolfe, K. W., Clayton, J. L., Elliott, S., Butler, N. N., Melnik, L. I., Alam, J., McLachlan, J. A., Jaffe, B. M., Beckman, B. S., and Burow, M. E. (2002) *Surgery* **132**, 293-301

104. Buschbeck, M., Hofbauer, S., Di Croce, L., Keri, G., and Ullrich, A. (2005) *EMBO Rep* **6**, 63-69

105. Clape, C., Fritz, V., Henriquet, C., Apparailly, F., Fernandez, P. L., Iborra, F., Avances, C., Villalba, M., Culine, S., and Fajas, L. (2009) *PLoS One* **4**, e7542

106. Arnoux, V., Nassour, M., L'Helgoualc'h, A., Hipskind, R. A., and Savagner, P. (2008) *Mol Biol Cell* **19**, 4738-4749

107. Mehta, P. B., Jenkins, B. L., McCarthy, L., Thilak, L., Robson, C. N., Neal, D. E., and Leung, H. Y. (2003) *Oncogene* **22**, 1381-1389

108. Kesavan, K., Lobel-Rice, K., Sun, W., Lapadat, R., Webb, S., Johnson, G. L., and Garrington, T. P. (2004) *J Cell Physiol* **199**, 140-148

109. Barros, J. C., and Marshall, C. J. (2005) *J Cell Sci* **118**, 1663-1671

110. Montero, J. C., Ocana, A., Abad, M., Ortiz-Ruiz, M. J., Pandiella, A., and Esparis-Ogando, A. (2009) *PLoS One* **4**, e5565

111. Davies, H., Bignell, G. R., Cox, C., Stephens, P., Edkins, S., Clegg, S., Teague, J., Woffendin, H., Garnett, M. J., Bottomley, W., Davis, N., Dicks, E., Ewing, R., Floyd, Y., Gray, K., Hall, S., Hawes, R., Hughes, J., Kosmidou, V., Menzies, A., Mould, C., Parker, A., Stevens, C., Watt, S., Hooper, S., Wilson, R., Jayatilake, H., Gusterson, B. A., Cooper, C., Shipley, J., Hargrave, D., Pritchard-Jones, K., Maitland, N., Chenevix-Trench, G., Riggins, G. J., Bigner, D. D., Palmieri, G., Cossu, A., Flanagan, A., Nicholson, A., Ho, J. W., Leung, S. Y., Yuen, S. T., Weber, B. L., Seigler, H. F., Darrow, T. L., Paterson, H., Marais, R., Marshall, C. J., Wooster, R., Stratton, M. R., and Futreal, P. A. (2002) *Nature* **417**, 949-954

112. Bosch, E., Cherwinski, H., Peterson, D., and McMahon, M. (1997) *Oncogene* **15**, 1021-1033

113. Yazdi, A. S., Palmedo, G., Flaig, M. J., Puchta, U., Reckwerth, A., Rutten, A., Mentzel, T., Hugel, H., Hantschke, M., Schmid-Wendtner, M. H., Kutzner, H., and Sander, C. A. (2003) *J Invest Dermatol* **121**, 1160-1162

114. Dankort, D., Curley, D. P., Cartlidge, R. A., Nelson, B., Karnezis, A. N., Damsky, W. E., Jr., You, M. J., DePinho, R. A., McMahon, M., and Bosenberg, M. (2009) *Nat Genet* **41**, 544-552

115. Hoeflich, K. P., Gray, D. C., Eby, M. T., Tien, J. Y., Wong, L., Bower, J., Gogineni, A., Zha, J., Cole, M. J., Stern, H. M., Murray, L. J., Davis, D. P., and Seshagiri, S. (2006) *Cancer Res* **66**, 999-1006

116. Tsai, J., Lee, J. T., Wang, W., Zhang, J., Cho, H., Mamo, S., Bremer, R., Gillette, S., Kong, J., Haass, N. K., Sproesser, K., Li, L., Smalley, K. S., Fong, D., Zhu, Y. L., Marimuthu, A., Nguyen, H., Lam, B., Liu, J., Cheung, I., Rice, J., Suzuki, Y., Luu, C., Settachatgul, C., Shellooe, R., Cantwell, J., Kim, S. H., Schlessinger, J., Zhang, K. Y., West, B. L., Powell, B., Habets, G., Zhang, C., Ibrahim, P. N., Hirth, P., Artis, D. R., Herlyn, M., and Bollag, G. (2008) *Proc Natl Acad Sci U S A* **105**, 3041-3046

117. Sala, E., Mologni, L., Truffa, S., Gaetano, C., Bollag, G. E., and Gambacorti-Passerini, C. (2008) *Mol Cancer Res* **6**, 751-759

118. Shepherd, C., Puzanov, I., and Sosman, J. A. (2010) *Curr Oncol Rep* **12**, 146-152

119. Cuevas, B. D., Winter-Vann, A. M., Johnson, N. L., and Johnson, G. L. (2006) *Oncogene* **25**, 4998-5010

120. Cazares, L. H., Troyer, D., Mendrinos, S., Lance, R. A., Nyalwidhe, J. O., Beydoun, H. A., Clements, M. A., Drake, R. R., and Semmes, O. J. (2009) *Clin Cancer Res* **15**, 5541-5551

121. Kim, H., Huang, W., Jiang, X., Pennicooke, B., Park, P. J., and Johnson, M. D. (2010) *Proc Natl Acad Sci U S A* **107**, 2183-2188

122. Samanta, A. K., Huang, H. J., Le, X. F., Mao, W., Lu, K. H., Bast, R. C., Jr., and Liao, W. S. (2009) *Cancer* **115**, 3897-3908

123. Deng, Y., Yang, J., McCarty, M., and Su, B. (2007) *Am J Physiol Cell Physiol* **293**, C1404-1411

124. Iriyama, T., Takeda, K., Nakamura, H., Morimoto, Y., Kuroiwa, T., Mizukami, J., Umeda, T., Noguchi, T., Naguro, I., Nishitoh, H., Saegusa, K., Tobiume, K., Homma, T., Shimada, Y., Tsuda, H., Aiko, S., Imoto, I., Inazawa, J., Chida, K., Kamei, Y., Kozuma, S., Taketani, Y., Matsuzawa, A., and Ichijo, H. (2009) *Embo J* **28**, 843-853

125. Hayakawa, Y., Hirata, Y., Nakagawa, H., Sakamoto, K., Hikiba, Y., Otsuka, M., Ijichi, H., Ikenoue, T., Tateishi, K., Akanuma, M., Ogura, K., Yoshida, H., Ichijo, H., Omata, M., and Maeda, S. (2010) *Gastroenterology* **138**, 1055-1067 e1051-1054

126. Patriotis, C., Makris, A., Bear, S. E., and Tsichlis, P. N. (1993) *Proc Natl Acad Sci U S A* **90**, 2251-2255

127. Ceci, J. D., Patriotis, C. P., Tsatsanis, C., Makris, A. M., Kovatch, R., Swing, D. A., Jenkins, N. A., Tsichlis, P. N., and Copeland, N. G. (1997) *Genes Dev* **11**, 688-700

128. Christoforidou, A. V., Papadaki, H. A., Margioris, A. N., Eliopoulos, G. D., and Tsatsanis, C. (2004) *Mol Cancer* **3**, 34

129. Hartkamp, J., Troppmair, J., and Rapp, U. R. (1999) *Cancer Res* **59**, 2195-2202

130. Cho, Y. Y., Bode, A. M., Mizuno, H., Choi, B. Y., Choi, H. S., and Dong, Z. (2004) *Cancer Res* **64**, 3855-3864

131. Lambert, J. M., Karnoub, A. E., Graves, L. M., Campbell, S. L., and Der, C. J. (2002) *J Biol Chem* **277**, 4770-4777

132. Velho, S., Oliveira, C., Paredes, J., Sousa, S., Leite, M., Matos, P., Milanezi, F., Ribeiro, A. S., Mendes, N., Licastro, D., Karhu, A., Oliveira, M. J., Ligtenberg, M., Hamelin, R., Carneiro, F., Lindblom, A., Peltomaki, P., Castedo, S., Schwartz, S., Jr., Jordan, P., Aaltonen, L. A., Hofstra, R. M., Suriano, G., Stupka, E., Fialho, A. M., and Seruca, R. (2010) *Hum Mol Genet* **19**, 697-706

133. Fedorov, O., Muller, S., and Knapp, S. (2010) *Nat Chem Biol* **6**, 166-169

134. Abell, A. N., Rivera-Perez, J. A., Cuevas, B. D., Uhlik, M. T., Sather, S., Johnson, N. L., Minton, S. K., Lauder, J. M., Winter-Vann, A. M., Nakamura, K., Magnuson, T., Vaillancourt, R. R., Heasley, L. E., and Johnson, G. L. (2005) *Mol Cell Biol* **25**, 8948-8959

135. Simpson, K. J., Selfors, L. M., Bui, J., Reynolds, A., Leake, D., Khvorova, A., and Brugge, J. S. (2008) *Nat Cell Biol* **10**, 1027-1038

136. Kiel, C., and Serrano, L. (2009) *Sci Signal* **2**, ra38

137. Nickischer, D., Laethem, C., Trask, O. J., Jr., Williams, R. G., Kandasamy, R., and Johnston, P. A. (2006) *Methods Enzymol* **414**, 389-418

138. Friedman, A., and Perrimon, N. (2006) *Nature* **444**, 230-234

139. Bond, D., and Foley, E. (2009) *PLoS Pathog* **5**, e1000655

140. Paumelle, R., Tulasne, D., Kherrouche, Z., Plaza, S., Leroy, C., Reveneau, S., Vandenbunder, B., and Fafeur, V. (2002) *Oncogene* **21**, 2309-2319

141. Hammoud, L., Burger, D. E., Lu, X., and Feng, Q. (2009) *Am J Physiol Cell Physiol* **296**, C735-745

142. Kajanne, R., Miettinen, P., Mehlem, A., Leivonen, S. K., Birrer, M., Foschi, M., Kahari, V. M., and Leppa, S. (2007) *J Cell Physiol* **212**, 489-497

143. Caceres, M., Tobar, N., Guerrero, J., Smith, P. C., and Martinez, J. (2008) *J Cell Biochem* **103**, 986-993

144. Huang, Z., Yan, D. P., and Ge, B. X. (2008) *Cell Signal* **20**, 2002-2012

145. Nishimura, M., Shin, M. S., Singhirunnusorn, P., Suzuki, S., Kawanishi, M., Koizumi, K., Saiki, I., and Sakurai, H. (2009) *Mol Cell Biol* **29**, 5529-5539

146. Lu, Z., Xu, S., Joazeiro, C., Cobb, M. H., and Hunter, T. (2002) *Mol Cell* **9**, 945-956

147. Hennessy, B. T., Gonzalez-Angulo, A. M., Stemke-Hale, K., Gilcrease, M. Z., Krishnamurthy, S., Lee, J. S., Fridlyand, J., Sahin, A., Agarwal, R., Joy, C., Liu, W., Stivers, D., Baggerly, K., Carey, M., Lluch, A., Monteagudo, C., He, X., Weigman, V., Fan, C., Palazzo, J., Hortobagyi, G. N., Nolden, L. K., Wang, N. J., Valero, V., Gray, J. W., Perou, C. M., and Mills, G. B. (2009) *Cancer Res* **69**, 4116-4124

148. Sticht, C., Freier, K., Knopfle, K., Flechtenmacher, C., Pungs, S., Hofele, C., Hahn, M., Joos, S., and Lichter, P. (2008) *Neoplasia* **10**, 462-470

149. Zen, K., Yasui, K., Nakajima, T., Zen, Y., Gen, Y., Mitsuyoshi, H., Minami, M., Mitsufuji, S., Tanaka, S., Itoh, Y., Nakanuma, Y., Taniwaki, M., Arii, S., Okanoue, T., and Yoshikawa, T. (2009) *Genes Chromosomes Cancer* **48**, 109-120

150. Sourvinos, G., Tsatsanis, C., and Spandidos, D. A. (1999) *Oncogene* **18**, 4968-4973

151. Karasarides, M., Chiloeches, A., Hayward, R., Niculescu-Duvaz, D., Scanlon, I., Friedlos, F., Ogilvie, L., Hedley, D., Martin, J., Marshall, C. J., Springer, C. J., and Marais, R. (2004) *Oncogene* **23**, 6292-6298

152. Samowitz, W. S., Sweeney, C., Herrick, J., Albertsen, H., Levin, T. R., Murtaugh, M. A., Wolff, R. K., and Slattery, M. L. (2005) *Cancer Res* **65**, 6063-6069

153. Cuevas, B. D., Abell, A. N., Witowsky, J. A., Yujiri, T., Johnson, N. L., Kesavan, K., Ware, M., Jones, P. L., Weed, S. A., DeBiasi, R. L., Oka, Y., Tyler, K. L., and Johnson, G. L. (2003) *Embo J* **22**, 3346-3355

154. Patsialou, A., Wyckoff, J., Wang, Y., Goswami, S., Stanley, E. R., and Condeelis, J. S. (2009) *Cancer Res* **69**, 9498-9506

155. Sartorius, C. A., Shen, T., and Horwitz, K. B. (2003) *Breast Cancer Res Treat* **79**, 287-299

156. Hollestelle, A., Elstrodt, F., Nagel, J. H., Kallemeijn, W. W., and Schutte, M. (2007) *Mol Cancer Res* **5**, 195-201

157. Jaeschke, A., and Davis, R. J. (2007) *Mol Cell* **27**, 498-508

158. Garcia-Hoz, C., Sanchez-Fernandez, G., Diaz-Meco, M. T., Moscat, J., Mayor, F., and Ribas, C. (2010) *J Biol Chem* **285**, 13480-13489

159. Sun, W., Wei, X., Kesavan, K., Garrington, T. P., Fan, R., Mei, J., Anderson, S. M., Gelfand, E. W., and Johnson, G. L. (2003) *Mol Cell Biol* **23**, 2298-2308

160. Versteeg, H. H., Schaffner, F., Kerver, M., Petersen, H. H., Ahamed, J., Felding-Habermann, B., Takada, Y., Mueller, B. M., and Ruf, W. (2008) *Blood* **111**, 190-199

161. Wang, X., Wang, M., Amarzguioui, M., Liu, F., Fodstad, O., and Prydz, H. (2004) *Int J Cancer* **112**, 994-1002

162. McCracken, S. R., Ramsay, A., Heer, R., Mathers, M. E., Jenkins, B. L., Edwards, J., Robson, C. N., Marquez, R., Cohen, P., and Leung, H. Y. (2008) *Oncogene* **27**, 2978-2988

163. Mishra, R., Barthwal, M. K., Sondarva, G., Rana, B., Wong, L., Chatterjee, M., Woodgett, J. R., and Rana, A. (2007) *J Biol Chem* **282**, 30393-30405

164. Yamashita, M., Ying, S. X., Zhang, G. M., Li, C., Cheng, S. Y., Deng, C. X., and Zhang, Y. E. (2005) *Cell* **121**, 101-113

165. Witowsky, J. A., and Johnson, G. L. (2003) *J Biol Chem* **278**, 1403-1406

166. Vitale, I., Senovilla, L., Galluzzi, L., Criollo, A., Vivet, S., Castedo, M., and Kroemer, G. (2008) *Cell Cycle* **7**, 1956-1961

167. Borysov, S. I., and Guadagno, T. M. (2008) *Mol Biol Cell* **19**, 2907-2915

168. Grueneberg, D. A., Degot, S., Pearlberg, J., Li, W., Davies, J. E., Baldwin, A., Endege, W., Doench, J., Sawyer, J., Hu, Y., Boyce, F., Xian, J., Munger, K., and Harlow, E. (2008) *Proc Natl Acad Sci U S A* **105**, 16472-16477

169. MacKeigan, J. P., Murphy, L. O., and Blenis, J. (2005) *Nat Cell Biol* **7**, 591-600

170. Solit, D. B., Garraway, L. A., Pratilas, C. A., Sawai, A., Getz, G., Basso, A., Ye, Q., Lobo, J. M., She, Y., Osman, I., Golub, T. R., Sebolt-Leopold, J., Sellers, W. R., and Rosen, N. (2006) *Nature* **439**, 358-362

171. Greenman, C., Stephens, P., Smith, R., Dalgliesh, G. L., Hunter, C., Bignell, G., Davies, H., Teague, J., Butler, A., Stevens, C., Edkins, S., O'Meara, S., Vastrik, I., Schmidt, E. E., Avis, T., Barthorpe, S., Bhamra, G., Buck, G., Choudhury, B., Clements, J., Cole, J., Dicks, E., Forbes, S., Gray, K., Halliday, K., Harrison, R., Hills, K., Hinton, J., Jenkinson, A., Jones, D., Menzies, A., Mironenko, T., Perry, J., Raine, K., Richardson, D., Shepherd, R., Small, A., Tofts, C., Varian, J., Webb, T., West, S., Widaa, S., Yates, A., Cahill, D. P., Louis, D. N., Goldstraw, P., Nicholson, A. G., Brasseur, F., Looijenga, L., Weber, B. L., Chiew, Y. E., DeFazio, A., Greaves, M. F., Green, A. R., Campbell, P., Birney, E., Easton, D. F., Chenevix-Trench, G., Tan, M. H., Khoo, S. K., Teh, B. T., Yuen, S. T., Leung, S. Y., Wooster, R., Futreal, P. A., and Stratton, M. R. (2007) *Nature* **446**, 153-158

172. Davies, H., Hunter, C., Smith, R., Stephens, P., Greenman, C., Bignell, G., Teague, J., Butler, A., Edkins, S., Stevens, C., Parker, A., O'Meara, S., Avis, T., Barthorpe, S., Brackenbury, L., Buck, G., Clements, J., Cole, J., Dicks, E., Edwards, K., Forbes, S., Gorton, M., Gray, K., Halliday, K., Harrison, R., Hills, K., Hinton, J., Jones, D., Kosmidou, V., Laman, R., Lugg, R., Menzies, A., Perry, J., Petty, R., Raine, K., Shepherd, R., Small, A., Solomon, H., Stephens, Y., Tofts, C., Varian, J., Webb, A., West, S., Widaa, S., Yates, A., Brasseur, F., Cooper, C. S., Flanagan, A. M., Green, A., Knowles, M., Leung, S. Y., Looijenga, L. H., Malkowicz, B., Pierotti, M. A., Teh, B. T., Yuen, S. T., Lakhani, S. R., Easton, D.

F., Weber, B. L., Goldstraw, P., Nicholson, A. G., Wooster, R., Stratton, M. R., and Futreal, P. A. (2005) *Cancer Res* **65**, 7591-7595

173. Guo, Z., Clydesdale, G., Cheng, J., Kim, K., Gan, L., McConkey, D. J., Ullrich, S. E., Zhuang, Y., and Su, B. (2002) *Mol Cell Biol* **22**, 5761-5768